MOSE
TECHNICAL REPORT

Doc.No : E-TRE-INA-245-0009.1
Version : 2.0
Date : 13 October 2015

MOSE: MOdeling Sites ESO Report Phase B

PI: Elena Masciadri
TEAM: Luca Fini, Franck Lascaux, Elena Masciadri, Alessio Turchi

INAF/Osservatorio Astrofisico di Arcetri
L.go Enrico Fermi 5
50125 Florence, Italy

ESO BOARD:
Florian Kerber, Harald Kuntschner, Pierre-Yves Madec, Marc Sarazin

ABSTRACT

The MOSE project (MOdeling ESO Sites) aims at proving the feasibility of the forecast of **(1)** all the classical atmospheric parameters (temperature, wind speed intensity and direction, relative humidity) and **(2)** the optical turbulence OT (C_N^2 profiles) with all the main integrated astro-climatic parameters derived from the C_N^2 i.e. the seeing (ε), the isoplanatic angle (θ_0), the wavefront coherence time (τ_0) above the two ESO sites of Cerro Paranal (site of the Very Large Telescope - VLT) and Cerro Armazones (site selected for the European Extremely Large Telescope - E-ELT).
For what concerns the atmospheric parameters the study aims at studying the ability of the model in reconstructing their vertical stratification along the troposphere and low stratosphere (around 20 km) and their estimation near the ground (the first 30 m). To constrain and validate the model a different set of measurements have been used that are provided by different instruments. At Cerro Paranal: Automatic Weather Station (AWS) [RD1] and radiosoungings [RD2]. At Cerro Armazones: Automatic Weather Station (AWS) and mast [RD3].
For what concerns the optical turbulence and derived integrated astroclimatic paramaters measurements from a Generalized Scidar (GS), a Differential Image Motion Monitor (DIMM) and a MASS (Multi Aperture Scintillation Sensor) running simultaneously during the PAR2007 Site testing campaign at Cerro Paranal [RD4] have been used for the model calibration and a preliminary model validation. Independent measurements from a DIMM and MASS taken routinely at Cerro Paranal since 19/08/1998[a] have been used for the final model validation.
In this technical report are summarized the deliverables according to MOSE Project - Phase B and minutes from review meetings (BSCW archive).

We refer the reader to the report of MOSE Phase A for the complementary part of this feasibility study. Phase B was necessary to tackle specific issues (or solve specific problems) to complete the study presented in Phase A. The structure of the Phase B report follows simply the structure of the management plan.

[a] http://archive.eso.org/asm/ambientserver

Contents

1 Work Package 1.1 - Model performances in reconstructing atmospheric parameters close to the ground using ECMWF ANALYSES as input and forcing: large statistical sample

This section is about the model reconstruction of the surface layer meteorological parameters. The main goal of the work package was to enrich the statistical sample and verify if the good preliminary results obtained above Cerro Paranal and Cerro Armazones [52] could be confirmed or not. For Cerro Paranal we could collect and investigate a rich homogeneous statistical sample of 129 nights uniformly distributed in different years (2007, 2010 and 2011). For Cerro Armazones the situation was more complicate. Indeed measurements done at Armazones have bene performed by different Institutions (ESO, TMT) using different instrumentation and covering different years. It was therefore not possible to perform for Armazones the same analysis done at Paranal on the same sample of nights. We decided therefore to consider for Armazones, two samples of nights. The first one done by 42 nights of the year 2007 with measurements done by the TMT. The second one done by 53 nights in the 2010 and 2011 years with measurements done by ESO. The samples are not as rich as that of Paranal but we could verify if instrumentation of ESO and TMT was consistent. At the end of Phase A indeed, we had observed that the temperature reconstructed by the model at 2m above Armazones showed a slightly larger discrepancy versus observation than what happened at Paranal. The validation of the model on samples of nights in which different instrumentation was used permitted us to conclude if the reason of the slightly different results obtained above Paranal and Armazones was due to the model or to the instrumentation. The conclusion of this analysis tells us that that are no evident problems in the instrumentation. We would like to achieve in the next future a sample as rich as that of Paranal, however results obtained with these two sample of 42 and 53 nights tell us that the model performances are very good also for the site of Cerro Armazones.

1.1 Cerro Paranal - 129 nights in 2007, 2010 and 2011 - Lascaux et al., 2015, MNRAS

An extensive study (focused on the wind speed, the wind direction and the temperature) and applied to 129 nights distributed on 2007, 2010 and 2011 has been summarized in **Lascaux, F., Masciadri, E., Fini, L., MNRAS, 2015, 449, 1664** [53]. We refer the reader to this paper for details. We included in the report only those elements not treated in the paper.

More precisely we treat here results obtained for the relative humidity. This parameter indeed could not be treated as the others.

In this part of Chile the weather is particularly dry, the relative humidity (RH) in the surface layer is typically below 30%. The frequency of the nights with a relative humidity above 80%, level at which the dome of the telescope has to be closed and observations are not allowed, is definitely very low (typically less than 5 nights for year). In all the other nights the RH does not really represent a critical issue in terms of scheduling of observations because the RH value is not high enough to affect the observations. The study of the relative humidity close to the ground is therefore not very critical and important for telescopes in this region. Also it has been observed in occasion of the TMT site characterization in this region (T. Travouillon, private communication), that the reliability of the relative humidity measurements, when values are so low, can hardly be assured. This makes difficult (and mostly useless) to investigate the model performances in reconstructing the RH on the same sample of nights selected for the analysis of the other parameters. A more interesting analysis might be to check the model performances in reconstructing the RH values in those few nights in each year where RH is higher than the threshold imposing to close the dome of the telescope. We refer the read to Annex of Lascaux et al., 2015 [53] paper for this analysis of the model performances in reconstructing the RH in which 13 nights in which the observed RH was particularly strong (close to 100%). The conclusion of that study tells us that the model reconstructs in a very satisfactory way the RH under this conditions.

Here, the 13 nights with very strong observed values for the RH were added to the sample of 129 nights (see Table 109) for a total of 142 nights. This was done to investigate the ability of the model to discriminate between nights with low and strong RH.

1.1.1 Relative humidity - Scattered plots

Fig. 1 displays the scattered plots of the model output relative humidity against the observed relative humidity, for Cerro Paranal, at 2 m and 30 m. Table 1 reports the values of the bias, the RMSE and the σ of the relative humidity for the 142 nights sample only (the relative humidity was not investigated in the Phase A report n. E-TRE-INA-245-0001, that is for the original 20 nights sample). From Fig.1 we can see that, when the observed RH is $< 20\%$ (i.e. most of time) the model always predicts a small value of RH even if in general it overestimates a little bit the observed one. However the important thing that we can retrieve from this figure in this context is that the model well discriminates statistically the small and the large RH values.

	RH (%)	
PARANAL	142 nights	
ΔX = 500 m	2 m	30 m
BIAS	8.6	9.4
RMSE	16	16
σ	13.6	13

Table 1: Near surface relative humidity **bias**, **RMSE** and bias-corrected RMSE σ (Meson-NH with the standard configuration - maximum ΔX = 500 m - minus Observations), at Cerro Paranal. For the specific case of the relative humidity, 13 nights with very strong observed values for the RH (close to 100%), were added to the sample (for a total of 142 nights) of the simulated nights.

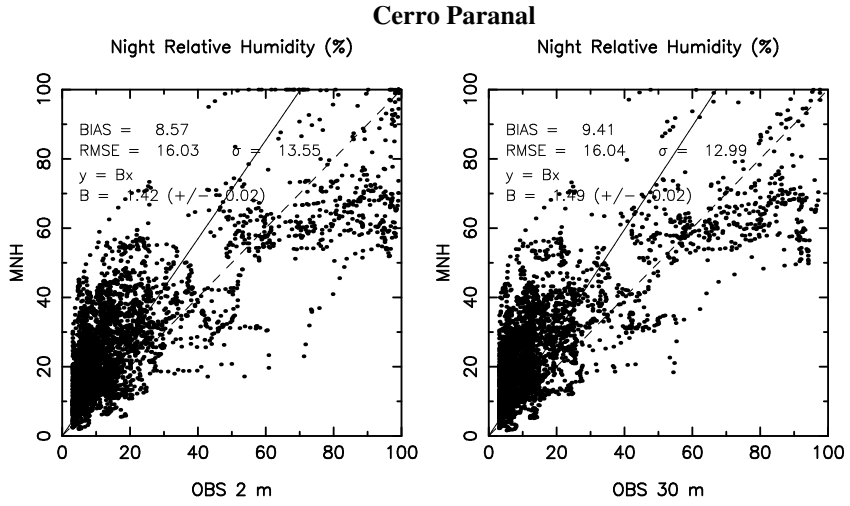

Figure 1: Scattered plot of Meso-NH **relative humidity** against observations, at 2 m and 30 m at **Cerro Paranal**, with the ΔX = 500 m configuration. For the specific case of the relative humidity, 13 nights with very strong observed values for the RH (close to 100%), were added to the sample (for a total of 142 nights) of the simulated nights.

1.1.2 Relative Humidity - Contingency tables

We report here the contingency tables (see the Phase A report or Lascaux et al., 2015[53] for a complete description of the contingency tables). The median, the first and third tertiles of the RH computed on the period 2006-2012 at 2 m and 30 m are respectively (12%, 9%, 18%) and (11%, 8%, 16%). These values are extremely low and it is therefore not useful to use these value as thresholds of the contingency tables. As we discussed

previously what is important is to verify if the model well distinguishes the low RH (a reasonable value is RH $< 30\%$) from the strong RH (a reasonable value is RH $> 60\%$). Tables 2 and Table 3 tells us that the all the PODs (1,2,3) calculated at 2 m and 30 m are very good. If the value of the threshold of the POD_3 is increased and from 60% we pass to 66% or even 70% (from Tables 4 to 7 for 2 m and 30 m) we can see that the ability of the model in isolating high RH decreases monotonically. This tells us that the model ability in reconstructing RH above Paranal is good in the sense that it can easily reconstruct a RH $> 60\%$. However it is more difficult to discriminate between strong values (for example 70 and 90 %).
In Lascaux et al. (2015)[53] are shown the temporal evolution of the observed and simulated RH all along the night for all the individual 13 nights in which the RH overcame the 80% threshold. In all cases the model could reconstruct a strong RH value.

		OBSERVATIONS		
	C. Paranal - 2 m	$RH < 30\%$	$30\% < RH < 60\%$	$RH > 60\%$
MODEL	$RH < 30\%$	2393	29	3
	$30\% < RH < 60\%$	775	208	98
	$RH > 60\%$	12	55	256

Total points = 3829; PC=74.6%; EBD=0.4%
POD_1=75.2%; POD_2=71.2%; POD_3=71.7%

Table 2: 3×3 contingency table for the RH during the night, at 2 m a.g.l. at Cerro Paranal. We use the Meso-NH ΔX = 500 m configuration. The threshold of POD_3 is 60%.

		OBSERVATIONS		
	C. Paranal - 30 m	$RH < 30\%$	$30\% < RH < 60\%$	$RH > 60\%$
MODEL	$RH < 30\%$	2320	20	0
	$30\% < RH < 60\%$	717	203	92
	$RH > 60\%$	12	72	220

Total points = 3656; PC=75.0%; EBD=0.3%
POD_1=76.2%; POD_2=68.8%; POD_3=70.5%

Table 3: 3×3 contingency table for the RH during the night, at 30 m a.g.l. at Cerro Paranal. We use the Meso-NH ΔX = 500 m configuration. The threshold of POD_3 is 60%.

		OBSERVATIONS		
	C. Paranal - 2 m	$RH < 30\%$	$30\% < RH < 66\%$	$RH > 66\%$
MODEL	$RH < 30\%$	2393	30	2
	$30\% < RH < 66\%$	778	262	150
	$RH > 66\%$	9	28	177

Total points = 3829; PC=73.9%; EBD=0.3%
POD_1=75.2%; POD_2=81.9%; POD_3=54%

Table 4: 3×3 contingency table for the RH during the night, at 2 m a.g.l. at Cerro Paranal. We use the Meso-NH $\Delta X = 500$ m configuration. The threshold of POD_3 is 66%.

		OBSERVATIONS		
	C. Paranal - 30 m	$RH < 30\%$	$30\% < RH < 66\%$	$RH > 66\%$
MODEL	$RH < 30\%$	2320	20	0
	$30\% < RH < 66\%$	721	275	125
	$RH > 66\%$	8	48	139

Total points = 3656; PC=74.8%; EBD=0.2%
POD_1=76.0%; POD_2=80.2%; POD_3=52.6%

Table 5: 3×3 contingency table for the RH during the night, at 30 m a.g.l. at Cerro Paranal. We use the Meso-NH $\Delta X = 500$ m configuration. The threshold of POD_3 is 66%.

		OBSERVATIONS		
	C. Paranal - 2 m	$RH < 30\%$	$30\% < RH < 70\%$	$RH > 70\%$
MODEL	$RH < 30\%$	2393	30	2
	$30\% < RH < 70\%$	780	286	183
	$RH > 70\%$	7	32	116

Total points = 3829; PC=73.0%; EBD=0.2%
POD_1=72.2%; POD_2=82.2%; POD_3=38.5%

Table 6: 3×3 contingency table for the RH during the night, at 2 m a.g.l. at Cerro Paranal. We use the Meso-NH $\Delta X = 500$ m configuration. The threshold of POD_3 is 70%.

		OBSERVATIONS		
	C. Paranal - 30 m	$RH < 30\%$	$30\% < RH < 70\%$	$RH > 70\%$
MODEL	$RH < 30\%$	2842	59	0
	$30\% < RH < 70\%$	289	176	149
	$RH > 70\%$	7	48	86

Total points = 3656; PC=74.1%; EBD=0.2%
POD_1=76.1%; POD_2=81.4%; POD_3=36.6%

Table 7: 3×3 contingency table for the RH during the night, at 30 m a.g.l. at Cerro Paranal. We use the Meso-NH ΔX = 500 m configuration. The threshold of POD_3 is 70%.

1.2 Cerro Armazones - 42 nights in 2007

In this section we consider only the 42 nights in 2007.

1.2.1 Scattered plots

Fig. 2 displays the scattered plots of the model output temperature against the observed temperature, for Cerro Armazones, at 2 m, 11 m, 20 m and 28 m. Fig. 3 and Fig. 4 display the scattered plots of the model output wind speed against the observed wind speed, for Cerro Armazones, at 2 m, 11 m, 20 m and 28 m. Fig. 5 displays the scattered plots of the model output wind direction against the observed wind direction, for Cerro Armazones, at 2 m, 11 m, 20 m and 28 m. The corresponding values for the bias, the RMSE (and the RMSE_{rel} for the wind direction), and the σ, of the temperature, the wind speed (with both ΔX=500 m and ΔX=100 m configurations) and the wind direction (with and without discarding wind speed inferior to 3 $\text{m}\cdot\text{s}^{-1}$), are reported in Tables 8, 9, 10, 11, 12, respectively, and compared to the values of the original 20 nights sample.

The results for the temperature are excellent. The bias remains very small between 0.10°C and 0.64°C in absolute value, and the RMSE is always inferior to 1.04°C at every levels. The bias at 2 m is still slightly larger than at Paranal but this difference is definitely not relevant. Moreover we developed a method to eliminate this problem with an additive bias coefficient for the calculation of the contingency tables. In conclusion, these results are comparable to the results obtained with the original 20 nights sample.

Concerning the wind speed, the bias and the RMSE are slightly higher with this sampel than with the 20 nights sample. Now with the ΔX=100 m configuration the bias is between -1.12 $\text{m}\cdot\text{s}^{-1}$ and -2.57 $\text{m}\cdot\text{s}^{-1}$ (the forecasted wind speed is always inferior to the observations), and the RMSE is in the range [2.89,3.82] $\text{m}\cdot\text{s}^{-1}$. The σ for the 2 samples are comparable. In any case, even if the gain on the bias at 2 m using the 100 m horizontal resolution seems to be less efficient at Armazones with respect to Paranal, introducing the multiplicative corrector coefficient in the calculation of the contingency tables, the problem is basically removed.

The wind direction is confirmed to be well predicted by the model, with a RMSE_{rel} always inferior to 20%.

	Absolute temperature (^{o}C)							
ARMAZONES	42 nights				20 nights			
Δ X =500 m	2 m	11 m	20 m	28 m	2 m	11 m	20 m	28 m
BIAS	0.64	-0.10	-0.15	-0.21	0.76	0.06	0.04	0.02
RMSE	1.04	0.86	0.92	0.97	1.06	0.80	0.84	0.86
σ	0.82	0.85	0.91	0.95	0.74	0.80	0.84	0.86

Table 8: Near surface temperature **bias**, **RMSE** and bias-corrected RMSE σ (Meson-NH minus Observations), at Cerro Armazones. Left: for the sample of 42 nights of 2007. Right: with the sample of 20 nights from Phase A

	Wind speed ($m \cdot s^{-1}$)							
ARMAZONES	42 nights				20 nights			
Δ X =500 m	2 m	11 m	20 m	28 m	2 m	11 m	20 m	28 m
BIAS	-5.44	-4.35	-2.56	-2.03	-3.59	-2.91	-1.40	-0.92
RMSE	6.80	5.53	3.86	3.48	4.52	3.97	2.78	2.54
σ	4.08	3.41	2.89	2.83	2.75	2.70	2.40	2.37

Table 9: Near surface wind speed **bias**, **RMSE** and bias-corrected RMSE σ (Meson-NH minus Observations), at Cerro Armazones, with the Δ X =500 m configuration. Left: for the sample of 42 nights of 2007. Right: with the sample of 20 nights from Phase A.

	Wind speed ($m \cdot s^{-1}$)							
ARMAZONES	42 nights				20 nights			
Δ X =100 m	2 m	11 m	20 m	28 m	2 m	11 m	20 m	28 m
BIAS	-2.57	-2.16	-1.32	-1.12	-1.50	-1.41	-0.68	-0.42
RMSE	3.82	3.39	2.89	2.91	2.62	2.75	2.46	2.55
σ	2.83	2.61	2.57	2.69	2.15	2.36	2.36	2.52

Table 10: Near surface wind speed **bias**, **RMSE** and bias-corrected RMSE σ (Meson-NH minus Observations), at Cerro Armazones, with the Δ X =100 m configuration. Left: for the sample of 42 nights of 2007.Right: with the sample of 20 nights from Phase A.

	Wind direction (^{o})							
ARMAZONES	42 nights				20 nights			
Δ X =500 m	2 m	11 m	20 m	28 m	2 m	11 m	20 m	28 m
BIAS	9.4	12.5	8.9	2.6	6.7	10.3	6.7	-0.8
RMSE	50.0	45.9	44.8	44.1	50.5	43.8	42.9	41.5
$RMSE_{rel}$	27.8%	25.5%	24.9%	24.5%	28.1%	24.3%	23.8%	23.1%
σ	49.1	44.2	43.9	44.0	50.1	42-6	42.4	41.5

Table 11: Near surface wind speed **bias**, **RMSE**, bias-corrected RMSE σ and relative RMSE (Meson-NH minus Observations), at Cerro Armazones, with the Δ X =500 m configuration. Left: for the sample of 42 nights of 2007. Right: for the sample of 20 nights from Phase A.

	Wind direction (^{o})							
ARMAZONES	42 nights				20 nights			
Δ X =500 m	2 m	11 m	20 m	28 m	2 m	11 m	20 m	28 m
BIAS	12.7	14.7	10.6	4.1	10.2	12.0	8.4	2.1
RMSE	34.9	36.0	33.9	31.4	37.7	35.8	32.6	30.4
$RMSE_{rel}$	19.4%	20.0%	18.8%	17.4%	20.9%	19.9%	18.1%	16.9%
σ	32.5	32.9	32.2	31.1	36.3	33.7	31.5	30.3

Table 12: Near surface wind speed **bias**, **RMSE**, bias-corrected RMSE σ and relative RMSE (Meson-NH minus Observations), at Cerro Armazones, with the Δ X =500 m configuration. Left: for the sample of 42 nights of 2007. Right: for the sample of 20 nights from Phase A. Data with wind speed inferior to 3 $m \cdot s^{-1}$ have been discarded.

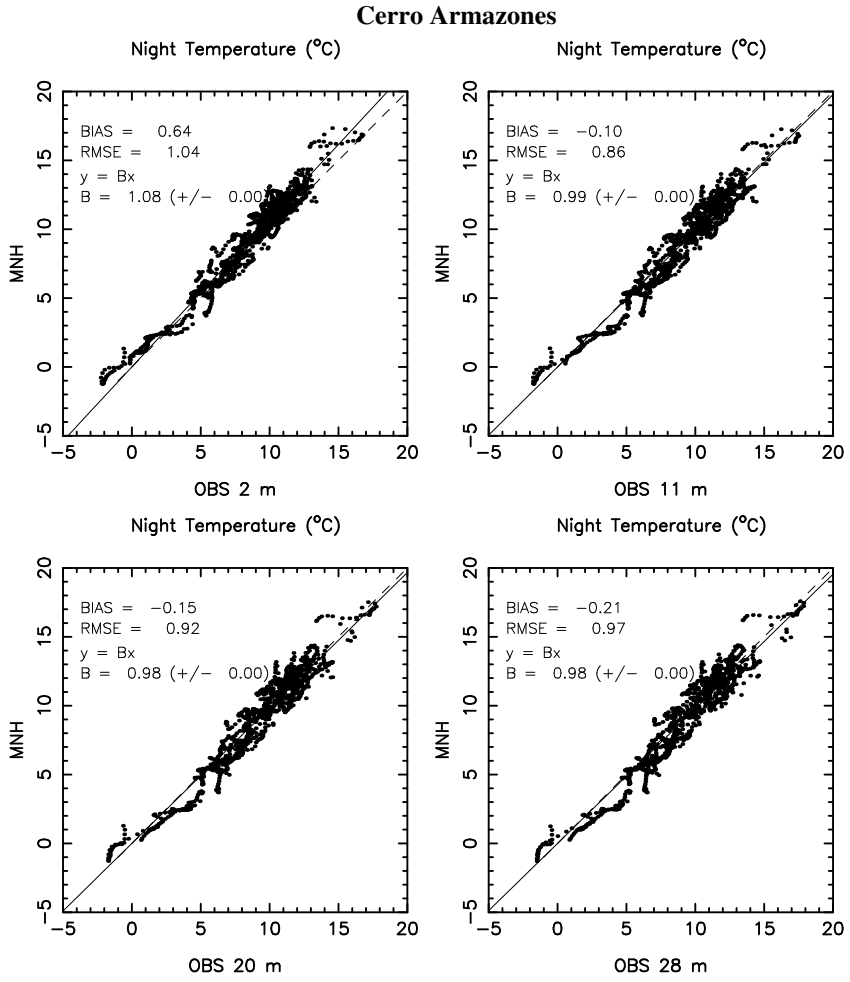

Figure 2: Scattered plot of Meso-NH **temperature** against observations, at 2 m, 11 m, 20 m and 28 m at **Cerro Armazones**, with the $\Delta X = 500$ m configuration.

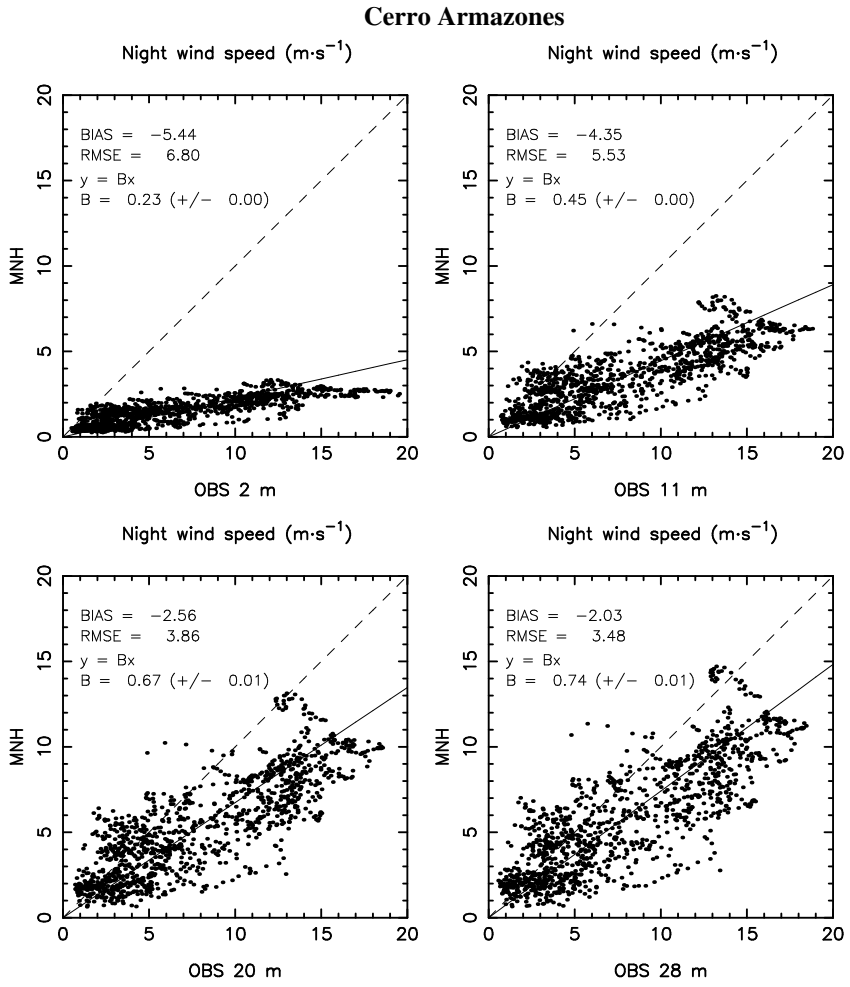

Figure 3: Scattered plot of Meso-NH **wind speed** against observations, at 2 m, 11 m, 20 m and 28 m at **Cerro Armazones**, with the $\Delta X = 500$ m configuration.

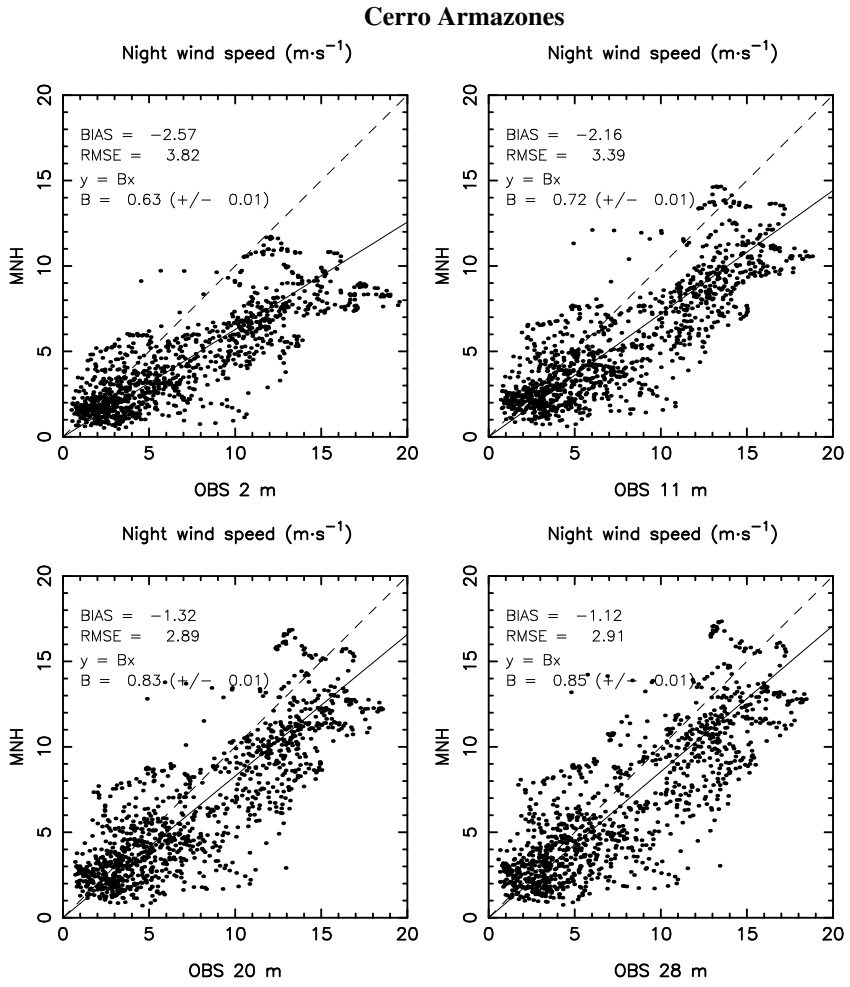

Figure 4: Scattered plot of Meso-NH **wind speed** against observations, at 2 m, 11 m, 20 m and 28 m at **Cerro Armazones**, with the $\Delta X = 100$ m configuration.

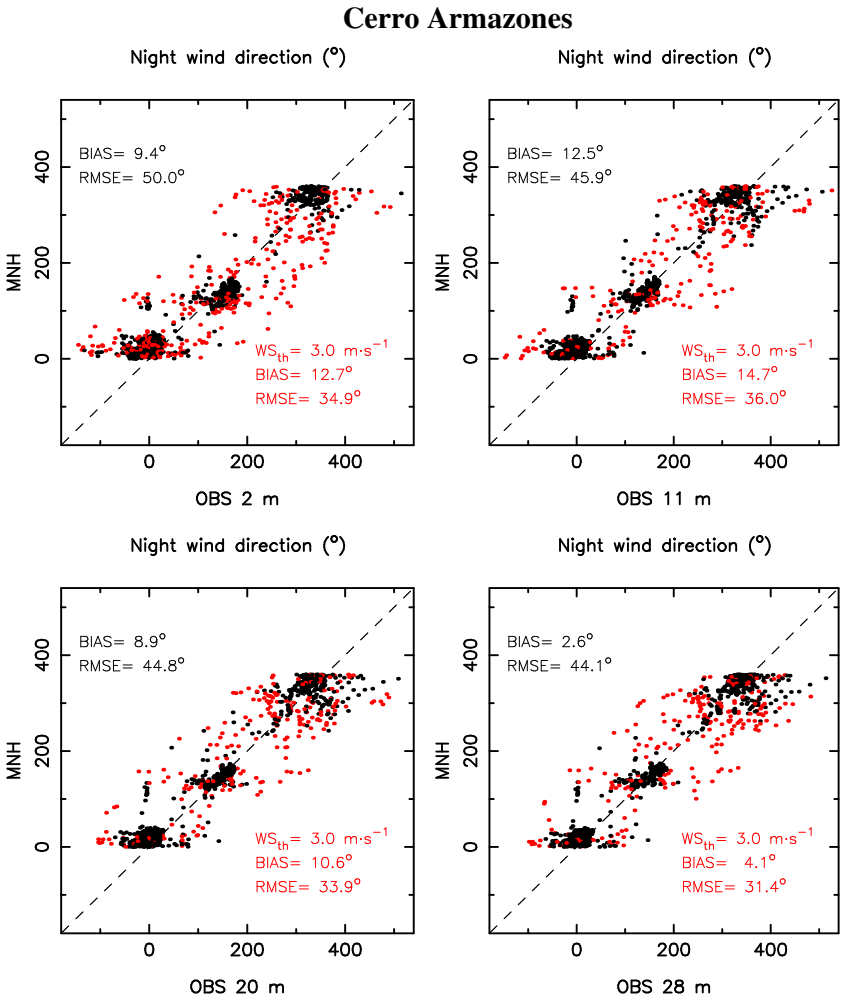

Figure 5: Scattered plot of Meso-NH **wind direction** against observations, at 2 m, 11 m, 20 m and 28 m at **Cerro Armazones**, with the $\Delta X = 500$ m configuration.

1.2.2 Temporal evolutions

In this section are reported the temporal evolutions of the averaged, the bias and the RMSE for the temperature, the wind speed and the wind direction near the surface at Cerro Armazones for the 42 nights sample (Fig. 6 for the temperature, Fig. 7 for the wind speed with the ΔX = 500 m configuration, Fig. 8 for the wind speed with the ΔX = 100 m configuration, Fig. 9 for the wind direction).

For the temperature, the bias and RMSE are confirmed to be excellent. During the night, he bias is below 0.5°C at levels 11 m, 20 m and 28 m, and between 0.5°C and 0.9°C at level 2 m. The RMSE is equal to, or slightly superior to, 1°C at all levels.

For the wind speed (with the ΔX = 100 m configuration), the bias during the night is between 2 m·s^{-1} and 3 m·s^{-1}. The RMSE is between 2.5 m·s^{-1} and 4 m·s^{-1}, depending in the level. As said previously, this residual RMSE can be eleiminated with the multiplicative coefficient of correction.

The average wind direction is well predicted. The temporal evolution of the RMSE during the night is between 40° and 50°, even better than for the original 20 nights sample. No filter has been applied for this computation, and so one can expect much better values when filtering the low level winds.

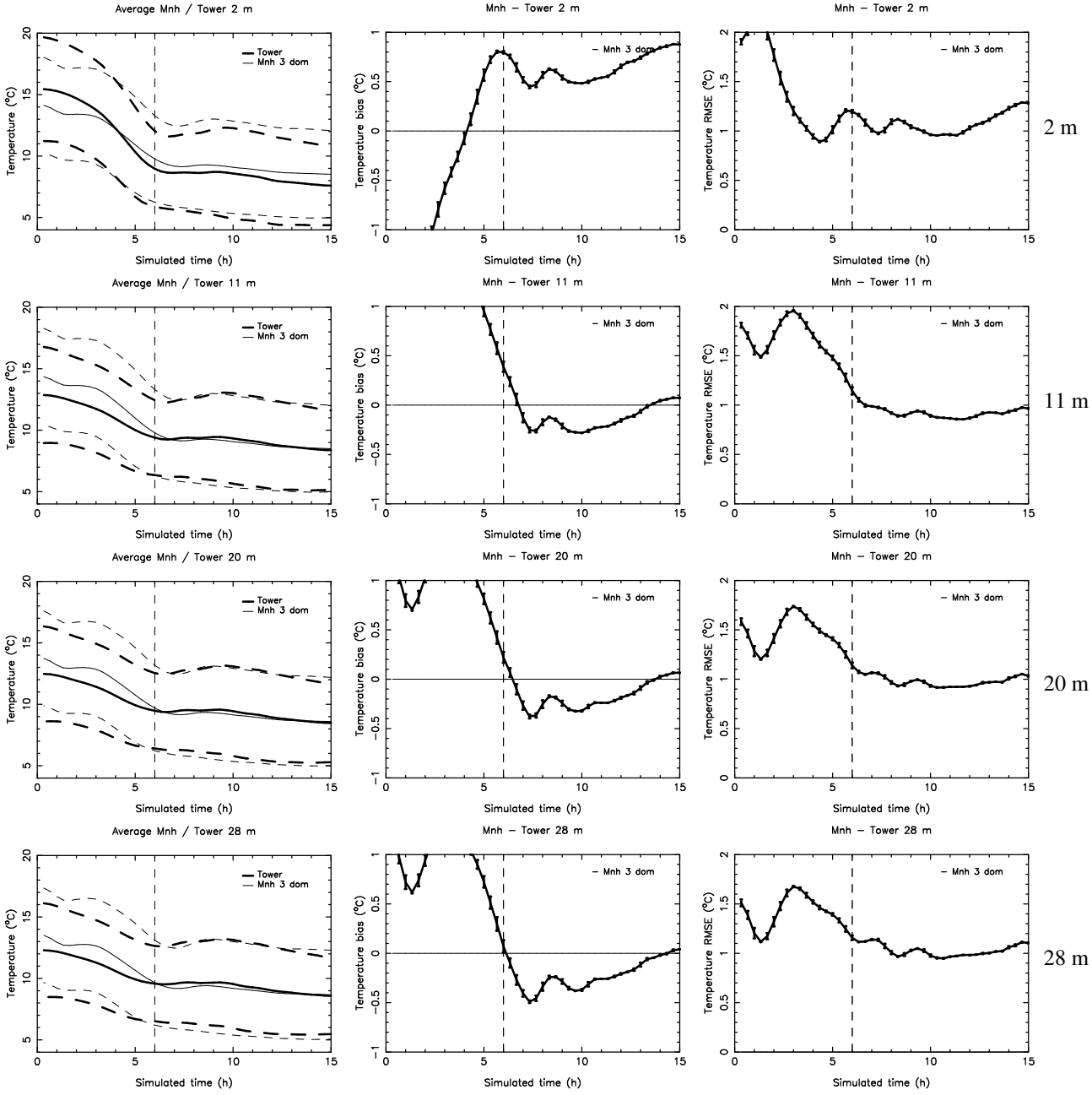

Figure 6: Temporal evolution of the **absolute temperature average** (the bold line is the observation average and the thin line is Meso-NH average), **bias** (Mnh - Observations) and **RMSE** at **Cerro Armazones**, at 2 m, 11 m, 20 m and 28 m. The x-axis represents the time from the beginning of the simulation (00 h is 18 UT of the day before, 06 h is 00 UT, and 15 h is 09 UT). The nights starts at around 06 h (00 UT - 20 LT) and is delimited by the vertical dashed line. Meso-NH is with the $\Delta X = 500$ m configuration. The error bars represent $\pm$ the standard deviation.

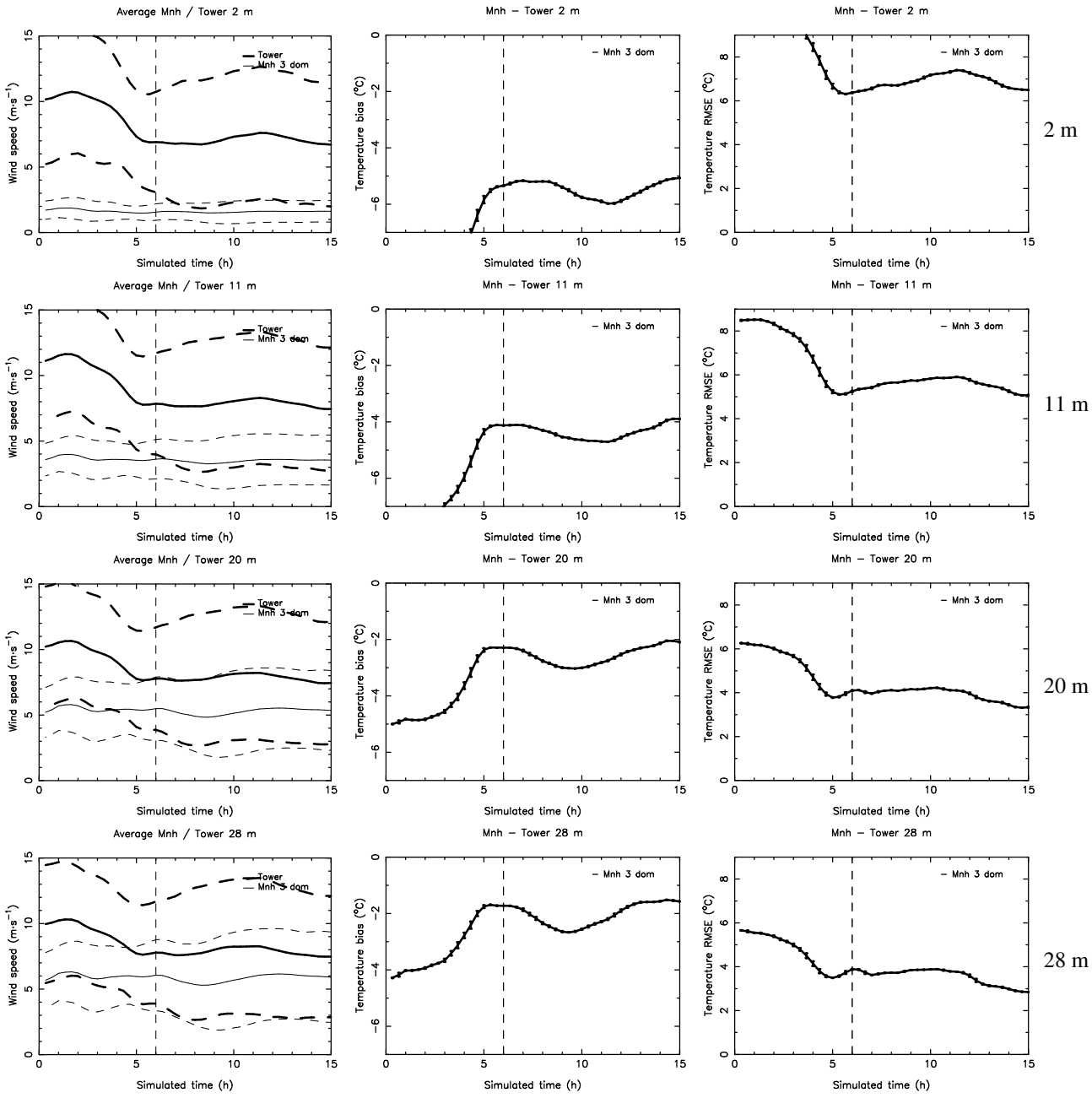

Figure 7: Same as Fig. 6 but for the **wind speed** at **Cerro Paranal** (top: at 10 m; bottom: at 30 m). Meso-NH is used with $\Delta X = 500$ m configuration.

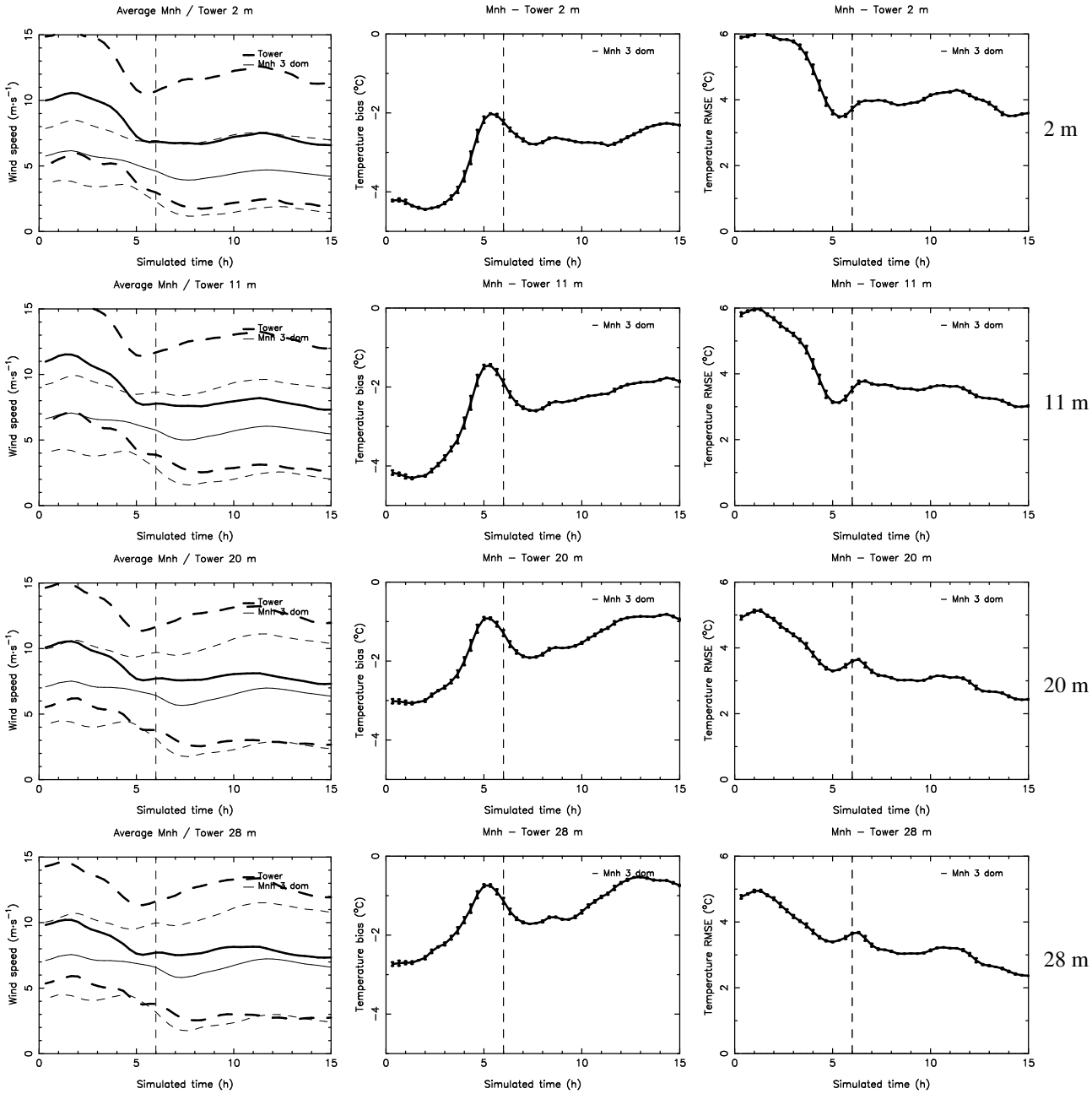

Figure 8: Same as Fig. 7 but Meso-NH is used in the $\Delta X = 100$ m configuration.

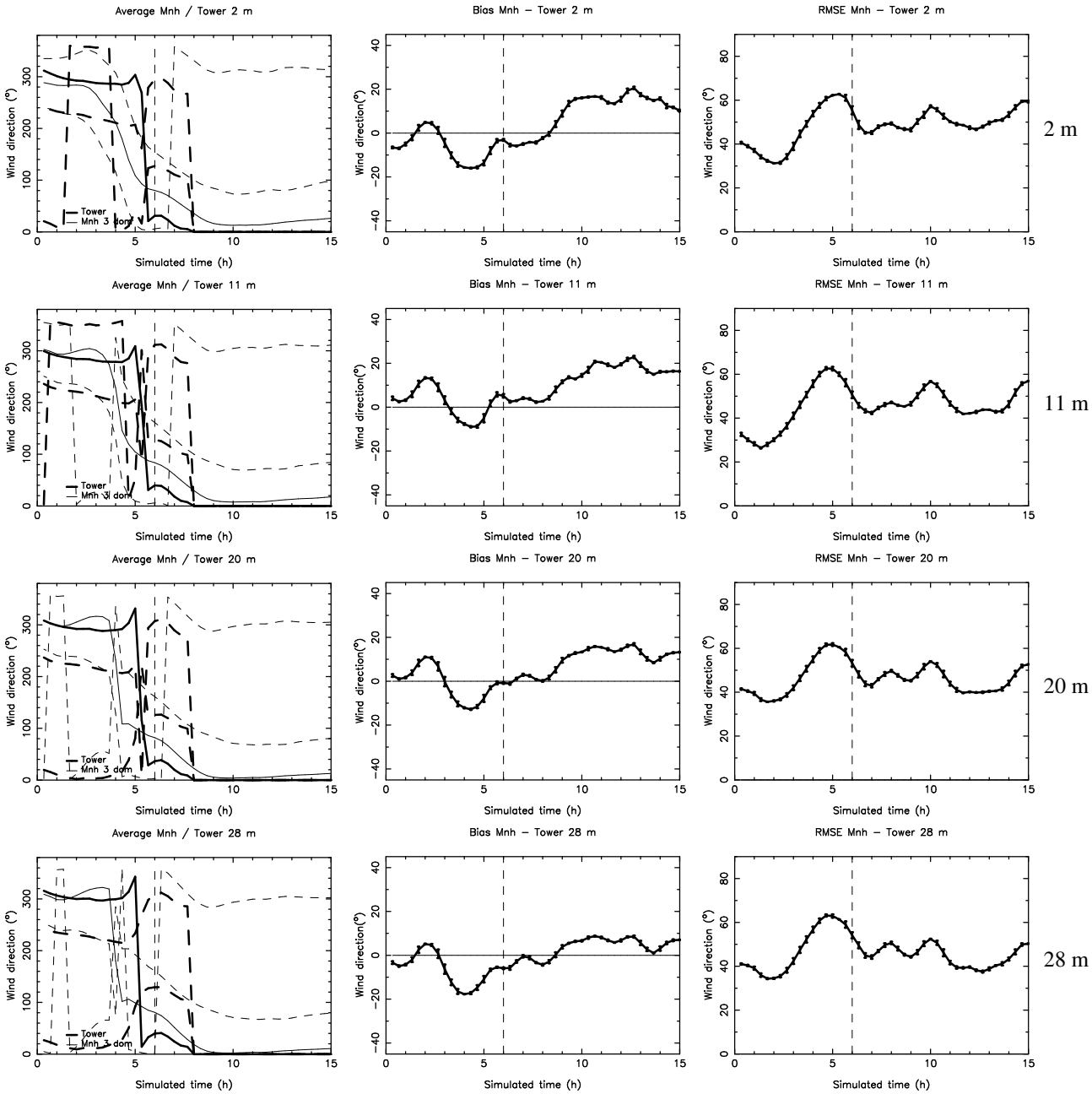

Figure 9: Same as Fig. 6 but for the **wind direction** at **Cerro Paranal** (top: at 10 m; bottom: at 30 m).

1.2.3 Contingency tables

In this section, we have constructed contingency tables for the surface meteorological parameters.

TEMPERATURE
Tables 13, 14, 15, 16, 17 are for the temperature. The results show that the model is able to predict with a very good accuracy an estimation of the surface temperature. The POD of the lowest, and highest temperatures, are almost perfect (close to 100%), and the POD of the temperature in-between is good (always higher than 51.5%). We show that at 2 m it can be improved from 51.5% to 66.1% (Table 14) at the first level if we correct the model values with the coefficient of correction evidenced in the previous sections, without alterating the other PODs. PCs are all over 85%.

Division by tertiles (climatology) C. Armazones - 2 m		**OBSERVATIONS** $T < 7°C$	$7°C < T < 9°C$	$T > 9°C$
MODEL	$T < 7°C$	302	20	0
	$7°C < T < 9°C$	30	118	4
	$T > 9°C$	14	91	568

Total points = 1134; PC=87.1%; EBD=0.1%
POD_1=90.7%; POD_2=51.5%; POD_3=99.3%

Table 13: 3×3 contingency table for the absolute temperature during the night, at 2 m a.g.l. at Cerro Armazones, for the year 2007 (42 nights considered). We use the Meso-NH ΔX = 500 m configuration.

Division by tertiles (climatology) C. Armazones - 2 m		**OBSERVATIONS** $T < 7°C$	$7°C < T < 9°C$	$T > 9°C$
MODEL	$T < 7°C$	296	65	0
	$7°C < T < 9°C$	13	193	40
	$T > 9°C$	0	34	493

Total points = 1134; PC=86.6%; EBD=0.0%
POD_1=95.8%; POD_2=66.1%; POD_3=92.5%

Table 14: 3×3 contingency table for the absolute temperature during the night, at 2 m a.g.l. at Cerro Armazones, for the year 2007 (42 nights considered). We use the Meso-NH ΔX = 500 m configuration and we correct the Meso-NH output with the well identified bias of ∼0.6°C between observation and simulation at 2 m.

Division by tertiles (climatology) C. Armazones - 11 m		**OBSERVATIONS** $T < 7.5°C$	$7.5°C < T < 10°C$	$T > 10°C$
MODEL	$T < 7.5°C$	296	65	0
	$7.5°C < T < 10°C$	13	193	40
	$T > 10°C$	0	34	493

Total points = 1134; PC=86.7%; EBD=0.0%
POD_1=95.8%; POD_2=66.1%; POD_3=92.5%

Table 15: 3×3 contingency table for the absolute temperature during the night, at 11 m a.g.l. at Cerro Armazones, for the year 2007 (42 nights considered). We use the Meso-NH ΔX = 500 m configuration.

Division by tertiles (climatology) C. Armazones - 20 m		**OBSERVATIONS** $T < 7.5°C$	$7.5°C < T < 10°C$	$T > 10°C$
MODEL	$T < 7.5°C$	286	74	0
	$7.5°C < T < 10°C$	15	193	33
	$T > 10°C$	0	33	500

Total points = 1134; PC=86.3%; EBD=0.0%
POD_1=95.0%; POD_2=64.3%; POD_3=93.8%

Table 16: 3×3 contingency table for the absolute temperature during the night, at 20 m a.g.l. at Cerro Armazones, for the year 2007 (42 nights considered). We use the Meso-NH ΔX = 500 m configuration.

Division by tertiles (climatology) C. Armazones - 28 m		**OBSERVATIONS** $T < 8°C$	$8°C < T < 10°C$	$T > 10°C$
MODEL	$T < 8°C$	323	85	0
	$8°C < T < 10°C$	16	135	37
	$T > 10°C$	0	32	506

Total points = 1134; PC=85.0%; EBD=0.0%
POD_1=95.2%; POD_2=53.6%; POD_3=93.2%

Table 17: 3×3 contingency table for the absolute temperature during the night, at 28 m a.g.l. at Cerro Armazones, for the year 2007 (42 nights considered). We use the Meso-NH ΔX = 500 m configuration.

WIND SPEED

Tables 18, 19, 20, 21 are for the wind speed. For the weakest and the strongest winds at 2 m (POD_1 and POD_3), the results are very good, with PODs between 66.5% and 85.5%. This is particularly useful for the detection of the strongest winds, that can prevent from the opening of the dome. The POD_2 (intermediate values) are harder to predict, with values between 39.6% and 52.3%, depending on the level, but still better than a random forecast (which would have PODs equal to 33%). For heights $\geq$ 10 m the POD_1 and POD_3 are basically always larger than 70%.

Division by tertiles (climatology) C. Armazones - 2 m		**OBSERVATIONS** $WS < 5\ m{\cdot}s^{-1}$	$5\ m{\cdot}s^{-1} < WS < 9.5\ m{\cdot}s^{-1}$	$WS > 9.5\ m{\cdot}s^{-1}$
MODEL	$WS < 5\ m{\cdot}s^{-1}$	435	100	10
	$5\ m{\cdot}s^{-1} < WS < 9.5\ m{\cdot}s^{-1}$	77	116	115
	$WS > 9.5\ m{\cdot}s^{-1}$	0	6	248

Total points = 1107; PC=72.2%; EBD=0.9%
POD_1=84.9%; POD_2=52.3%; POD_3=66.5%

Table 18: 3×3 contingency table for the wind speed during the night, at 2 m a.g.l. at Cerro Armazones. We use the Meso-NH ΔX = 100 m configuration with the wind corrected by the multiplicative bias.

Division by tertiles (climatology) C. Armazones - 11 m		**OBSERVATIONS** $WS < 6\ m{\cdot}s^{-1}$	$6\ m{\cdot}s^{-1} < WS < 10.5\ m{\cdot}s^{-1}$	$WS > 10.5\ m{\cdot}s^{-1}$
MODEL	$WS < 6\ m{\cdot}s^{-1}$	407	97	4
	$6\ m{\cdot}s^{-1} < WS < 10.5\ m{\cdot}s^{-1}$	93	87	73
	$WS > 10.5\ m{\cdot}s^{-1}$	12	27	307

Total points = 1107; PC=72.4%; EBD=1.4%
POD_1=79.5%; POD_2=41.2%; POD_3=79.9%

Table 19: 3×3 contingency table for the wind speed during the night, at 11 m a.g.l. at Cerro Armazones. We use the Meso-NH ΔX = 100 m configuration with the wind corrected by the multiplicative bias.

Division by tertiles (climatology) C. Armazones - 20 m		**OBSERVATIONS** $WS < 6\ m{\cdot}s^{-1}$	$6\ m{\cdot}s^{-1} < WS < 10.5\ m{\cdot}s^{-1}$	$WS > 10.5\ m{\cdot}s^{-1}$
MODEL	$WS < 6\ m{\cdot}s^{-1}$	447	106	8
	$6\ m{\cdot}s^{-1} < WS < 10.5\ m{\cdot}s^{-1}$	75	81	104
	$WS > 10.5\ m{\cdot}s^{-1}$	1	14	271

Total points = 1107; PC=72.2%; EBD=0.8%
POD_1=85.5%; POD_2=40.3%; POD_3=70.8%

Table 20: 3×3 contingency table for the wind speed during the night, at 20 m a.g.l. at Cerro Armazones. We use the Meso-NH ΔX = 100 m configuration with the wind corrected by the multiplicative bias.

Division by tertiles (climatology) C. Armazones - 28 m		**OBSERVATIONS** $WS < 6\ m{\cdot}s^{-1}$	$6\ m{\cdot}s^{-1} < WS < 11\ m{\cdot}s^{-1}$	$WS > 11\ m{\cdot}s^{-1}$
MODEL	$WS < 6\ m{\cdot}s^{-1}$	437	104	4
	$6\ m{\cdot}s^{-1} < WS < 11\ m{\cdot}s^{-1}$	85	95	99
	$WS > 11\ m{\cdot}s^{-1}$	1	41	241

Total points = 1107; PC=69.8%; EBD=0.5%
POD_1=83.6%; POD_2=39.6%; POD_3=70.1%

Table 21: 3×3 contingency table for the wind speed during the night, at 28 m a.g.l. at Cerro Armazones. We use the Meso-NH ΔX = 100 m configuration with the wind corrected by the multiplicative bias.

WIND DIRECTION

Tables 22, 23, are for the wind direction. The numbers vary a little with respect to Lascaux et al. (2015)[53] treating Paranal. The model reconstructs in a very good way (POD(N) order of 90% and POD(SE) order of 85%) the wind directions for those direction from which the wind flows more frequently i.e. the North and South-East (see Fig.10). The POD(W) is some how low for the West direction but the wind basically never flows from this direction.

		OBSERVATIONS			
C. Armazones - all levels		N-E	S-E	S-W	N-W
MODEL	N-E	583	24	5	357
	S-E	26	350	23	27
	S-W	6	22	32	10
	N-W	107	15	38	500

Total points = 4194; PC=68.9%; EBD=2.5%
$POD(NE)$=80.7%; $POD(SE)$=85.2%
$POD(SW)$=32.7%; $POD(NW)$=55.9%

Table 22: 4×4 contingency table for the wind direction α during the night, at 2 m, 11 m, 20 m and 28 m a.g.l. at Cerro Armazones. We use the Meso-NH ΔX = 500 m configuration. We filter out the observed wind inferior to 3 $m{\cdot}s^{-1}$. NE corresponds to $0° < \alpha < 90°$; SE corresponds to $90° < \alpha < 180°$; SW corresponds to $180° < \alpha < 270°$; NW corresponds to $270° < \alpha < 360°$.

		OBSERVATIONS			
C. Armazones - all levels		N	E	S	W
MODEL	N	1246	64	13	155
	E	22	102	40	6
	S	9	44	235	8
	W	85	11	16	69

Total points = 4194; PC=77.4%; EBD=1.8%
$POD(N)$=91.5%; $POD(E)$=46.2%
$POD(S)$=77.3%; $POD(W)$=29.0%

Table 23: 4×4 contingency table for the wind direction α during the night, at 2 m, 11 m, 20 m and 28 m a.g.l. at Cerro Armazones. We use the Meso-NH ΔX = 500 m configuration. We filter out the observed wind inferior to 3 $m{\cdot}s^{-1}$. N corresponds to $-45° < \alpha < 45°$; E corresponds to $45° < \alpha < 135°$; S corresponds to $135° < \alpha < 225°$; W corresponds to $225° < \alpha < 315°$.

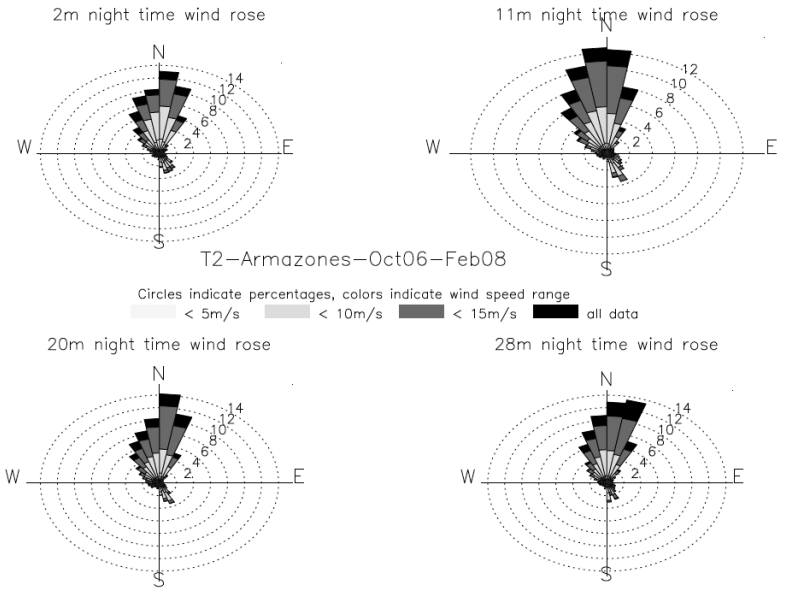

Figure 10: Wind rose at Armazones - Extracted from the TMT "Report on the meteorological condition up to 30 m" http://sitedata.tmt.org/.

1.2.4 Individual nights model performances

In this section we present the analysis done on the model performances in reconstructing the atmospheric parameters, night by night, on the 42 nights sample, at Cerro Armazones. Fig. 11 and Table 24 show the results for the temperature. Fig. 12 and Table 25 show the results for the wind speed. Fig. 13 and Table 26 show the results for the wind direction.

The results (bias, RMSE, bias-corrected RMSE) are summarized in Tables 24, 25, 26, and compared with the original 20 nights sample. The results are very similar between the 20 nights sample and the 42 nights sample, for all parameters. The RMSE for the temperature is in the range [0.76,0.88]°C, the RMSE for the wind speed is in the range [2.25,2.58] $m{\cdot}s^{-1}$, and the RMSE for the wind direction is in the range [21.90,28.50]°, with the filtering of the lowest wind speed (inferior to 3 $m{\cdot}s^{-1}$).

Also in this case, the results might be improved introducing the coefficient of correction as we did for the contingency tables.

Absolute temperature (^{o}C)

	ARMAZONES - 20 nights				ARMAZONES - 42 nights			
	2 m	11 m	20 m	28 m	2 m	11 m	20 m	28 m
BIAS	$0.64^{+1.02}_{+0.46}$	$0.01^{+0.28}_{-0.25}$	$0.05^{+0.37}_{-0.45}$	$0.07^{+0.50}_{-0.58}$	$0.57^{+0.87}_{+0.38}$	$-0.08^{+0.09}_{-0.51}$	$-0.10^{+0.10}_{-0.60}$	$-0.19^{+0.16}_{-0.75}$
RMSE	$0.87^{+1.20}_{+0.72}$	$0.74^{+0.98}_{+0.54}$	$0.77^{+0.98}_{+0.60}$	$0.85^{+1.02}_{+0.66}$	$0.82^{+1.17}_{+0.65}$	$0.76^{+1.04}_{+0.60}$	$0.78^{+1.07}_{+0.62}$	$0.88^{+1.09}_{+0.69}$
σ	$0.51^{+0.58}_{+0.45}$	$0.53^{+0.70}_{+0.47}$	$0.57^{+0.68}_{+0.49}$	$0.61^{+0.64}_{+0.47}$	$0.52^{+0.68}_{+0.39}$	$0.54^{+0.71}_{+0.42}$	$0.56^{+0.71}_{+0.39}$	$0.56^{+0.66}_{+0.42}$

Table 24: Near surface median, **bias**, **RMSE** and **bias-corrected RMSE** σ (Meson-NH minus Observations), of the **temperature** from the single nights values, from the original 20 nights sample on the left, and from the extended 42 nights sample on the right (see Fig. 11). In small fonts, the 1st and 3rd quartiles.

Wind speed ($m{\cdot}s^{-1}$)

	ARMAZONES - 20 nights			
	2 m	11 m	20 m	28 m
BIAS	$-0.99^{-0.38}_{-2.98}$	$-1.08^{-0.19}_{-2.73}$	$-0.55^{+0.17}_{-1.97}$	$-0.10^{+0.68}_{-1.76}$
RMSE	$1.76^{+3.25}_{+1.13}$	$2.11^{+3.22}_{+1.57}$	$2.14^{+2.47}_{+1.43}$	$2.02^{+2.62}_{+1.45}$
σ	$1.01^{+1.38}_{+0.70}$	$1.19^{+1.62}_{+0.93}$	$1.34^{+1.73}_{+1.03}$	$1.42^{+1.82}_{+1.06}$

	ARMAZONES - 42 nights			
	2 m	11 m	20 m	28 m
BIAS	$-2.06^{-0.50}_{-4.35}$	$-2.00^{-0.25}_{-4.13}$	$-1.31^{+0.15}_{-2.94}$	$-1.11^{+0.30}_{-2.49}$
RMSE	$2.25^{+4.50}_{+1.44}$	$2.58^{+4.54}_{+1.68}$	$2.36^{+3.27}_{+1.58}$	$2.35^{+3.39}_{+1.53}$
σ	$1.15^{+1.46}_{+0.81}$	$1.23^{+1.63}_{+0.98}$	$1.33^{+1.73}_{+1.08}$	$1.37^{+1.84}_{+1.15}$

Table 25: Near surface median, **bias**, **RMSE** and **bias-corrected RMSE** σ (Meson-NH minus Observations), of the **wind speed** with the ΔX = 100 m configuration, from the single nights values, from the original 20 nights sample on the top, and from the extended 42 nights sample on the bottom (see Fig. 12). In small fonts, the 1st and 3rd quartiles.

Wind direction (°)

	ARMAZONES - 20 nights			
	2 m	11 m	20 m	28 m
BIAS	$5.76^{+25.77}_{-17.91}$	$5.91^{+22.69}_{-5.13}$	$1.34^{+17.00}_{-5.40}$	$-3.36^{+16.45}_{-12.82}$
RMSE	$28.63^{+46.45}_{+16.42}$	$27.38^{+50.01}_{+16.19}$	$28.28^{+46.43}_{+13.26}$	$27.73^{+43.92}_{+13.99}$
σ	$13.98^{+27.04}_{+10.42}$	$20.06^{+37.66}_{+11.00}$	$17.25^{+34.16}_{+11.18}$	$16.65^{+34.15}_{+11.63}$

	ARMAZONES - 42 nights			
	2 m	11 m	20 m	28 m
BIAS	$10.54^{+26.26}_{-8.76}$	$14.30^{+26.20}_{+0.86}$	$10.28^{+20.30}_{+0.12}$	$4.18^{+16.31}_{-4.52}$
RMSE	$28.19^{+41.90}_{+15.81}$	$28.50^{+45.56}_{+16.70}$	$24.52^{+44.58}_{+13.32}$	$21.90^{+41.09}_{+12.44}$
σ	$13.65^{+22.61}_{+8.45}$	$14.93^{+35.80}_{+7.56}$	$14.08^{+35.23}_{+7.86}$	$13.96^{+33.73}_{+8.23}$

Table 26: Near surface median, **bias**, **RMSE** and **bias-corrected RMSE** σ (Meson-NH minus Observations), of the **wind direction**, from the single nights values, from the original 20 nights sample on the top, and from the extended 42 nights sample on the bottom (see Fig. 13). In small fonts, the 1st and 3rd quartiles.

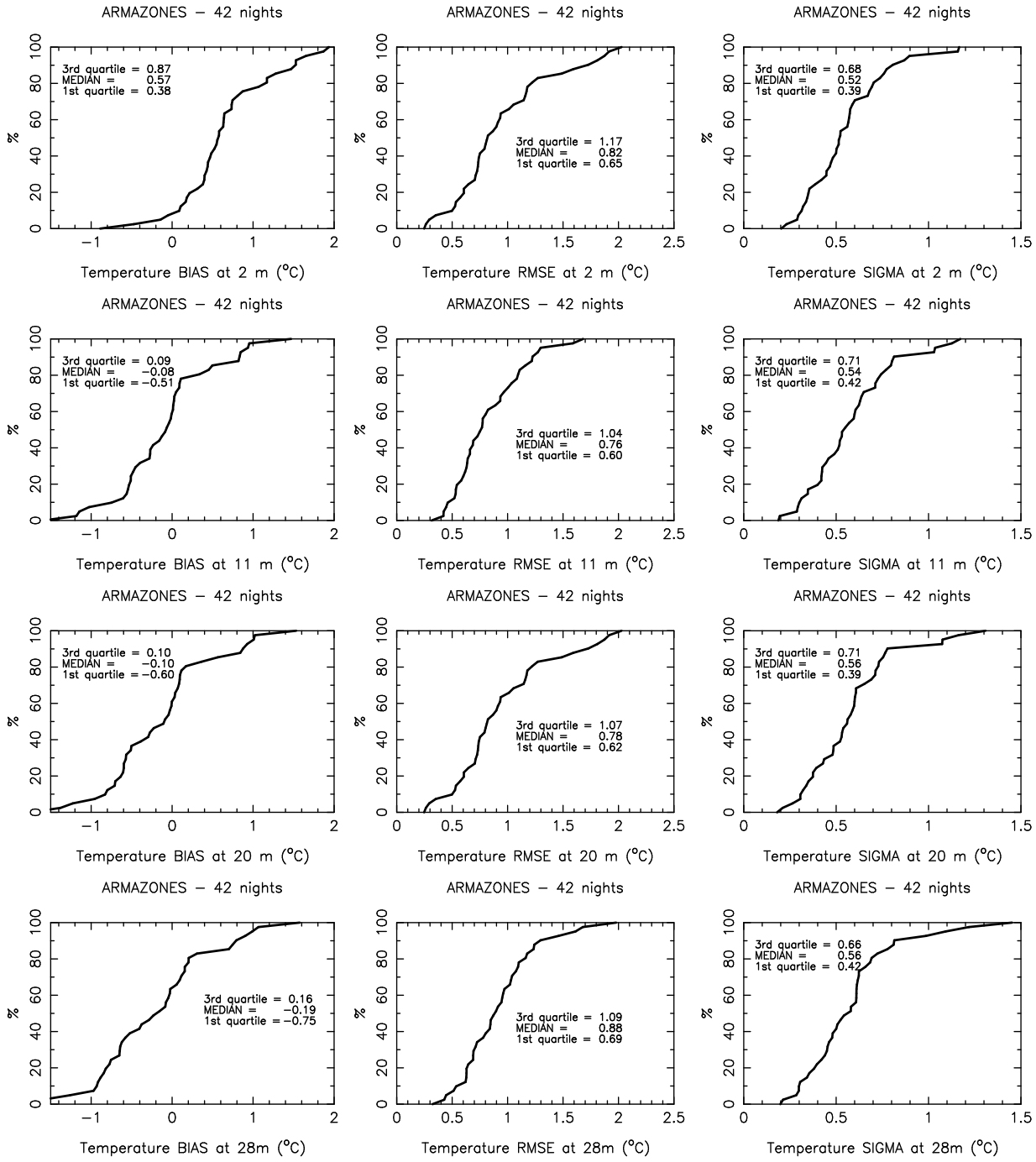

Figure 11: Cumulative distributions of the single nights bias (left), RMSE (middle) and bias-corrected RMSE (right) for the absolute temperature at Cerro Armazones, for the sample of 42 nights in 2007.

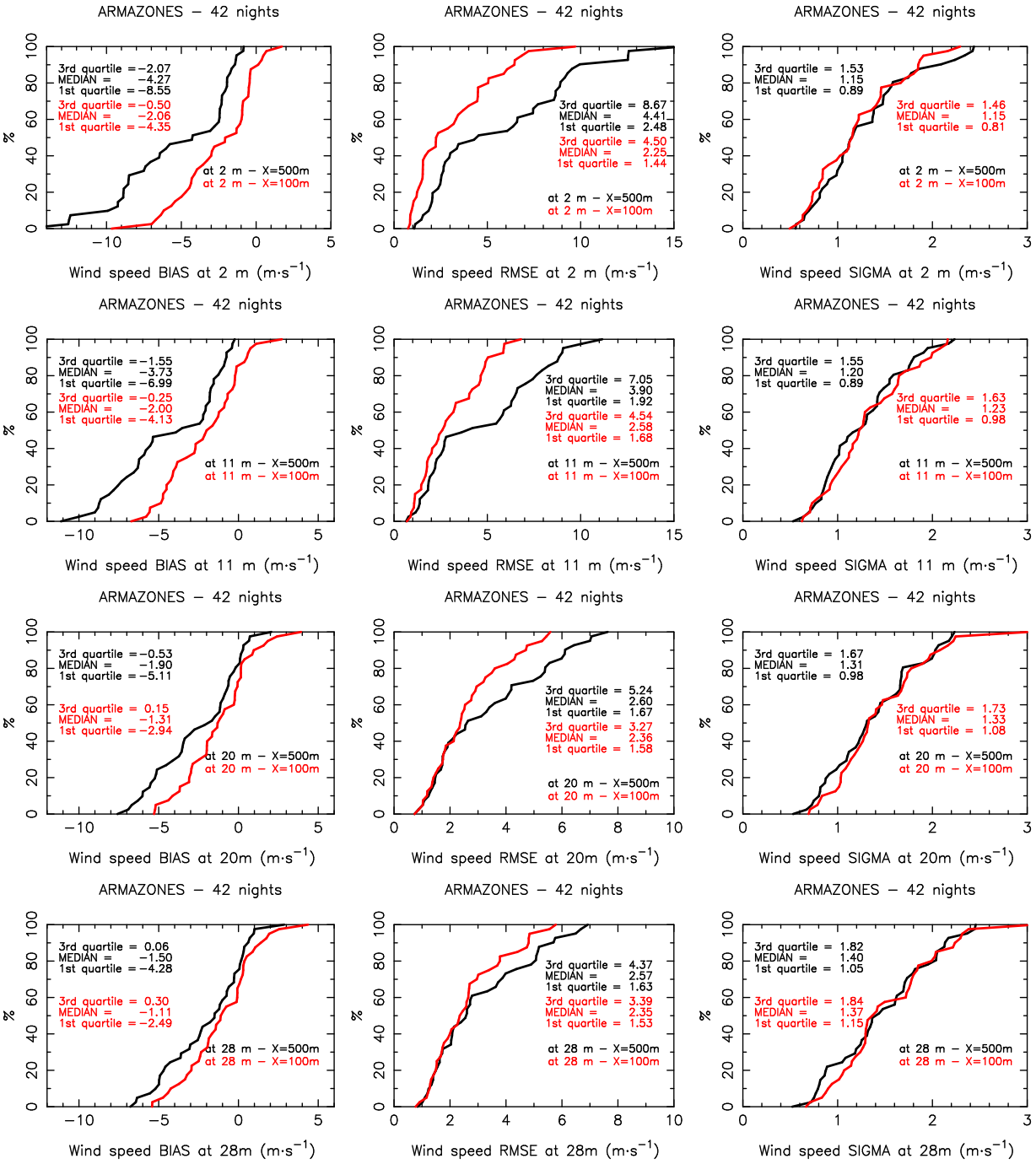

Figure 12: Cumulative distributions of the single nights bias (left), RMSE (middle) and bias-corrected RMSE (right) for the wind speed at Cerro Armazones, for the sample of 42 nights in 2007. The results for both $\Delta X = 500$ m (in black) and $\Delta X = 100$ m (in red) configurations are reported.

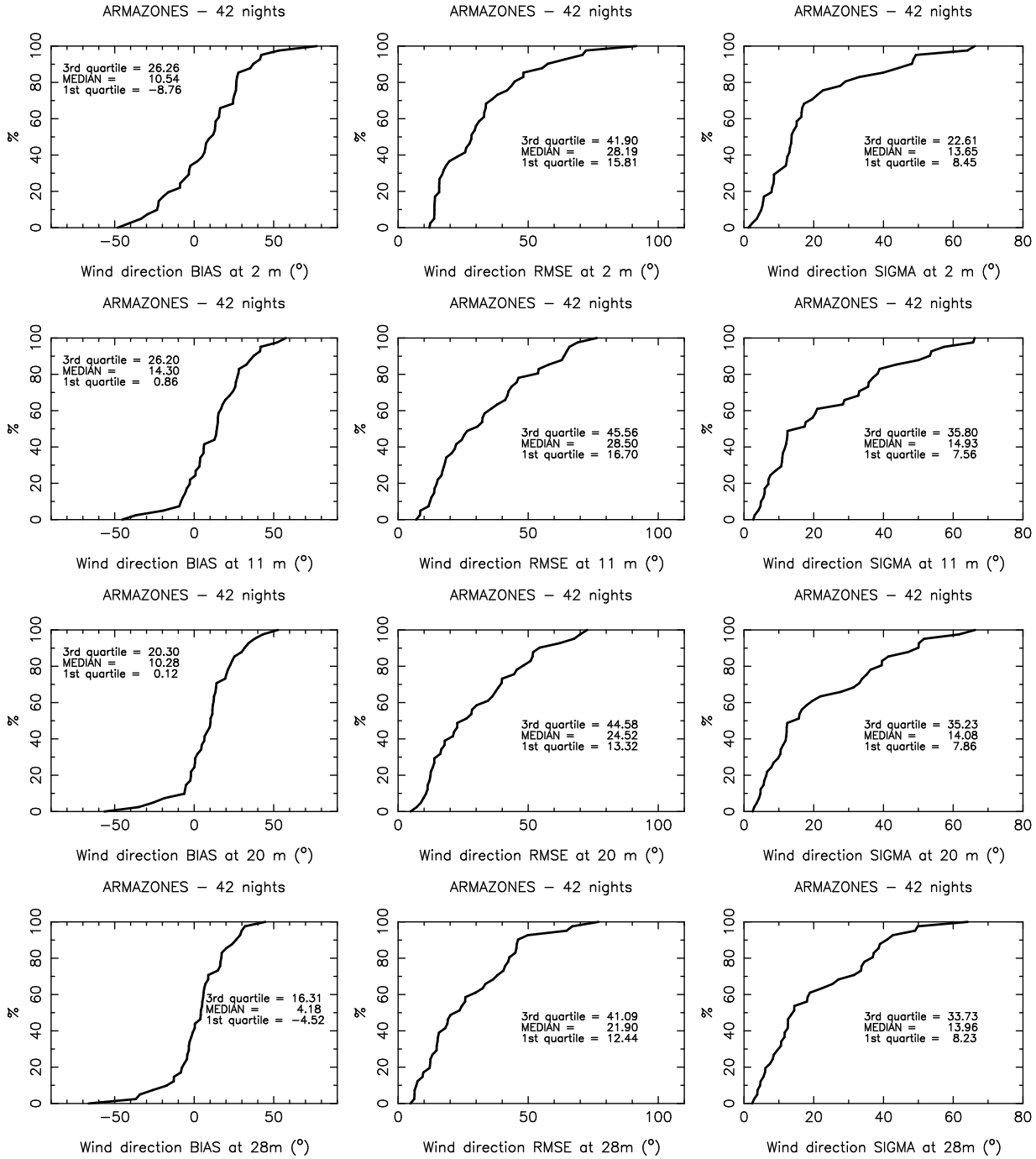

Figure 13: Cumulative distributions of the single nights bias (left), RMSE (middle) and bias-corrected RMSE (right) for the wind direction at Cerro Armazones, for the sample of 42 nights in 2007. The data with a wind velocity inferior to 3 m·s^{-1} are filtered out from the sample.

1.3 Cerro Armazones - 53 nights in 2010 and 2011

In this section we consider only the 53 nights in 2010 an 2011.

1.3.1 Scattered plots

Fig. 14 displays the scattered plots of the model output temperature against the observed temperature, for Cerro Armazones, at 2 m, 10 m and 30 m. Fig. 15 displays the scattered plots of the model output wind speed against the observed wind speed, for Cerro Armazones, at 20 m and 30 m. Fig. 16 displays the scattered plots of the model output wind direction against the observed wind direction, for Cerro Armazones, at 10 m and 30 m. The corresponding values for the bias, the RMSE (and the RMSE_{rel} for the wind direction), and the σ, of the temperature, the wind speed (with both ΔX=500 m and ΔX=100 m configurations) and the wind direction (with and without discarding wind speed inferior to 3 $\text{m}\cdot\text{s}^{-1}$), are reported in Tables 27, 28, 29, 30, 31, respectively, and compared to the values of the original 20 nights sample. In the comparison we have to take into account that measurements done for the 20 nights in 2007 have been done with the TMT instrumentation i.e. at four heights: 2 m, 11 m, 20 m and 28 m. For this 53 nights sample, only observations at 10 m and 30 m are available, except for the temperature where observations are available at 2 m too.

For the temperature, the results are very similar to what we found with the 20 nights of Phase A study. The RMSE is in the interval [0.91,1.02]°C. The RMSE for the wind speed is slightly higher (3.21 $\text{m}\cdot\text{s}^{-1}$ at 30 m and 3.90 $\text{m}\cdot\text{s}^{-1}$ at 10 m), with the ΔX = 100 m configuration. The results for the wind direction are still excellent. Indeed, the RMSE_{rel} is around 24%. Globally, we observe a very similar result on the sample of nights having the ESO instrumentation and those nights having the TMT instrumentation.

	Absolute temperature (°C)						
ARMAZONES	53 nights			20 nights			
Δ X =500 m	2 m	10 m	30 m	2 m	11 m	20 m	28 m
BIAS	0.55	-0.05	-0.19	0.76	0.06	0.04	0.02
RMSE	1.02	0.91	1.01	1.06	0.80	0.84	0.86
σ	0.86	0.91	1.00	0.74	0.80	0.84	0.86

Table 27: Near surface temperature **bias**, **RMSE** and bias-corrected RMSE σ (Meson-NH minus Observations), at Cerro Armazones. Left: for the sample of 53 nights of 2010 and 2011. Right: with the sample of 20 nights from Phase A

	Wind speed ($\text{m}\cdot\text{s}^{-1}$)					
ARMAZONES	53 nights		20 nights			
Δ X =500 m	10 m	30 m	2 m	11 m	20 m	28 m
BIAS	-5.24	-2.75	-3.59	-2.91	-1.40	-0.92
RMSE	6.32	4.09	4.52	3.97	2.78	2.54
σ	3.53	3.03	2.75	2.70	2.40	2.37

Table 28: Near surface wind speed **bias**, **RMSE** and bias-corrected RMSE σ (Meson-NH minus Observations), at Cerro Armazones, with the Δ X =500 m configuration. Left: for the sample of 53 nights of 2010 and 2011. Right: with the sample of 20 nights from Phase A.

	Wind speed ($m \cdot s^{-1}$)					
ARMAZONES	53 nights		20 nights			
Δ X =100 m	10 m	30 m	2 m	11 m	20 m	28 m
BIAS	-2.76	-1.59	-1.50	-1.41	-0.68	-0.42
RMSE	3.90	3.21	2.62	2.75	2.46	2.55
σ	2.76	2.79	2.15	2.36	2.36	2.52

Table 29: Near surface wind speed **bias**, **RMSE** and bias-corrected RMSE σ (Meson-NH minus Observations), at Cerro Armazones, with the Δ X =100 m configuration. Left: for the sample of 53 nights of 2010 and 2011.Right: with the sample of 20 nights from Phase A.

	Wind direction (^{o})					
ARMAZONES	53 nights		20 nights			
Δ X =500 m	10 m	30 m	2 m	11 m	20 m	28 m
BIAS	11.6	15.1	6.7	10.3	6.7	-0.8
RMSE	43.1	44.3	50.5	43.8	42.9	41.5
$RMSE_{rel}$	23.9%	24.6%	28.1%	24.3%	23.8%	23.1%
σ	41.5	41.6	50.1	42.6	42.4	41.5

Table 30: Near surface wind speed **bias**, **RMSE**, bias-corrected RMSE σ and relative RMSE (Meson-NH minus Observations), at Cerro Armazones, with the Δ X =500 m configuration. Left: for the sample of 53 nights of 2010 and 2011. Right: for the sample of 20 nights from Phase A.

	Wind direction (^{o})					
ARMAZONES	53 nights		20 nights			
Δ X =500 m	10 m	30 m	2 m	11 m	20 m	28 m
BIAS	10.3	15.4	10.2	12.0	8.4	2.1
RMSE	33.8	36.4	37.7	35.8	32.6	30.4
$RMSE_{rel}$	18.8%	20.2%	20.9%	19.9%	18.1%	16.9%
σ	32.2	33.0	36.3	33.7	31.5	30.3

Table 31: Near surface wind speed **bias**, **RMSE**, bias-corrected RMSE σ and relative RMSE (Meson-NH minus Observations), at Cerro Armazones, with the Δ X =500 m configuration. Left: for the sample of 53 nights of 2010 and 2011. Right: for the sample of 20 nights from Phase A. Data with wind speed inferior to 3 $m \cdot s^{-1}$ have been discarded.

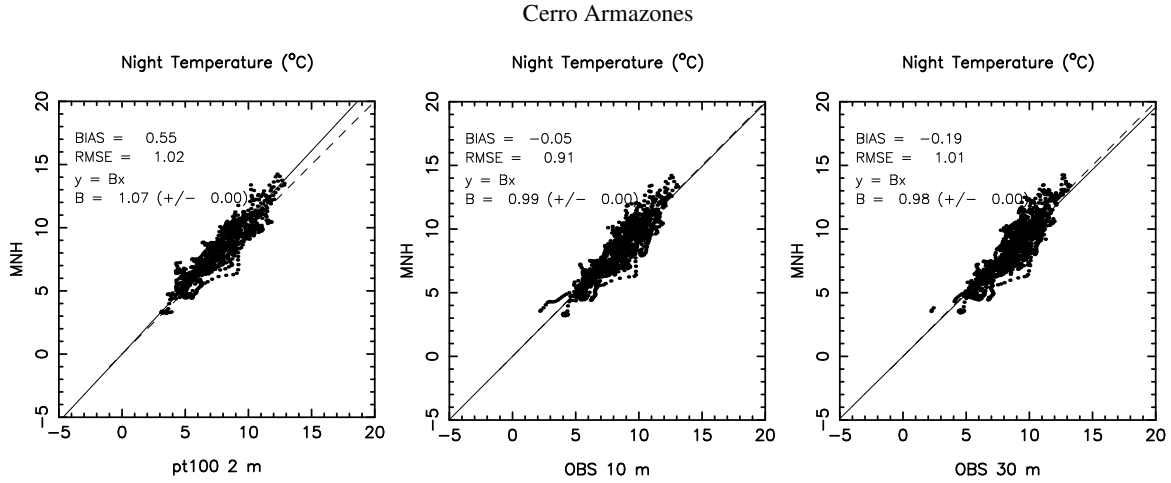

Figure 14: Scattered plot of Meso-NH **temperature** against observations, at 2 m, 10 m and 30 m at **Cerro Armazones**, with the $\Delta X = 500$ m configuration (53 nights in 2010-2011).

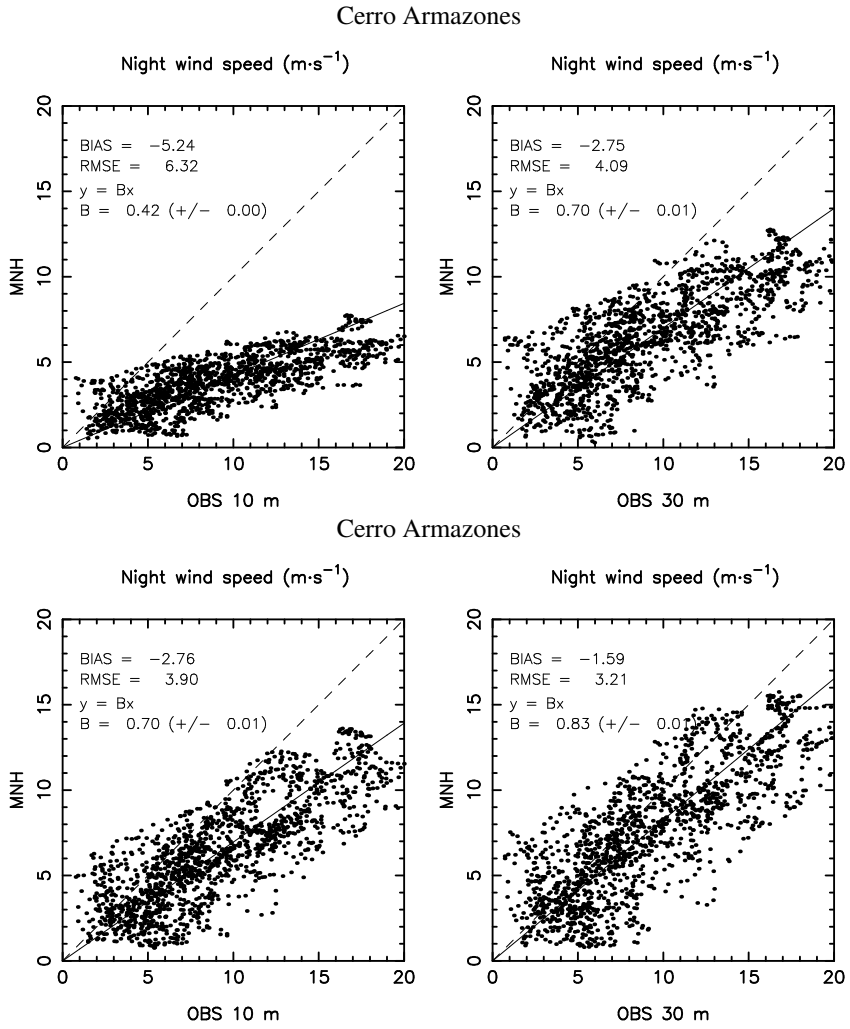

Figure 15: Scattered plot of Meso-NH **wind speed** against observations, at 10 m and 30 m at **Cerro Armazones** (53 nights in 2010-2011). Top figures: with the ΔX = 500 m configuration. Bottom figures: with the ΔX = 100 m configuration.

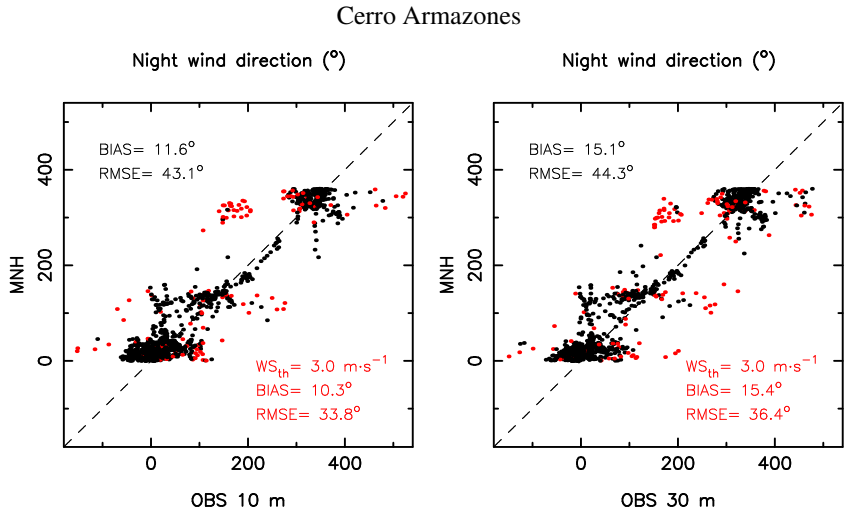

Figure 16: Scattered plot of Meso-NH **wind direction** against observations, at 10 m and 30 m at **Cerro Armazones** (53 nights in 2010-2011), with the $\Delta X = 500$ m configuration.

1.3.2 Temporal evolutions

In this section are reported the temporal evolutions of the averaged, the bias and the RMSE for the temperature, the wind speed and the wind direction near the surface at Cerro Armazones for the 53 nights sample (Fig. 17 for the temperature, Fig. 18 for the wind speed with the ΔX = 500 m configuration, Fig. 19 for the wind speed with the ΔX = 100 m configuration, Fig. 20 for the wind direction).

For the temperature, the bias and RMSE are confirmed to be excellent. During the night, he bias is below 0.5°C at levels 10 m and 30 m, and around 0.5°C at level 2 m. The RMSE is equal to, or slightly superior to, 1°C at all levels.

For the wind speed (with the ΔX = 100 m configuration), the bias during the night is between 1.5 m·s^{-1} and 3.5 m·s^{-1}. The RMSE is between 3 m·s^{-1} and 4 m·s^{-1}, depending in the level.

The temporal evolution of the RMSE during the night is between 40° and 50°, even better than for the original 20 nights sample. No filter has been applied for this computation, and so one can expect much better values when filtering the low level winds.

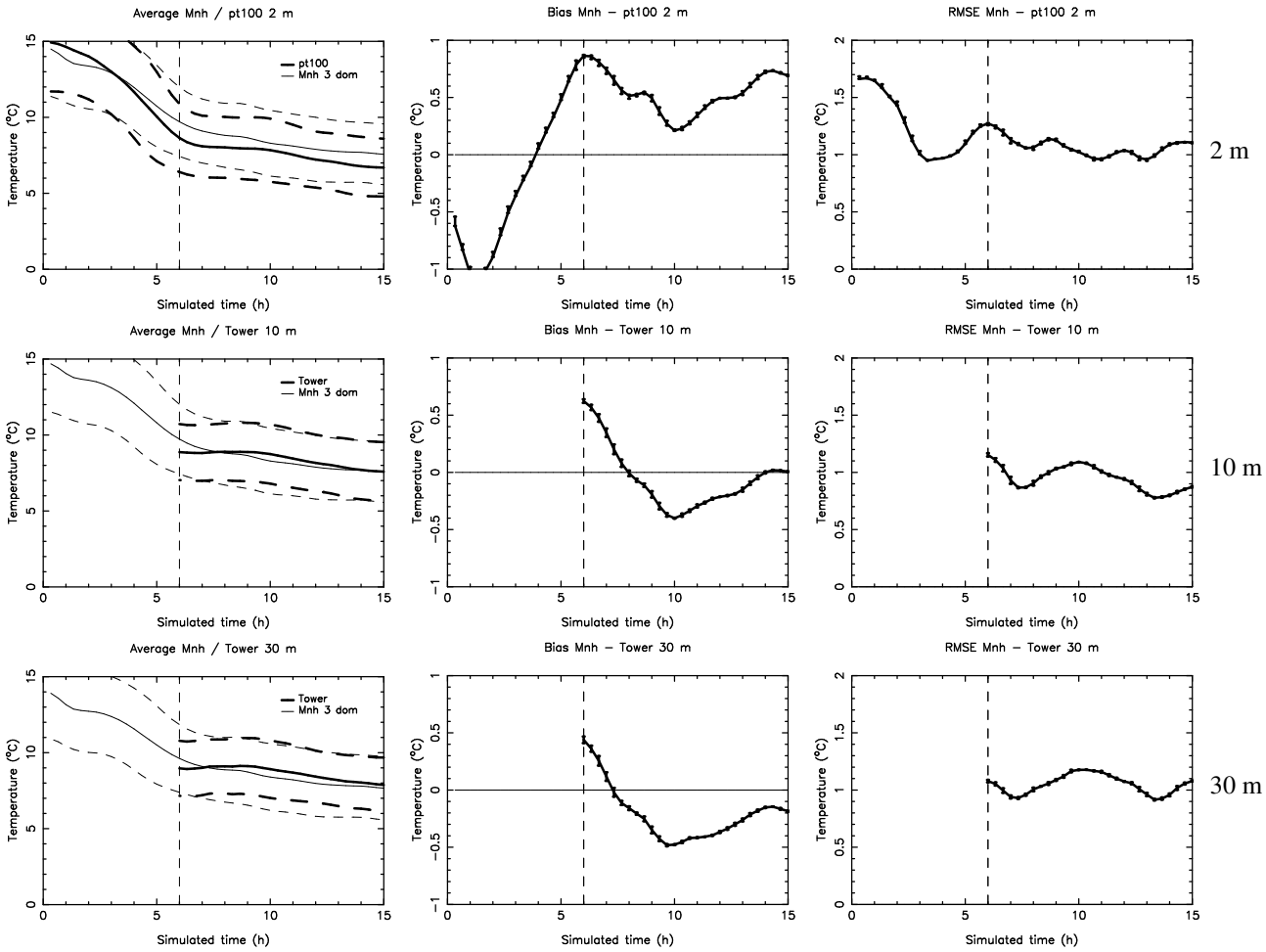

Figure 17: Temporal evolution of the **absolute temperature average** (the bold line is the observation average and the thin line is Meso-NH average), **bias** (Mnh - Observations) and **RMSE** at **Cerro Armazones** (top: at 10 m; bottom: at 30 m). The sample is 53 nights in 2010-2011. The x-axis represents the time from the beginning of the simulation (00 h is 18 UT of the day before, 06 h is 00 UT, and 15 h is 09 UT). The nights starts at around 06 h (00 UT - 20 LT) and is delimited by the vertical dashed line. Meso-NH is with the $\Delta X = 500$ m configuration. The error bars represent $\pm$ the standard deviation. Almost no observations during daytime were available for the period considered (53 nights in 2010-2011).

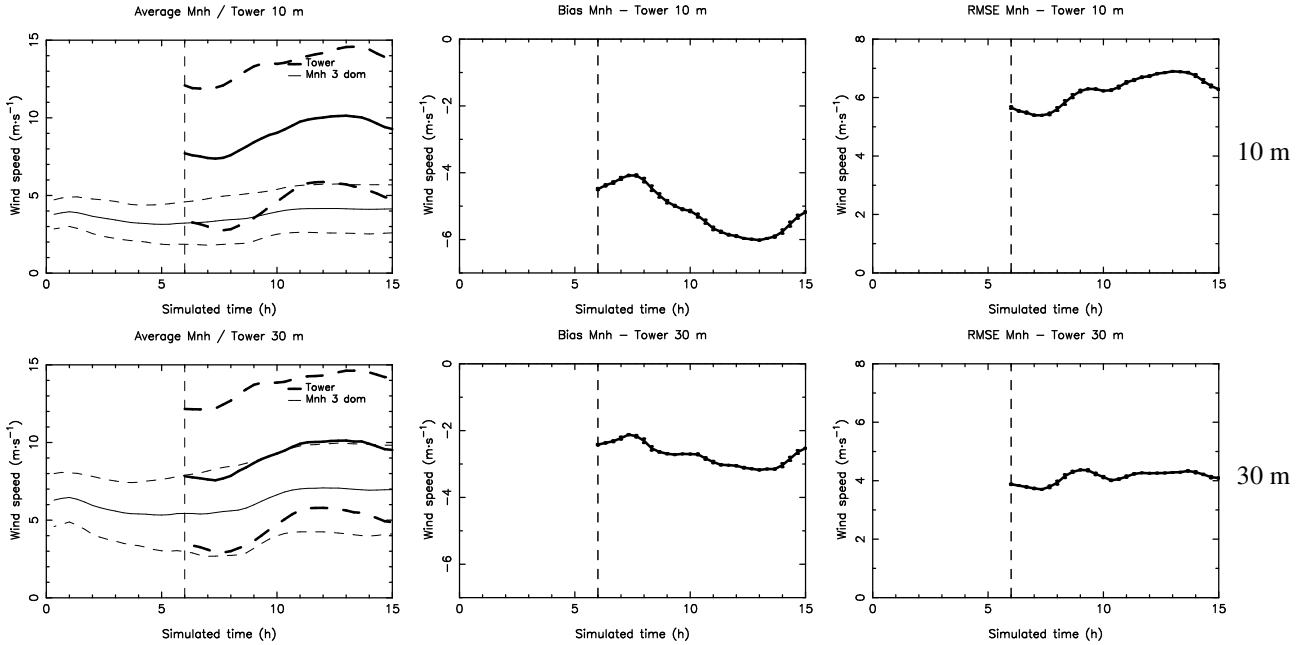

Figure 18: Same as Figure 17 but for the **wind speed** at Cerro Armazones with the $\Delta X = 500$ m configuration.

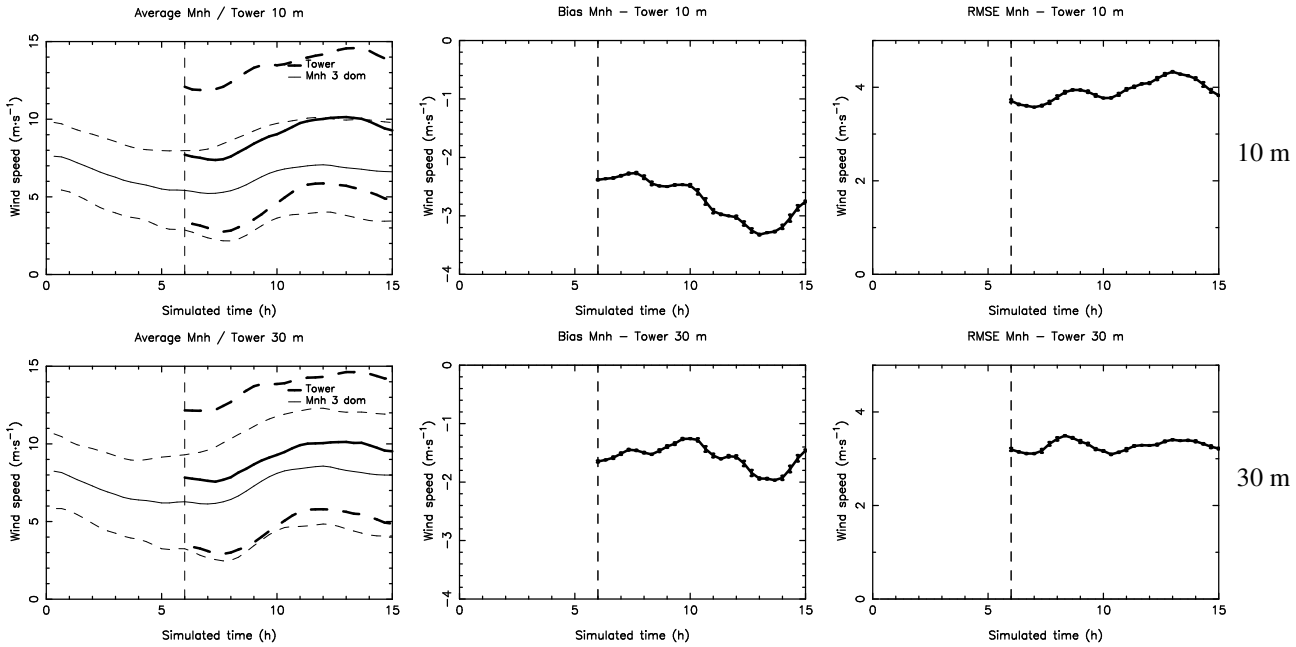

Figure 19: Same as Figure 17 but for the **wind speed** at Cerro Armazones with the $\Delta X = 100$ m configuration.

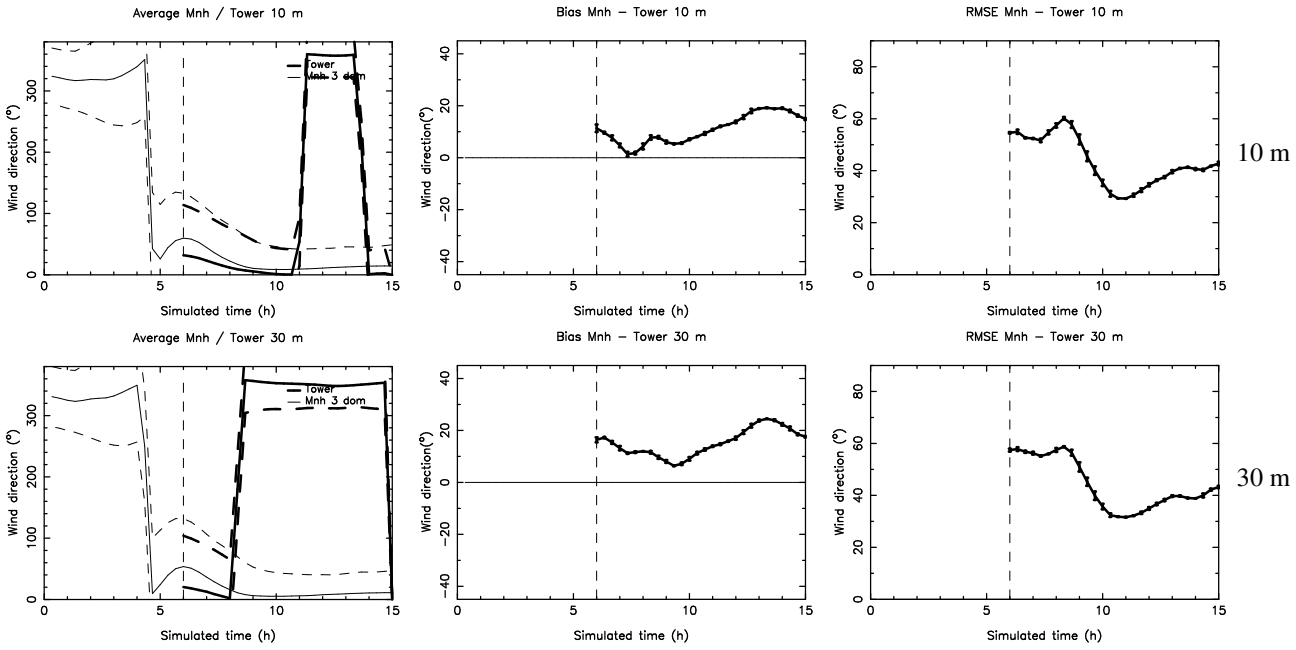

Figure 20: Same as Figure 17 but for the **wind direction** at Cerro Armazones.

1.3.3 Contingency tables

In this section, we have constructed contingency tables for the surface meteorological parameters.

TEMPERATURE
Tables 32, 33, 34, 35 are for the temperature. Once again, the results show that the model is able to predict with a very good accuracy an estimation of the surface temperature. All the PODs are excellent (between 51.1% and 94.4%). The lowest PODs are for the intermediate values (POD_2). PCs are all over 71.2%.

Division by tertiles (climatology) C. Armazones - 2 m		**OBSERVATIONS** $T < 7°C$	$7°C < T < 9°C$	$T > 9°C$
MODEL	$T < 7°C$	344	23	2
	$7°C < T < 9°C$	89	252	20
	$T > 9°C$	04	129	223

Total points = 1082; PC=75.7%; EBD=0.2%
POD_1=79.4%; POD_2=62.4%; POD_3=91.0%

Table 32: 3×3 contingency table for the absolute temperature during the night, at 2 m a.g.l. at Cerro Armazones, for the years 2010-2011 (53 nights considered). We use the Meso-NH ΔX = 500 m configuration.

Division by tertiles (climatology) C. Armazones - 2 m		**OBSERVATIONS** $T < 7°C$	$7°C < T < 9°C$	$T > 9°C$
MODEL	$T < 7°C$	402	66	4
	$7°C < T < 9°C$	31	256	52
	$T > 9°C$	0	82	189

Total points = 1082; PC=78.3%; EBD=0.4%
POD_1=92.8%; POD_2=63.4%; POD_3=77.1%

Table 33: 3×3 contingency table for the absolute temperature during the night, at 2 m a.g.l. at Cerro Armazones, for the years 2010-2010 (53 nights considered). We use the Meso-NH ΔX = 500 m configuration and we correct the Meso-NH output with the well identified bias of ∼0.6°C between observation and simulation at 2 m.

Division by tertiles (climatology) C. Armazones - 10 m		OBSERVATIONS $T < 7.5°C$	$7.5°C < T < 10°C$	$T > 10°C$
MODEL	$T < 7.5°C$	436	124	0
	$7.5°C < T < 10°C$	26	426	88
	$T > 10°C$	00	107	224

Total points = 1431; PC=75.9%; EBD=0.0%
POD_1=94.4%; POD_2=64.8%; POD_3=71.8%

Table 34: 3×3 contingency table for the absolute temperature during the night, at 10 m a.g.l. at Cerro Armazones, for the years 2010-2011 (53 nights considered). We use the Meso-NH ΔX = 500 m configuration.

Division by tertiles (climatology) C. Armazones - 30 m		OBSERVATIONS $T < 8°C$	$8°C < T < 10°C$	$T > 10°C$
MODEL	$T < 8°C$	471	174	4
	$8°C < T < 10°C$	31	292	97
	$T > 10°C$	00	105	252

Total points = 1426; PC=71.2%; EBD=0.3%
POD_1=93.8%; POD_2=51.1%; POD_3=71.4%

Table 35: 3×3 contingency table for the absolute temperature during the night, at 30 m a.g.l. at Cerro Armazones, for the years 2010-2011 (53 nights considered). We use the Meso-NH ΔX = 500 m configuration.

WIND SPEED

Tables 36, 37 are for the wind speed. For the weakest and the strongest winds (POD_1 and POD_3), the results are good, with PODs between 64.4% and 80.9%. The POD_2 (intermediate values) are almost as good, with values between 57.8% and 65.3%.

Division by tertiles (climatology) C. Armazones - 10 m		**OBSERVATIONS** $WS < 6m{\cdot}s^{-1}$	$6m{\cdot}s^{-1} < WS < 10.5m{\cdot}s^{-1}$	$WS > 10.5m{\cdot}s^{-1}$
MODEL	$WS < 6m{\cdot}s^{-1}$	295	106	7
	$6m{\cdot}s^{-1} < WS < 10.5m{\cdot}s^{-1}$	125	283	92
	$WS > 10.5m{\cdot}s^{-1}$	03	101	419

Total points = 1431; PC=69.7%; EBD=0.7%
POD_1=69.7%; POD_2=57.8%; POD_3=80.9%

Table 36: 3×3 contingency table for the wind speed during the night, at 10 m a.g.l. at Cerro Armazones, for the years 2010-2011 (53 nights considered). We use the Meso-NH ΔX = 100 m configuration with the wind corrected by the multiplicative bias.

Division by tertiles (climatology) C. Armazones - 30 m		**OBSERVATIONS** $WS < 6m{\cdot}s^{-1}$	$6m{\cdot}s^{-1} < WS < 11m{\cdot}s^{-1}$	$WS > 11m{\cdot}s^{-1}$
MODEL	$WS < 6m{\cdot}s^{-1}$	318	115	10
	$6m{\cdot}s^{-1} < WS < 11m{\cdot}s^{-1}$	108	322	170
	$WS > 11m{\cdot}s^{-1}$	01	56	326

Total points = 1426; PC=67.7%; EBD=0.8%
POD_1=74.5%; POD_2=65.3%; POD_3=64.4%

Table 37: 3×3 contingency table for the wind speed during the night, at 30 m a.g.l. at Cerro Armazones, for the years 2010-2011 (53 nights considered). We use the Meso-NH ΔX = 100 m configuration with the wind corrected by the multiplicative bias.

WIND DIRECTION

Tables 38, 39, are for the wind direction. The numbers vary a little with respect to what we found with the sample of 42 nights (and TMT instrumentation) and what we found at Paranal (see Lascaux et al. (2015)[53]), but the conclusions are still valid. The model shows a very good performance in reconstructing the wind direction particularly in those directions from which the wind flows more frequently.

		OBSERVATIONS			
C. Armazones - all levels		N-E	S-E	S-W	N-W
MODEL	N-E	1104	25	6	729
	S-E	89	147	25	8
	S-W	0	1	36	9
	N-W	61	46	12	493

Total points = 2791; PC=63.8%; EBD=2.1%
$POD(NE)$=88.0%; $POD(SE)$=67.1%
$POD(SW)$=45.6%; $POD(NW)$=39.8%

Table 38: 4×4 contingency table for the wind direction α during the night, at 10 m and 30 m a.g.l. at Cerro Armazones. We use the Meso-NH ΔX = 500 m configuration. We filter out the observed wind inferior to 3 $m{\cdot}s^{-1}$. NE corresponds to $0° < \alpha < 90°$; SE corresponds to $90° < \alpha < 180°$; SW corresponds to $180° < \alpha < 270°$; NW corresponds to $270° < \alpha < 360°$.

		OBSERVATIONS			
C. Armazones - all levels		N	E	S	W
MODEL	N	1951	140	26	171
	E	108	111	22	8
	S	11	51	66	4
	W	65	1	23	33

Total points = 2791; PC=77.4%; EBD=1.6%
$POD(N)$=91.4%; $POD(E)$=36.6%
$POD(S)$=48.2%; $POD(W)$=15.3%

Table 39: 4×4 contingency table for the wind direction α during the night, at 10 m and 30 m a.g.l. at Cerro Armazones. We use the Meso-NH ΔX = 500 m configuration. We filter out the observed wind inferior to 3 $m{\cdot}s^{-1}$. N corresponds to $-45° < \alpha < 45°$; E corresponds to $45° < \alpha < 135°$; S corresponds to $135° < \alpha < 225°$; W corresponds to $225° < \alpha < 315°$.

1.3.4 Individual nights model performances

In this section we present the analysis done on the model performances in reconstructing the atmospheric parameters, night by night, on the 53 nights sample, at Cerro Armazones. Fig. 21 and Table 40 show the results for the temperature. Fig. 22 and Table 41 show the results for the wind speed. Fig. 23 and Table 42 show the results for the wind direction.

The results (bias, RMSE, bias-corrected RMSE) are summarized in Tables 40, 41, 42, and compared with the original 20 nights sample. The results are very similar between the 20 nights sample and the 53 nights sample, for all parameters. The median RMSE for the temperature is in the range [0.81,0.85]°C, the median RMSE for the wind speed is in the range [2.51,2.92] $m{\cdot}s^{-1}$, and the median RMSE for the wind direction is in the range [26.65,29.36]°, with the filtering of the lowest wind speed (inferior to 3 $m{\cdot}s^{-1}$).

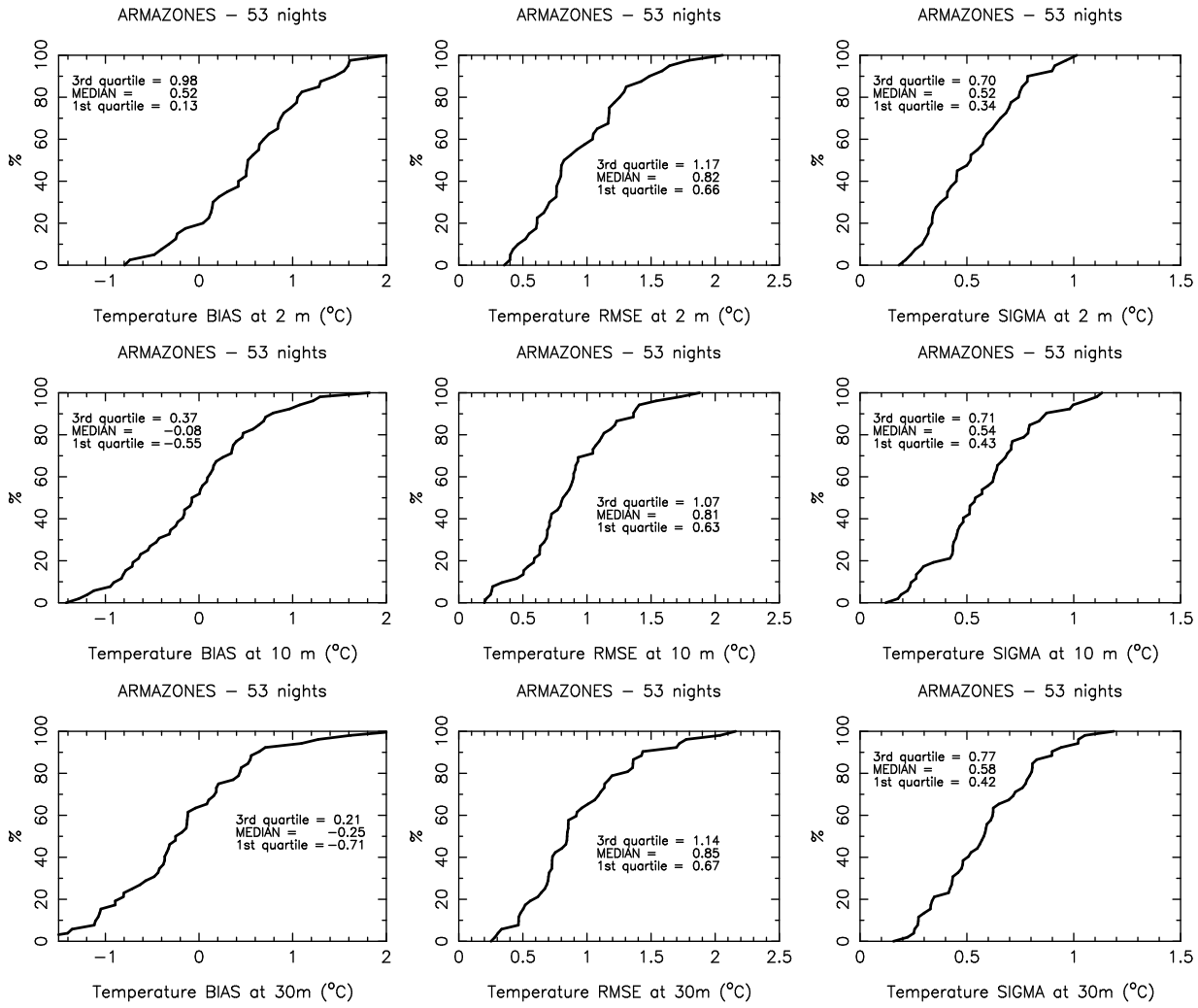

Figure 21: Cumulative distributions of the single nights bias (left), RMSE (middle) and bias-corrected RMSE (right) for the absolute temperature at Cerro Armazones, for the sample of 53 nights in 2010 and 2011.

The main conclusions obtained on the analysis of the atmospherical parameters at Armazones are summarized here:
(1) The value sof bias, RMSE and σ that we had found on a the sample of 20 nights have been substantially

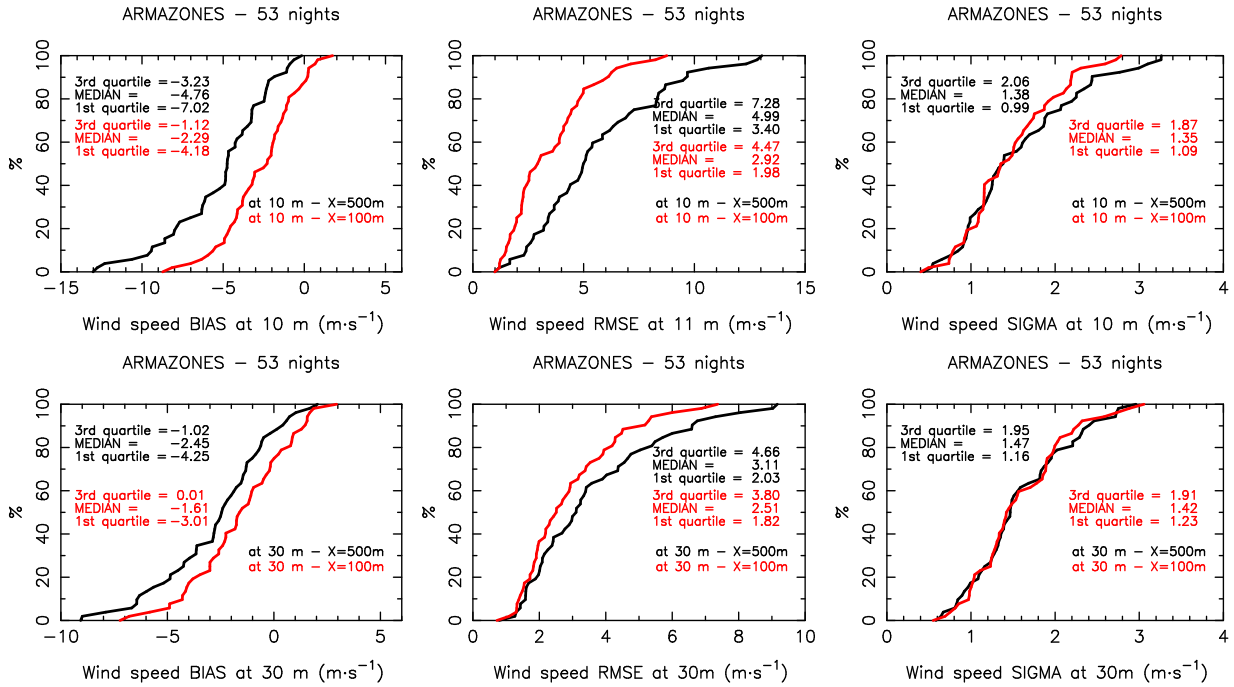

Figure 22: Cumulative distributions of the single nights bias (left), RMSE (middle) and bias-corrected RMSE (right) for the wind speed at Cerro Armazones, for the sample of 53 nights in 2010 and 2011. The results for both ΔX = 500 m (in black) and ΔX = 100 m (in red) configurations are reported.

Absolute temperature (^{o}C)

	ARMAZONES - 20 nights				ARMAZONES - 53 nights		
	2 m	11 m	20 m	28 m	2 m	10 m	30 m
BIAS	$0.64^{+1.02}_{+0.46}$	$0.01^{+0.28}_{-0.25}$	$0.05^{+0.37}_{-0.45}$	$0.07^{+0.50}_{-0.58}$	$0.52^{+0.98}_{+0.13}$	$-0.08^{+0.37}_{-0.55}$	$-0.25^{+0.21}_{-0.71}$
RMSE	$0.87^{+1.20}_{+0.72}$	$0.74^{+0.98}_{+0.54}$	$0.77^{+0.98}_{+0.60}$	$0.85^{+1.02}_{+0.66}$	$0.82^{+1.17}_{+0.66}$	$0.81^{+1.07}_{+0.63}$	$0.85^{+1.14}_{+0.67}$
σ	$0.51^{+0.58}_{+0.45}$	$0.53^{+0.70}_{+0.47}$	$0.57^{+0.68}_{+0.49}$	$0.61^{+0.64}_{+0.47}$	$0.52^{+0.70}_{+0.34}$	$0.54^{+0.71}_{+0.43}$	$0.58^{+0.77}_{+0.42}$

Table 40: Near surface median, **bias**, **RMSE** and **bias-corrected RMSE** σ (Meson-NH minus Observations), of the **temperature** from the single nights values, from the original 20 nights sample on the left, and from the extended 53 nights sample on the right (see Fig. 21). In small fonts, the 1st and 3rd quartiles.

confirmed on a richer statistical sample (42 and 53 nights) in different years and instrumentation (TMT and ESO).
(2) The temporal evolution all along the night of bias, RMSE and σ as well as the average of the atmospherical parameters present similar trends (or even better) than what we obtained with a sample of 20 nights.
(3) The calculation for individual nights (cumulative distribution, etc.) also confirm the results obtained with the sample of 20 nights.
(4) We proved that introducing multiplicative and additive coefficient of correction it is possible to decrease (and in some cases eliminate) the residual bias and RMSE.
(5) The contingency tables of all the atmospherical parameters confirm the results and in some cases (wind direction for example) are even better.

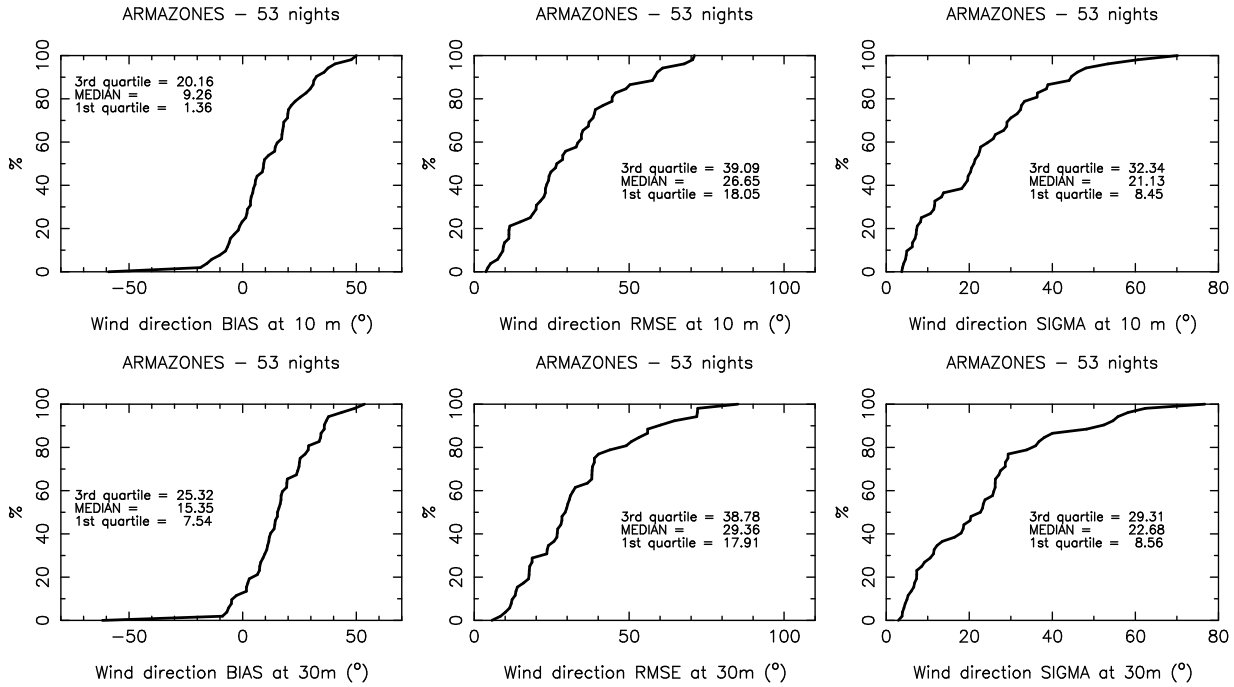

Figure 23: Cumulative distributions of the single nights bias (left), RMSE (middle) and bias-corrected RMSE (right) for the wind direction at Cerro Armazones, for the sample of 53 nights in 2010 and 2011. The data with a wind velocity inferior to 3 m·s^{-1} are filtered out from the sample.

	Wind speed ($m{\cdot}s^{-1}$)					
	ARMAZONES - 20 nights				ARMAZONES - 53 nights	
	2 m	11 m	20 m	28 m	10 m	30 m
BIAS	$-0.99^{-0.38}_{-2.98}$	$-1.08^{-0.19}_{-2.73}$	$-0.55^{+0.17}_{-1.97}$	$-0.10^{+0.68}_{-1.76}$	$-2.29^{-1.12}_{-4.18}$	$-1.61^{+0.01}_{-3.01}$
RMSE	$1.76^{+3.25}_{+1.13}$	$2.11^{+3.22}_{+1.57}$	$2.14^{+2.47}_{+1.43}$	$2.02^{+2.62}_{+1.45}$	$2.92^{+4.47}_{+1.98}$	$2.51^{+3.80}_{+1.82}$
σ	$1.01^{+1.38}_{+0.70}$	$1.19^{+1.62}_{+0.93}$	$1.34^{+1.73}_{+1.03}$	$1.42^{+1.82}_{+1.06}$	$1.42^{+1.91}_{+1.23}$	$1.35^{+1.87}_{+1.09}$

Table 41: Near surface median, **bias**, **RMSE** and **bias-corrected RMSE** σ (Meson-NH minus Observations), of the **wind speed** from the single nights values, from the original 20 nights sample on the left, and from the extended 53 nights sample on the right (see Fig. 22). In small fonts, the 1st and 3rd quartiles.

Wind direction (°)

	ARMAZONES - 20 nights				ARMAZONES - 53 nights	
	2 m	11 m	20 m	28 m	10 m	30 m
BIAS	$5.76^{+25.77}_{-17.91}$	$5.91^{+22.69}_{-5.13}$	$1.34^{+17.00}_{-5.40}$	$-3.36^{+16.45}_{-12.82}$	$9.26^{+20.16}_{+1.36}$	$15.35^{+25.32}_{+7.54}$
RMSE	$28.63^{+46.45}_{+16.42}$	$27.38^{+50.01}_{+16.19}$	$28.28^{+46.43}_{+13.26}$	$27.73^{+43.92}_{+13.99}$	$26.65^{+39.09}_{+18.05}$	$29.36^{+38.78}_{+17.91}$
σ	$13.98^{+27.04}_{+10.42}$	$20.06^{+37.66}_{+11.00}$	$17.25^{+34.16}_{+11.18}$	$16.65^{+34.15}_{+11.63}$	$21.13^{+32.34}_{+8.45}$	$22.68^{+29.31}_{+8.56}$

Table 42: Near surface median, **bias**, **RMSE** and **bias-corrected RMSE** σ (Meson-NH minus Observations), of the **wind direction** from the single nights values, from the original 20 nights sample on the left, and from the extended 53 nights sample on the right (see Fig. 23). In small fonts, the 1st and 3rd quartiles.

2 Work Package 1.2 - Model performances in reconstructing the atmospherical parameters on the 20 nights

This section is about the model performances in reconstructing the surface layer meteorological parameters. The main goal of this item was to check how results obtained in Phase A were modified using a moving average of 1 hour plus a resampling of 20 minutes on all the simulations and observations. The readers can jump this section and look at directly Session 1 and Session 3 if they are not interested on this specific point. With respect to the figures reported in Section 5 of the technical report from Phase A (n. E-TRE-INA-245-0001) All figures have been re-generated with the following method:

- Step 1: a filter using a moving average of 1 hour have been applied on both data and model outputs;
- Step 2: a resampling with a time interval of 20 minutes have been applied;
- Step 3: all statistical computations (bias, RMSE, bias-corrected RMSE σ) have been performed on the resulting samples.

On every scattered plot (Figures 24-27), every point is taken from the samples after Step 2. On every temporal evolution plot (Figures 28-35), every lines connect points taken from the samples after Step 3. All the bias and RMSE from the scattered plots are reported in the tables of Sections 1.1.1, 1.2.1 and 1.3.1. Concerning the temporal evolution of the wind direction bias, an inaccuracy in the Figures 18 and 19 from the MOSE Phase A report have been corrected. The bias is now really the difference (model - observation) and not (observation - model) as erroneously previously reported. In Figures 28 to 35, the error bars of the temporal evolution of bias and RMSE are now much smaller: the moving average of 1 hour applied to every sample prior to the resampling, acted as a filter for the highest frequencies. This analysis has been requested by the ESO Board at the end of the Phase A. In the successive sub-sections the reader will find the new results. Here we anticipate that the main conclusions obtained in Phase A are confirmed. The model performances in reconstructing the surface atmospjercal parameters appear to be very satisfactory and justify the extension of the analysis to a larger sample (see Section 1).

2.1 Scattered plots

In this section we reported the figures of all the outputs. The only important message is that all the conclusions obtained in Phase A are confirmed. The individual outputs and values are of course slightly different just because we implemented a filtering of the low frequencies with a different re-sampling (20 min instead of 10 min).

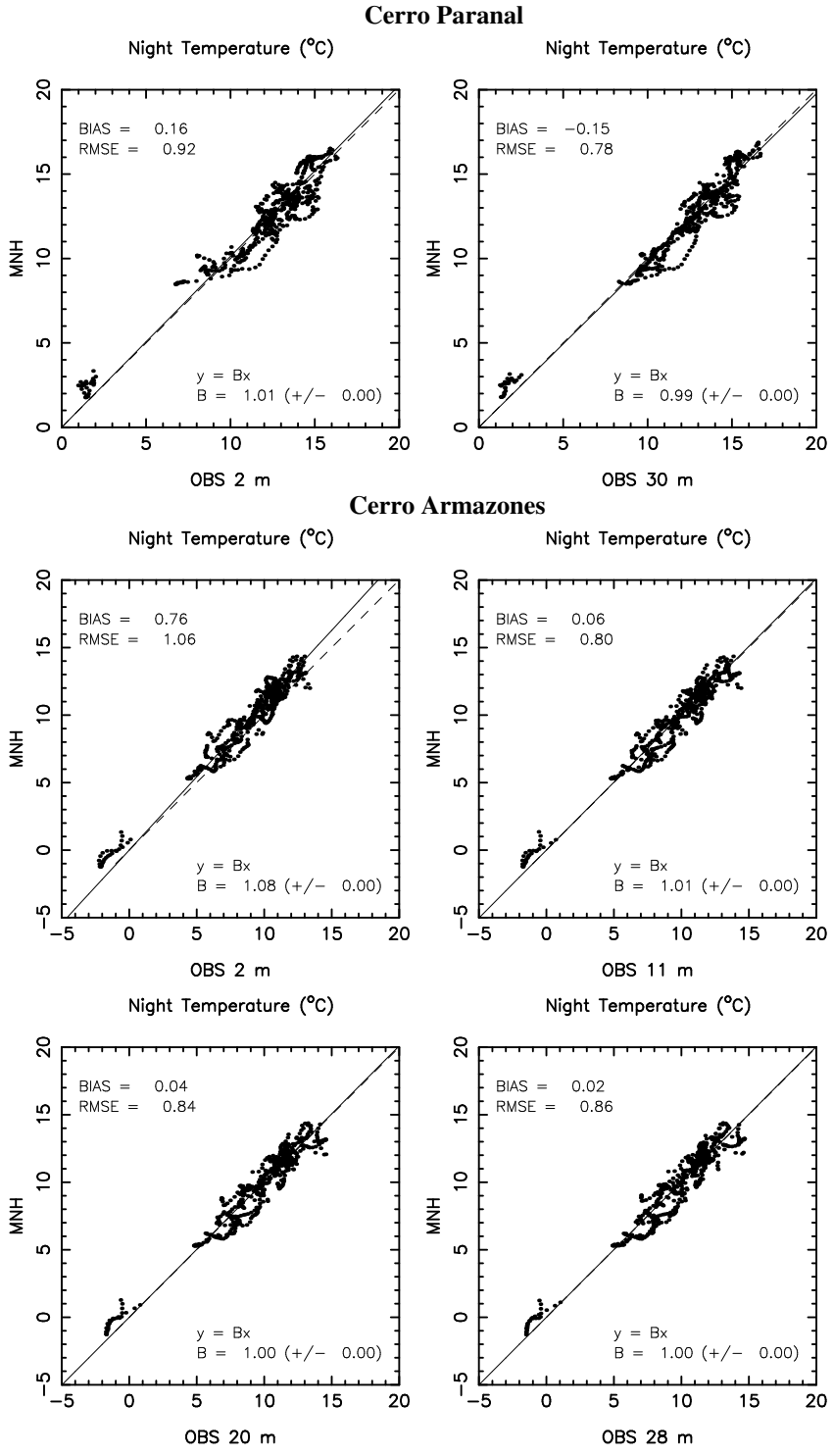

Figure 24: Scattered plot of Meso-NH **temperature** against observations, at 2 m and 30 m at **Cerro Paranal** (top figures); at 2 m, 11 m, 20 m and 28 m at **Cerro Armazones** (central and bottom figures).

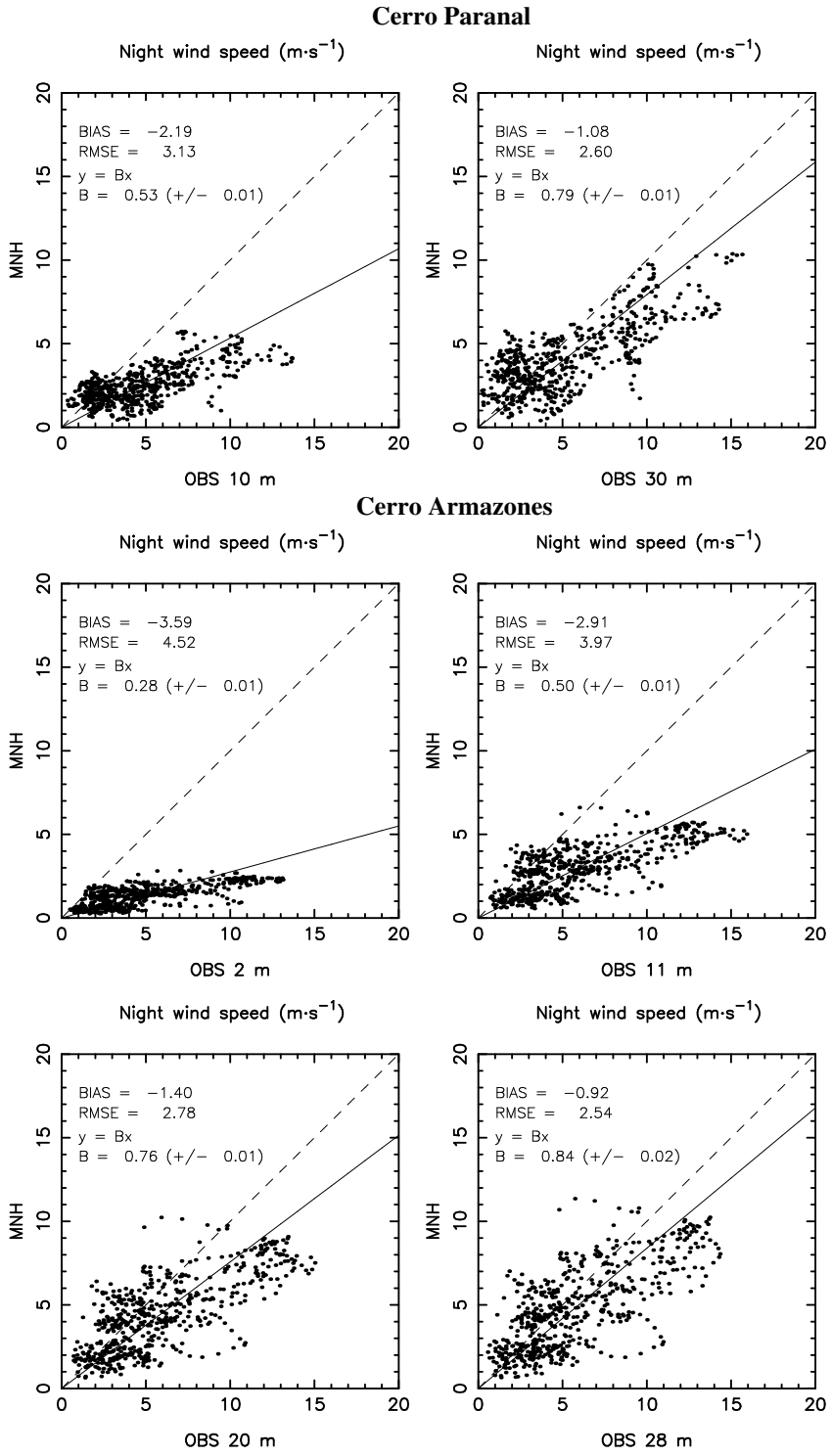

Figure 25: Scattered plot of Meso-NH **wind speed** against observations, at 10 m and 30 m at **Cerro Paranal** (top figures); at 2 m, 11 m, 20 m and 28 m at **Cerro Armazones** (central and bottom figures).

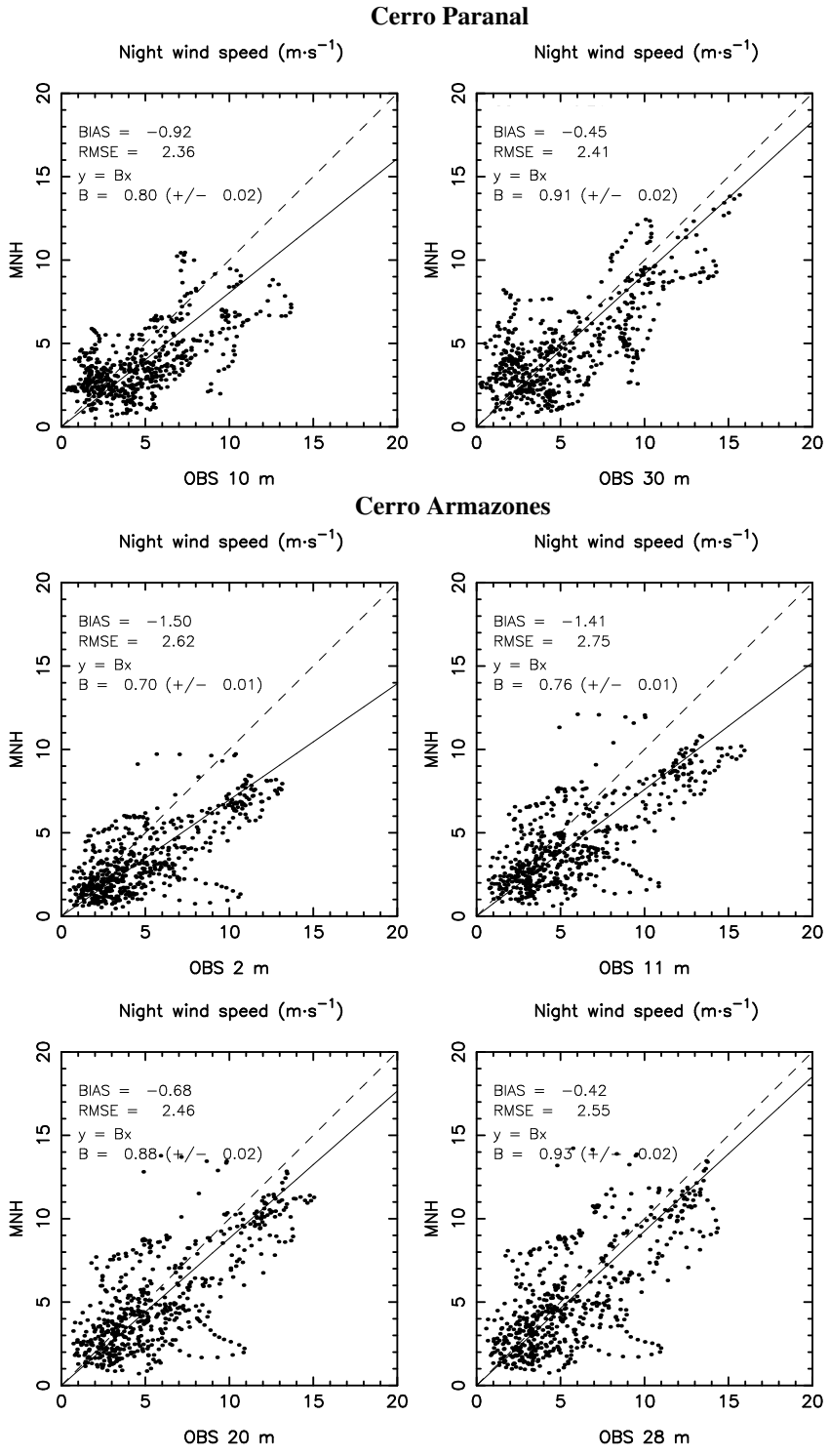

Figure 26: Same as Fig. 25, but with the high horizontal configuration for Meso-NH.

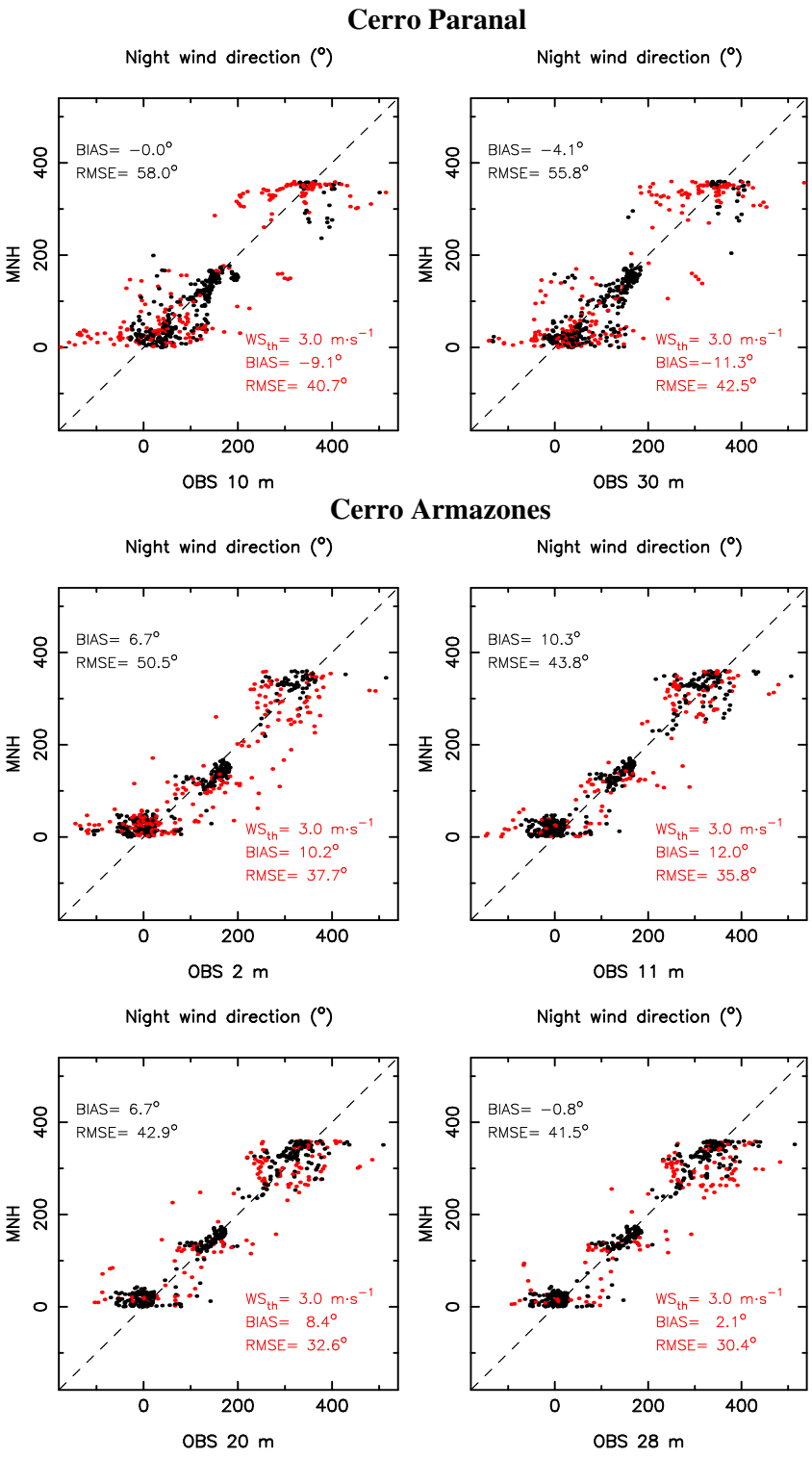

Figure 27: Scattered plot of Meso-NH **wind direction** against observations, at 10 m and 30 m at **Cerro Paranal** (top figures); at 2 m, 11 m, 20 m and 28 m at **Cerro Armazones** (central and bottom figures). Every point represents the average over an interval of 30 minutes.

2.2 Temporal evolutions

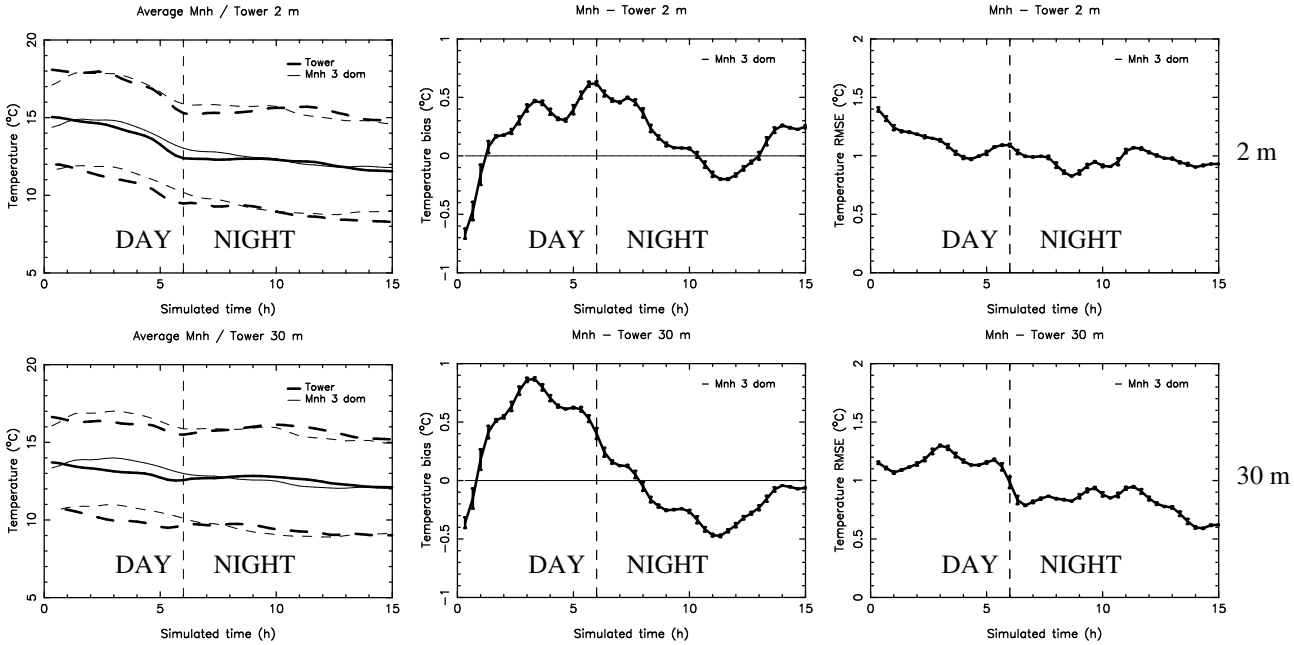

Figure 28: Temporal evolution of the **absolute temperature average** (the bold line is the observation average and the thin line is Meso-NH average), **bias** (Mnh - Observations) and **RMSE** at **Cerro Paranal** (top: at 2 m); bottom: at 30 m). The x-axis represents the time from the beginning of the simulation (00 h is 18 UT of the day before, 06 h is 00 UT, and 15 h is 09 UT). The nights starts at around 06 h (00 UT - 20 LT) and is delimited by the vertical dashed line. Meso-NH is with the $\Delta X = 500$ m configuration. The error bars represent $\pm$ the standard deviation.

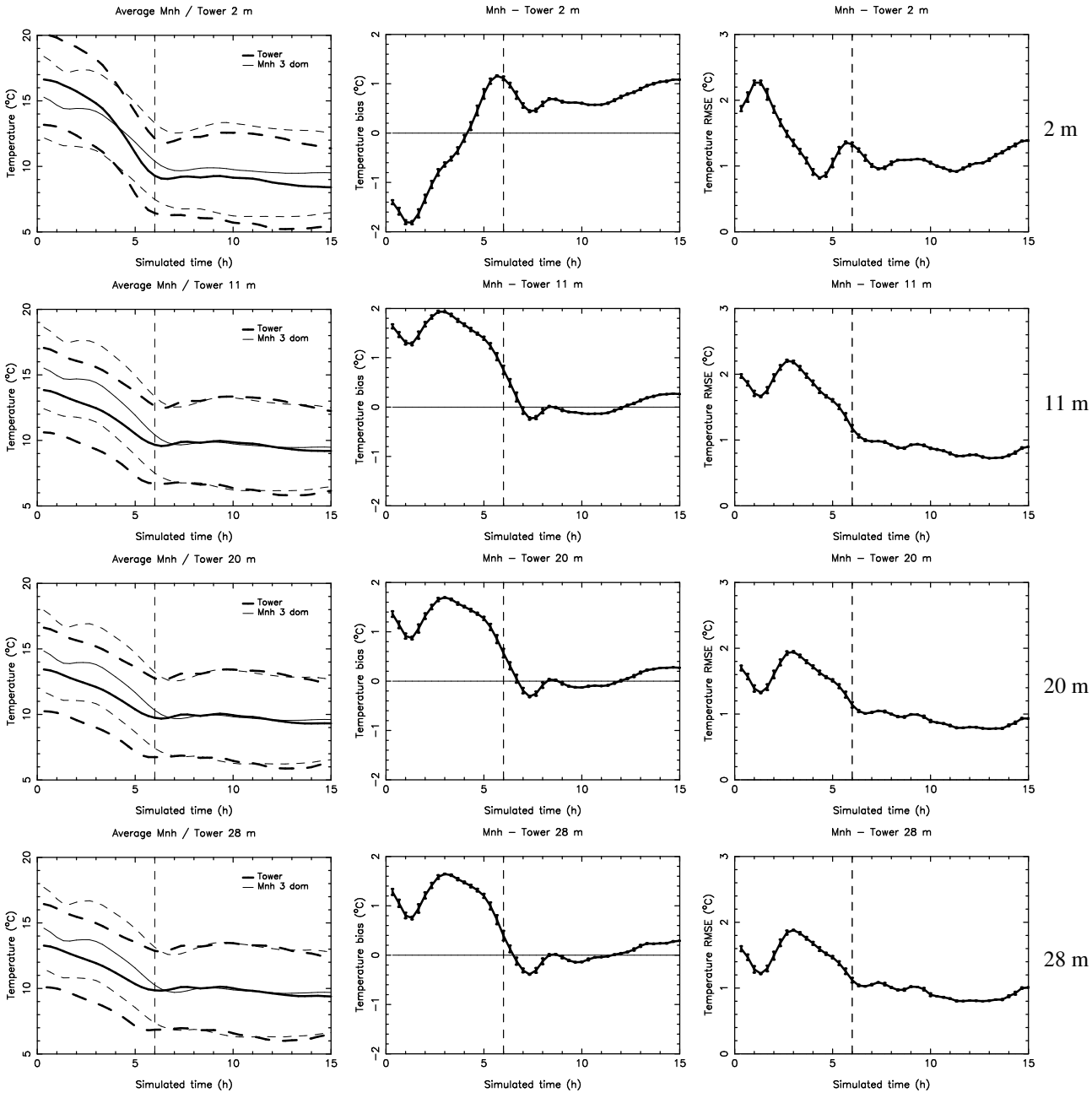

Figure 29: Same as Fig. 28 but for the **absolute temperature** at **Cerro Armazones** (from top to bottom: at 2 m, 11 m, 20 m and 28 m).

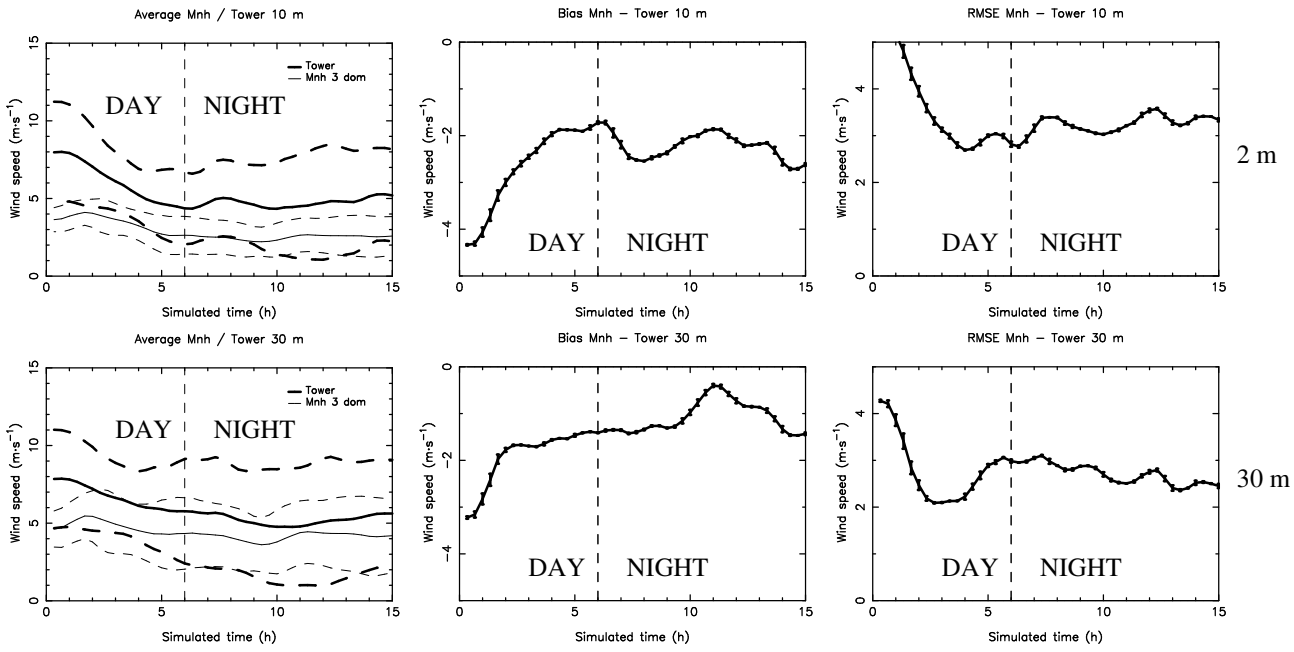

Figure 30: Same as Fig. 28 but for the **wind speed** at **Cerro Paranal** (top: at 10 m; bottom: at 30 m). Meso-NH is used with ΔX = 500 m configuration.

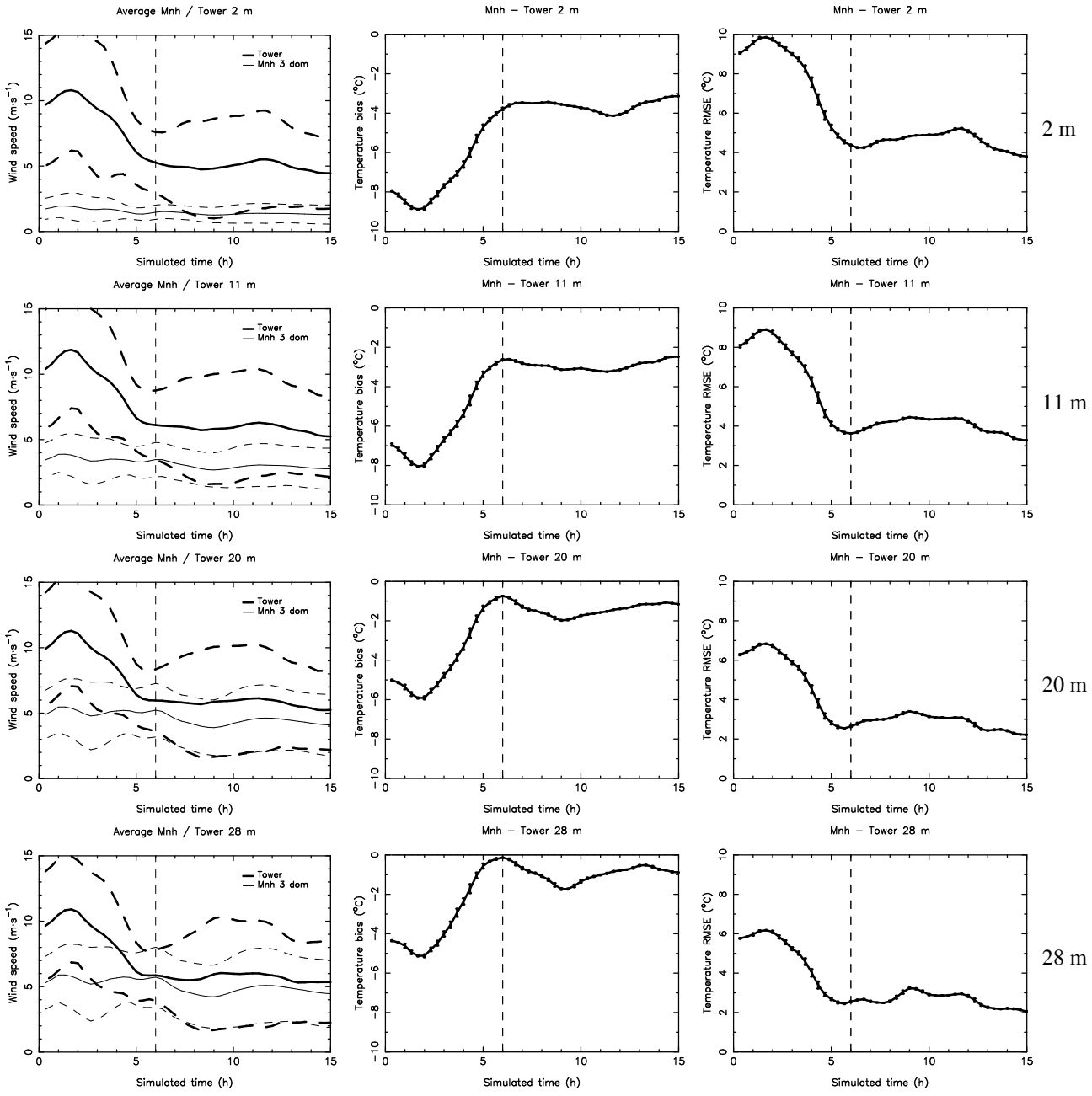

Figure 31: Same as Fig. 28 but for the **wind speed** at **Cerro Armazones** (from top to bottom: at 2 m, 11 m, 20 m and 28 m). Meso-NH is used with $\Delta X = 500$ m configuration.

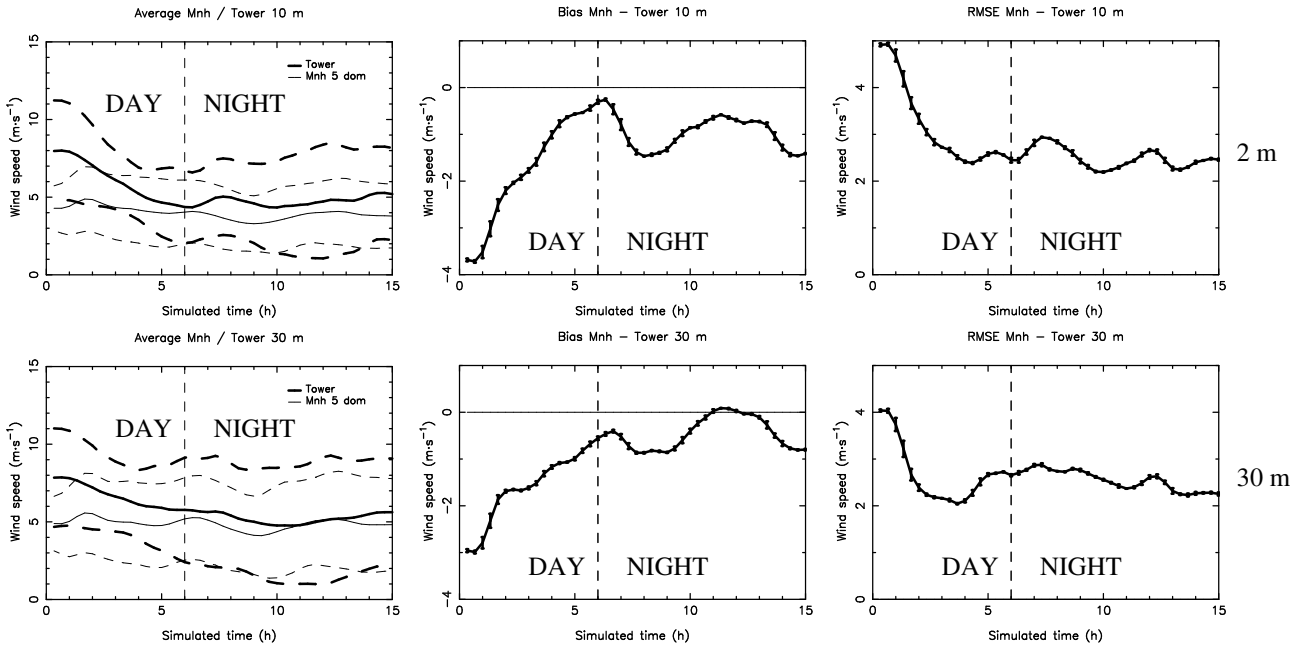

Figure 32: Same as Fig. 30 but Meso-NH is used in the $\Delta X = 100$ m configuration.

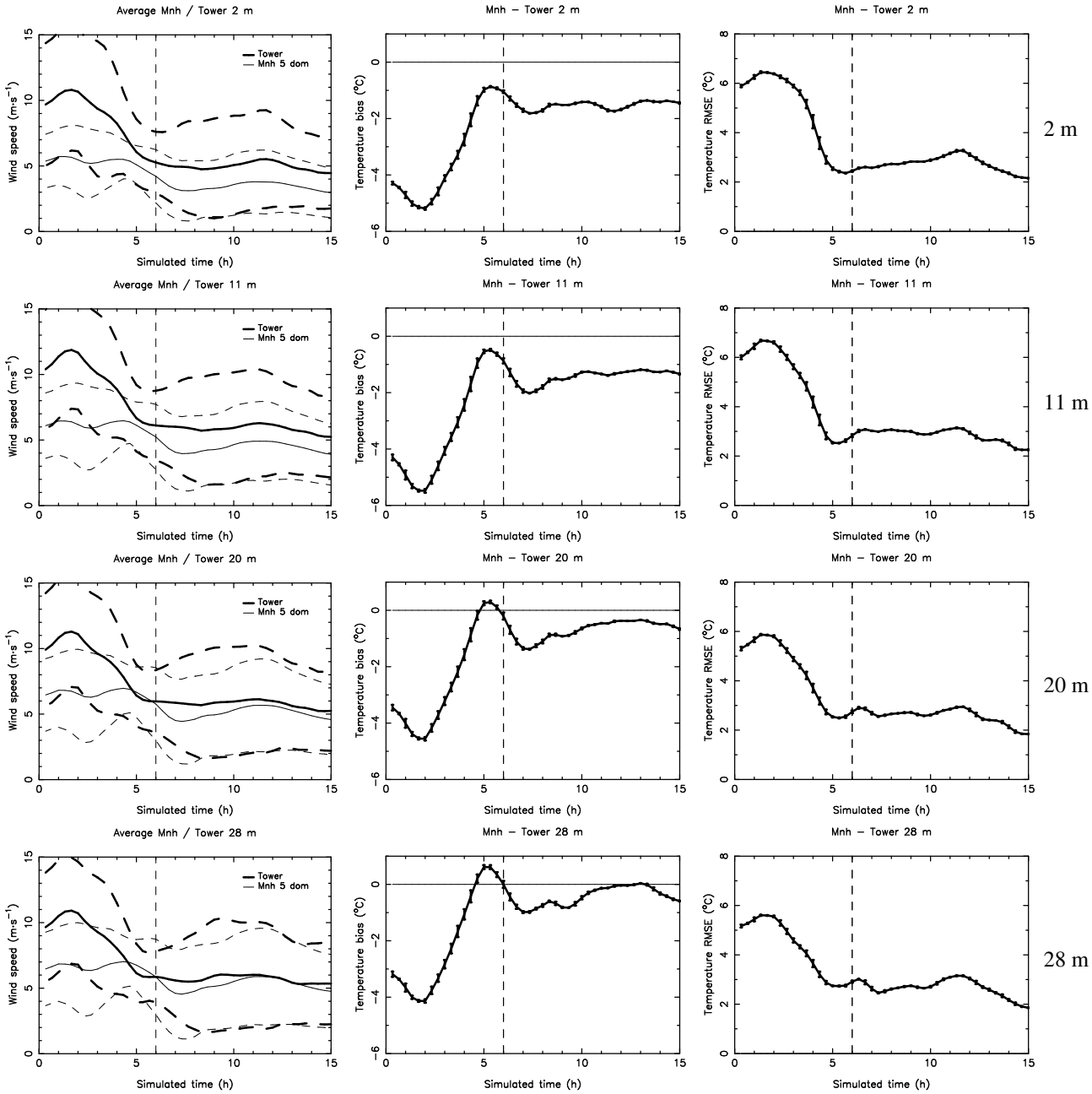

Figure 33: Same as Fig. 31 but Meso-NH is used in the $\Delta X = 100$ m configuration.

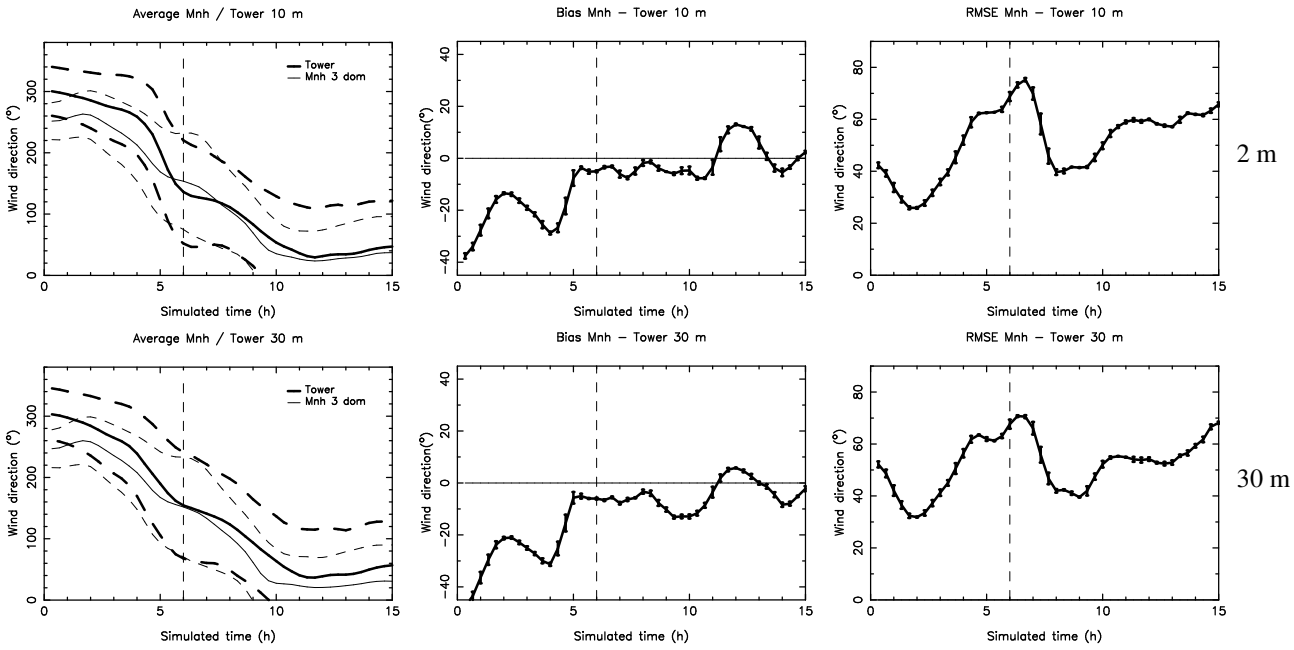

Figure 34: Same as Fig. 28 but for the **wind direction** at **Cerro Paranal** (top: at 10 m; bottom: at 30 m). The bias is now really the difference (model - observation) and not (observation - model).

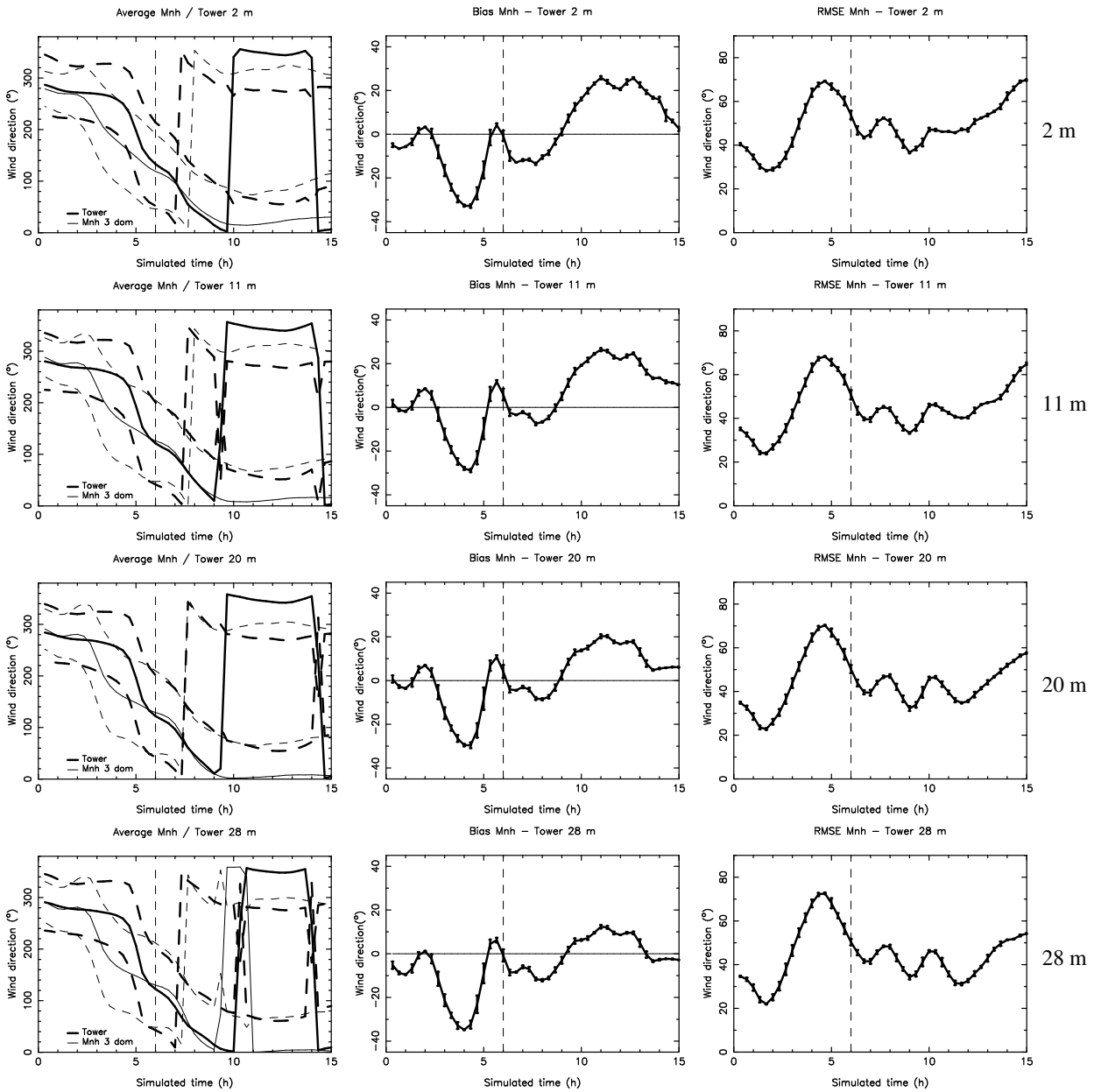

Figure 35: Same as Fig. 28 but for the **wind direction** at **Cerro Armazones** (from top to bottom: at 2 m, 11 m, 20 m and 28 m). The bias is now really the difference (model - observation) and not (observation - model).

2.3 Contingency tables

TEMPERATURE

Division by tertiles (climatology) C. Paranal - 2 m		**OBSERVATIONS** $T < 11°C$	$11°C < T < 13.5°C$	$T > 13.5°C$
MODEL	$T < 11°C$	122	17	0
	$11°C < T < 13.5°C$	0	149	57
	$T > 13.5°C$	0	41	154

Total points = 540; PC=78.7%; EBD=0%
POD_1=100%; POD_2=72.0%; POD_3=73.0%

Table 43: 3×3 contingency table for the absolute temperature during the night, at 2 m a.g.l. at Cerro Paranal. We use the Meso-NH ΔX = 500 m configuration. The sample is the original 20 nights sample from 2007.

Division by tertiles (climatology) C. Paranal - 30 m		**OBSERVATIONS** $T < 11.5°C$	$11.5°C < T < 13.5°C$	$T > 13.5°C$
MODEL	$T < 11.5°C$	135	15	0
	$11.5°C < T < 13.5°C$	0	114	48
	$T > 13.5°C$	0	30	198

Total points = 540; PC=82.8%; EBD=0%
POD_1=100%; POD_2=71.7%; POD_3=80.5%

Table 44: 3×3 contingency table for the absolute temperature during the night, at 30 m a.g.l. at Cerro Paranal. We use the Meso-NH ΔX = 500 m configuration. The sample is the original 20 nights sample from 2007.

Division by tertiles (climatology) C. Armazones - 2 m		**OBSERVATIONS** $T < 7°C$	$7°C < T < 9°C$	$T > 9°C$
MODEL	$T < 7°C$	94	22	0
	$7°C < T < 9°C$	13	73	16
	$T > 9°C$	0	9	313

Total points = 540; PC=88.9%; EBD=0%
POD_1=87.9%; POD_2=70.2%; POD_3=95.1%

Table 45: 3×3 contingency table for the absolute temperature during the night, at 2 m a.g.l. at Cerro Armazones. We use the Meso-NH ΔX = 500 m configuration and we correct the Meso-NH output with the well identified bias of ∼0.6°C between observation and simulation at 2 m. The sample is the original 20 nights sample from 2007.

Division by tertiles (climatology) C. Armazones - 11 m		**OBSERVATIONS** $T < 7.5°C$	$7.5°C < T < 10°C$	$T > 10°C$
MODEL	$T < 7.5°C$	86	25	0
	$7.5°C < T < 10°C$	13	99	21
	$T > 10°C$	0	11	285

Total points = 540; PC=87.0%; EBD=0%
POD_1=86.9%; POD_2=73.3%; POD_3=93.1%

Table 46: 3×3 contingency table for the absolute temperature during the night, at 11 m a.g.l. at Cerro Armazones. We use the Meso-NH ΔX = 500 m configuration. The sample is the original 20 nights sample from 2007.

Division by tertiles (climatology) C. Armazones - 20 m		**OBSERVATIONS** $T < 7.5°C$	$7.5°C < T < 10°C$	$T > 10°C$
MODEL	$T < 7.5°C$	77	32	0
	$7.5°C < T < 10°C$	15	99	19
	$T > 10°C$	0	11	287

Total points = 540; PC=85.7%; EBD=0%
POD_1=83.7%; POD_2=69.7%; POD_3=93.8%

Table 47: 3×3 contingency table for the absolute temperature during the night, at 20 m a.g.l. at Cerro Armazones. We use the Meso-NH ΔX = 500 m configuration. The sample is the original 20 nights sample from 2007.

Division by tertiles (climatology) C. Armazones - 28 m		**OBSERVATIONS** $T < 8°C$	$8°C < T < 10°C$	$T > 10°C$
MODEL	$T < 8°C$	98	30	0
	$8°C < T < 10°C$	11	73	26
	$T > 10°C$	0	10	292

Total points = 540; PC=85.7%; EBD=0%
POD_1=89.9%; POD_2=64.6%; POD_3=91.8%

Table 48: 3×3 contingency table for the absolute temperature during the night, at 28 m a.g.l. at Cerro Armazones. We use the Meso-NH ΔX = 500 m configuration. The sample is the original 20 nights sample from 2007.

WIND SPEED

Division by tertiles (climatology) C. Paranal - 10 m		**OBSERVATIONS** $WS < 4\ m{\cdot}s^{-1}$	$4\ m{\cdot}s^{-1} < WS < 7\ m{\cdot}s^{-1}$	$WS > 7\ m{\cdot}s^{-1}$
MODEL	$WS < 4\ m{\cdot}s^{-1}$	173	72	4
	$4\ m{\cdot}s^{-1} < WS < 7\ m{\cdot}s^{-1}$	69	91	39
	$WS > 7\ m{\cdot}s^{-1}$	5	20	67

Total points = 540; PC=61.3%; EBD=1.7%
POD_1=70.0%; POD_2=49.7%; POD_3=60.9%

Table 49: 3×3 contingency table for the wind speed during the night, at 10 m a.g.l. at Cerro Paranal. We use the Meso-NH ΔX = 100 m configuration with the wind corrected by the multiplicative bias. The sample is the original 20 nights sample from 2007.

Division by tertiles (climatology) C. Paranal - 30 m		**OBSERVATIONS** $WS < 4\ m{\cdot}s^{-1}$	$4\ m{\cdot}s^{-1} < WS < 8\ m{\cdot}s^{-1}$	$WS > 8\ m{\cdot}s^{-1}$
MODEL	$WS < 4\ m{\cdot}s^{-1}$	153	66	3
	$4\ m{\cdot}s^{-1} < WS < 8\ m{\cdot}s^{-1}$	85	83	48
	$WS > 8\ m{\cdot}s^{-1}$	9	7	86

Total points = 540; PC=59.6%; EBD=2.2%
POD_1=61.9%; POD_2=53.2%; POD_3=62.8%

Table 50: 3×3 contingency table for the wind speed during the night, at 30 m a.g.l. at Cerro Paranal. We use the Meso-NH ΔX = 100 m configuration with the wind corrected by the multiplicative bias. The sample is the original 20 nights sample from 2007.

Division by tertiles (climatology) C. Armazones - 2 m		**OBSERVATIONS** $WS < 5\ m{\cdot}s^{-1}$	$5\ m{\cdot}s^{-1} < WS < 9.5\ m{\cdot}s^{-1}$	$WS > 9.5\ m{\cdot}s^{-1}$
MODEL	$WS < 5\ m{\cdot}s^{-1}$	276	56	6
	$5\ m{\cdot}s^{-1} < WS < 9.5\ m{\cdot}s^{-1}$	64	55	22
	$WS > 9.5\ m{\cdot}s^{-1}$	0	5	56

Total points = 540; PC=71.7%; EBD=1.1%
POD_1=81.1%; POD_2=47.4%; POD_3=66.7%

Table 51: 3×3 contingency table for the wind speed during the night, at 2 m a.g.l. at Cerro Armazones. We use the Meso-NH ΔX = 100 m configuration with the wind corrected by the multiplicative bias. The sample is the original 20 nights sample from 2007.

Division by tertiles (climatology) C. Armazones - 11 m		**OBSERVATIONS** $WS < 6\ m{\cdot}s^{-1}$	$6\ m{\cdot}s^{-1} < WS < 10.5\ m{\cdot}s^{-1}$	$WS > 10.5\ m{\cdot}s^{-1}$
MODEL	$WS < 6\ m{\cdot}s^{-1}$	259	60	2
	$6\ m{\cdot}s^{-1} < WS < 10.5\ m{\cdot}s^{-1}$	64	43	11
	$WS > 10.5\ m{\cdot}s^{-1}$	12	18	71

Total points = 540; PC=69.1%; EBD=2.6%
POD_1=77.3%; POD_2=35.5%; POD_3=84.5%

Table 52: 3×3 contingency table for the wind speed during the night, at 11 m a.g.l. at Cerro Armazones. We use the Meso-NH ΔX = 100 m configuration with the wind corrected by the multiplicative bias. The sample is the original 20 nights sample from 2007.

Division by tertiles (climatology) C. Armazones - 20 m		**OBSERVATIONS** $WS < 6\ m{\cdot}s^{-1}$	$6\ m{\cdot}s^{-1} < WS < 10.5\ m{\cdot}s^{-1}$	$WS > 10.5\ m{\cdot}s^{-1}$
MODEL	$WS < 6\ m{\cdot}s^{-1}$	286	59	3
	$6\ m{\cdot}s^{-1} < WS < 10.5\ m{\cdot}s^{-1}$	56	45	20
	$WS > 10.5\ m{\cdot}s^{-1}$	1	12	58

Total points = 540; PC=72.0%; EBD=0.7%
POD_1=83.4%; POD_2=38.8%; POD_3=71.6%

Table 53: 3×3 contingency table for the wind speed during the night, at 20 m a.g.l. at Cerro Armazones. We use the Meso-NH ΔX = 100 m configuration with the wind corrected by the multiplicative bias. The sample is the original 20 nights sample from 2007.

Division by tertiles (climatology) C. Armazones - 28 m		**OBSERVATIONS** $WS < 6\ m{\cdot}s^{-1}$	$6\ m{\cdot}s^{-1} < WS < 11\ m{\cdot}s^{-1}$	$WS > 11\ m{\cdot}s^{-1}$
MODEL	$WS < 6\ m{\cdot}s^{-1}$	285	58	0
	$6\ m{\cdot}s^{-1} < WS < 11\ m{\cdot}s^{-1}$	60	48	16
	$WS > 11\ m{\cdot}s^{-1}$	1	30	42

Total points = 540; PC=69.4%; EBD=0.2%
POD_1=82.4%; POD_2=35.3%; POD_3=72.4%

Table 54: 3×3 contingency table for the wind speed during the night, at 28 m a.g.l. at Cerro Armazones. We use the Meso-NH ΔX = 100 m configuration with the wind corrected by the multiplicative bias. The sample is the original 20 nights sample from 2007.

WIND DIRECTION

		OBSERVATIONS			
C. Paranal - all levels		N-E	S-E	S-W	N-W
MODEL	N-E	325	78	18	65
	S-E	27	235	28	10
	S-W	5	1	0	0
	N-W	38	10	6	38

Total points = 884 ; PC=67.6%; EBD=4.9%
$POD(NE)$=82.3%; $POD(SE)$=72.5%
$POD(SW)$=0%; $POD(NW)$=33.6%

Table 55: 4×4 contingency table for the wind direction α during the night, at 10 m, and 30 m a.g.l. at Cerro Paranal. We use the Meso-NH ΔX = 500 m configuration. We filter out the data with an observed wind inferior to 3 $m{\cdot}s^{-1}$. NW corresponds to $0° < \alpha < 90°$; SW corresponds to $90° < \alpha < 180°$; SE corresponds to $180° < \alpha < 270°$; NE corresponds to $270° < \alpha < 360°$. The sample is the original 20 nights sample from 2007.

		OBSERVATIONS			
C. Paranal - all levels		N	E	S	W
MODEL	N	269	149	24	21
	E	30	123	50	3
	S	6	15	157	6
	W	24	5	1	1

Total points = 884; PC=62.2% ; EBD=4.3%
$POD(N)$=81.8%; $POD(E)$=42.1%
$POD(S)$=67.7%; $POD(W)$=3.2%

Table 56: 4×4 contingency table for the wind direction α during the night, at 10 m, and 30 m a.g.l. at Cerro Paranal. We use the Meso-NH ΔX = 500 m configuration. We filter out the observed wind inferior to 3 $m{\cdot}s^{-1}$. N corresponds to $-45° < \alpha < 45°$; E corresponds to $45° < \alpha < 135°$; S corresponds to $135° < \alpha < 225°$; W corresponds to $225° < \alpha < 315°$. The sample is the original 20 nights sample from 2007.

		OBSERVATIONS			
C. Armazones - all levels		N-E	S-E	S-W	N-W
MODEL	N-E	254	21	5	174
	S-E	14	210	14	5
	S-W	1	4	29	7
	N-W	56	4	34	188

Total points = 1996 ; PC=66.8%; EBD=1.5%
$POD(NE)$=78.2%; $POD(SE)$=87.9%
$POD(SW)$=35.4%; $POD(NW)$=50.3%

Table 57: 4×4 contingency table for the wind direction α during the night, at 2 m, 11 m, 20 m, and 28 m a.g.l. at Cerro Armazones. We use the Meso-NH ΔX = 500 m configuration. We filter out the data with an observed wind inferior to 3 $m{\cdot}s^{-1}$. NW corresponds to $0° < \alpha < 90°$; SW corresponds to $90° < \alpha < 180°$; SE corresponds to $180° < \alpha < 270°$; NE corresponds to $270° < \alpha < 360°$. The sample is the original 20 nights sample from 2007.

		OBSERVATIONS			
C. Armazones - all levels		N	E	S	W
MODEL	N	500	46	7	95
	E	3	79	23	3
	S	0	16	137	2
	W	42	2	8	57

Total points = 1996; PC=75.8% ; EBD=1.2%
$POD(N)$=97.4%; $POD(E)$=55.2%
$POD(S)$=78.3%; $POD(W)$=36.3%

Table 58: 4×4 contingency table for the wind direction α during the night, at 2 m, 11 m, 20 m, and 28 m a.g.l. at Cerro Armazones. We use the Meso-NH ΔX = 500 m configuration. We filter out the observed wind inferior to 3 $m{\cdot}s^{-1}$. N corresponds to $-45° < \alpha < 45°$; E corresponds to $45° < \alpha < 135°$; S corresponds to $135° < \alpha < 225°$; W corresponds to $225° < \alpha < 315°$. The sample is the original 20 nights sample from 2007.

2.4 Single nights statistics

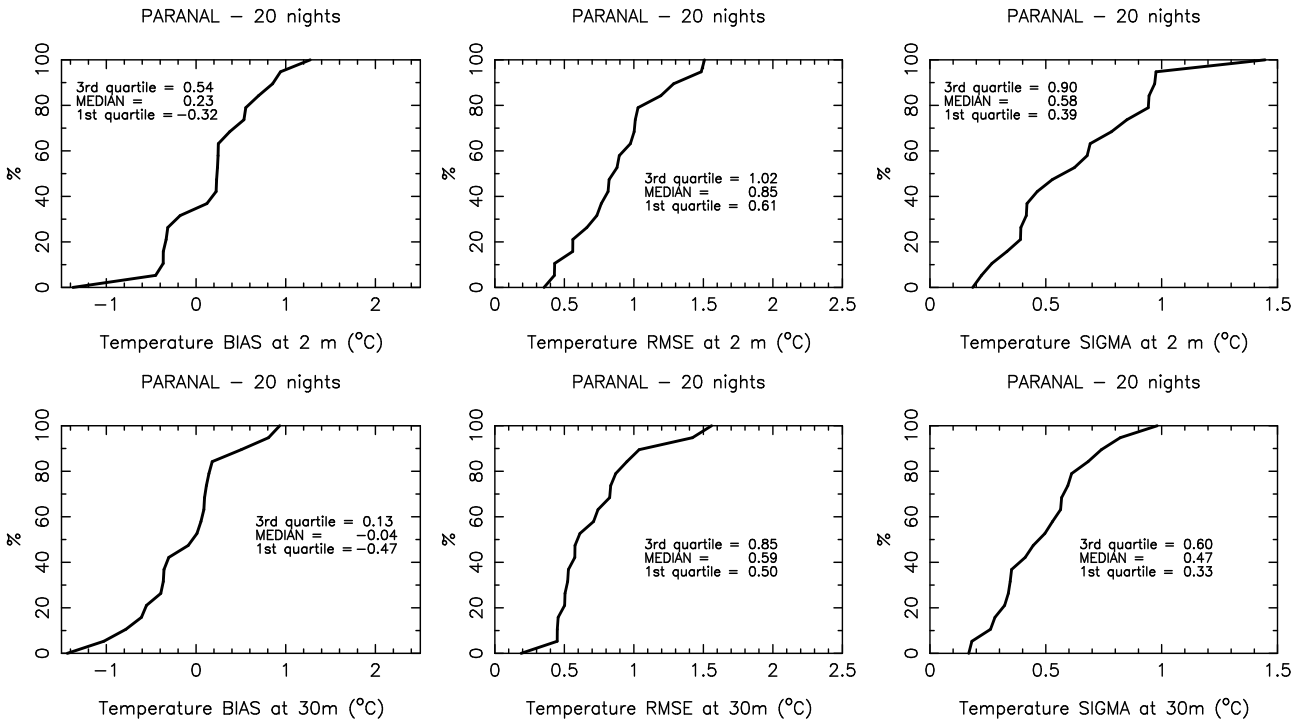

Figure 36: Cumulative distributions of the single nights bias (left), RMSE (middle) and bias-corrected RMSE (right) for the absolute temperature at Cerro Paranal, for the sample of 20 nights of 2007 (from the Phase A).

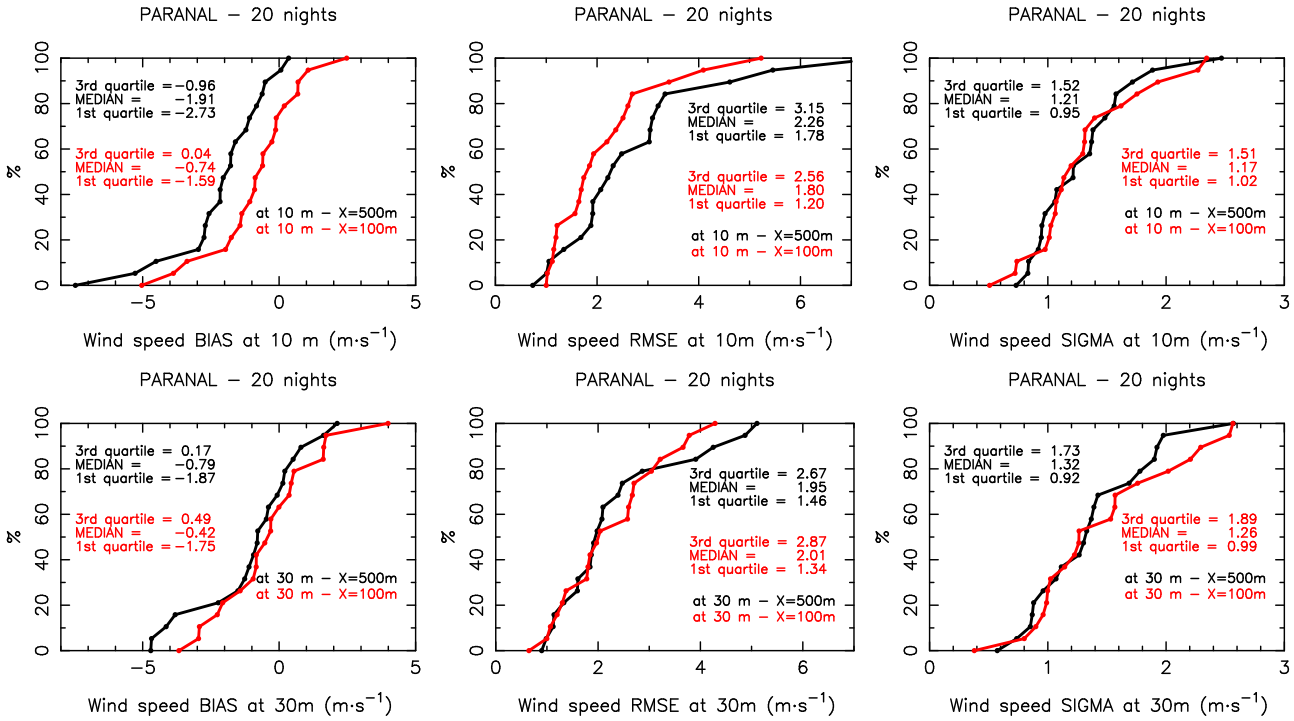

Figure 37: Cumulative distributions of the single nights bias (left), RMSE (middle) and bias-corrected RMSE (right) for the wind speed at Cerro Paranal, for the sample of 20 nights of 2007 (from the Phase A). In black, with the ΔX = 500 m configuration; in red, with the ΔX = 100 m configuration.

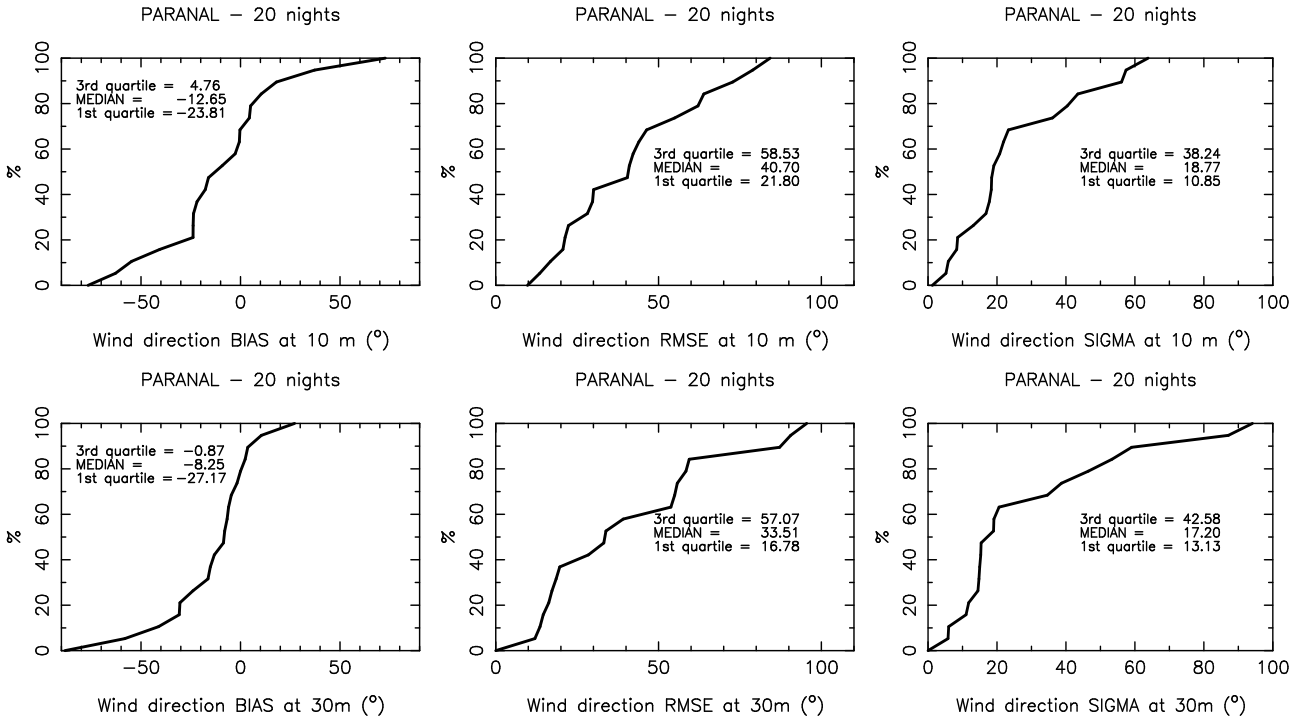

Figure 38: Cumulative distributions of the single nights bias (left), RMSE (middle) and bias-corrected RMSE (right) for the wind speed at Cerro Paranal, for the sample of 20 nights of 2007 (from the Phase A). The data with a wind velocity inferior to 3 m·s^{-1} are filtered out from the sample.

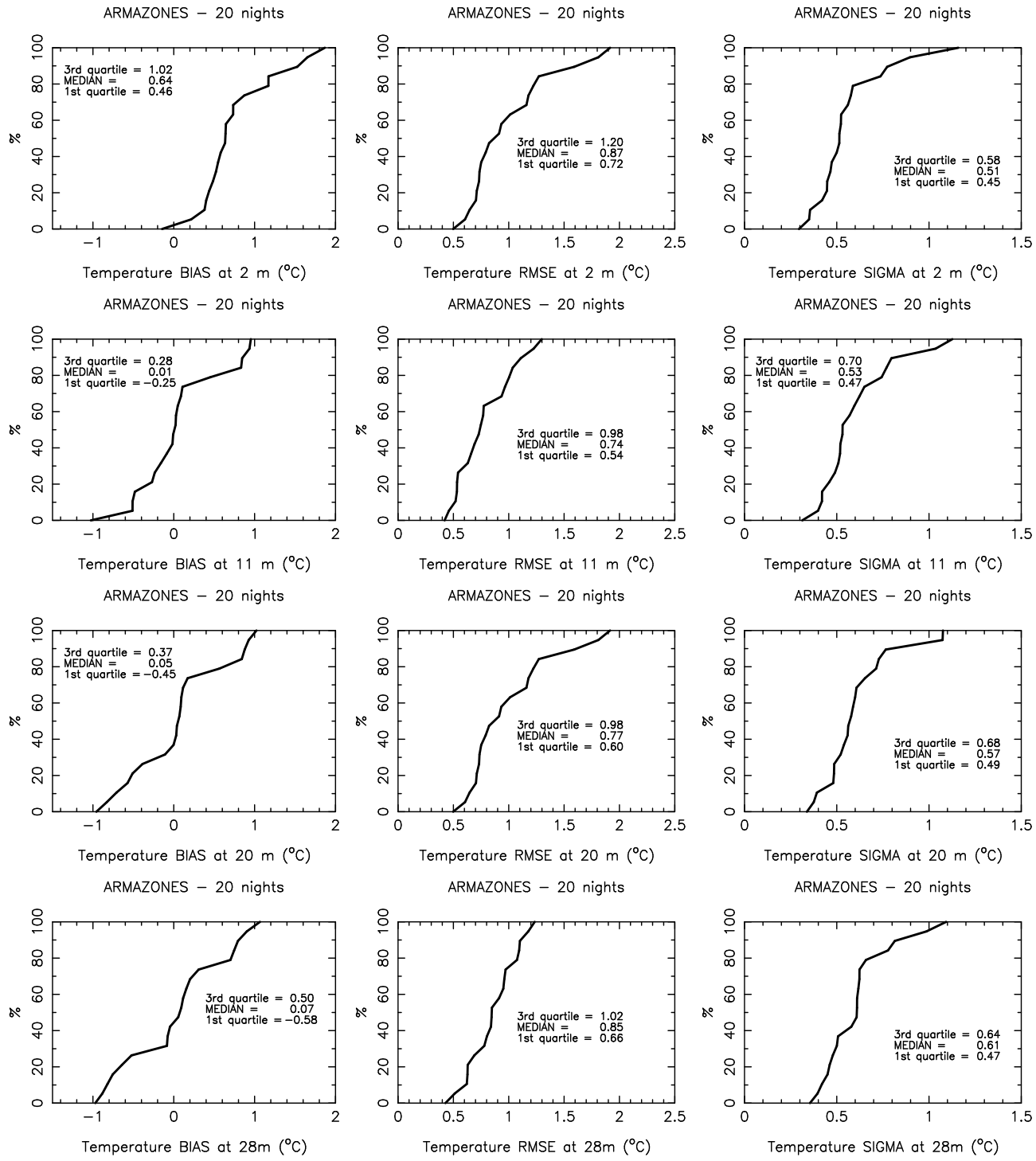

Figure 39: Cumulative distributions of the single nights bias (left), RMSE (middle) and bias-corrected RMSE (right) for the absolute temperature at Cerro Armazones, for the sample of 20 nights of 2007 (from the Phase A).

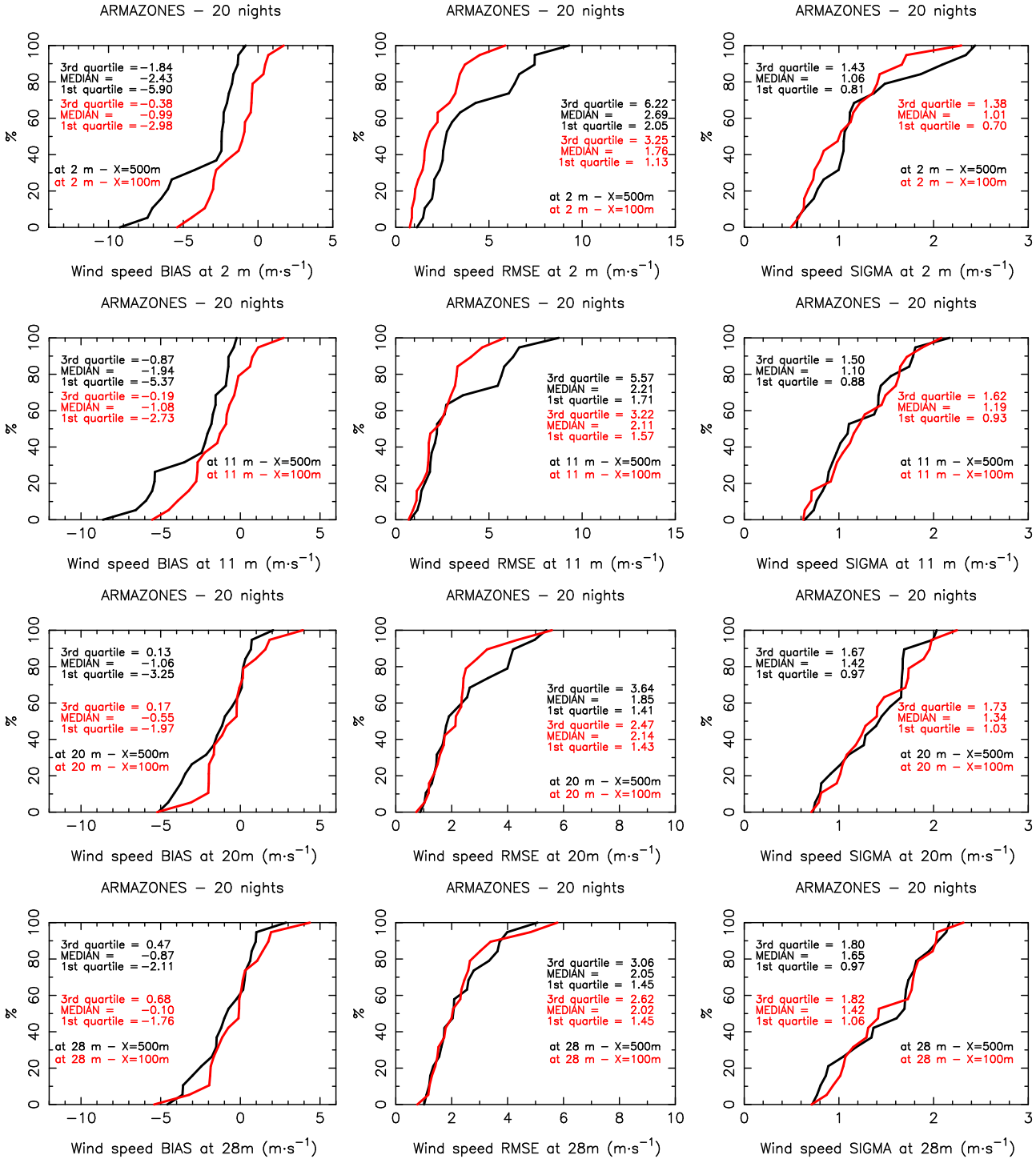

Figure 40: Cumulative distributions of the single nights bias (left), RMSE (middle) and bias-corrected RMSE (right) for the wind speed at Cerro Armazones, for the sample of 20 nights of 2007 (from the Phase A). In black, with the ΔX = 500 m configuration; in red, with the ΔX = 100 m configuration.

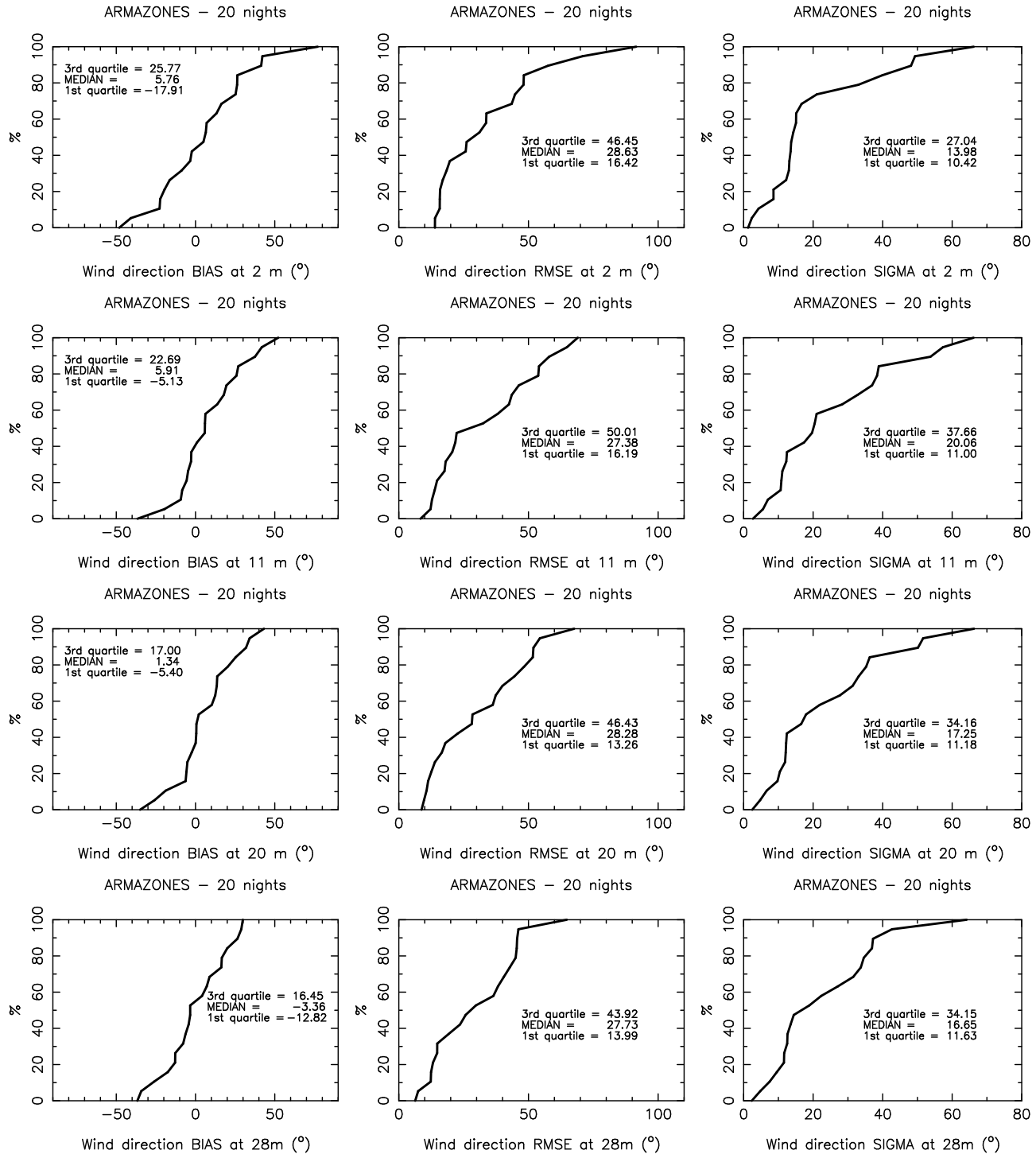

Figure 41: Cumulative distributions of the single nights bias (left), RMSE (middle) and bias-corrected RMSE (right) for the wind speed at Cerro Armazones, for the sample of 20 nights of 2007 (from the Phase A). The data with a wind velocity inferior to 3 m·s^{-1} are filtered out from the sample.

3 Work Package 1.3 - Model performances in reconstructing atmospheric parameters close to the ground using ECMWF FORECASTS as input and forcing: large statistical sample

In this section we report the statistical analysis of the forecasts of the 129 nights, for the surface meteorological parameters. Instead of using the ECMWF analyses (section 1) as initial and forcing conditions, we used the ECMWF forecasts, in order to evaluate if the good performance of the model is maintained with the use of initial conditions similar to a real-time configuration. The initialization and forcing data are the same that are supposed to be used for the operational configuration. We take all the forecasts calculated at 12:00 UT of the day (J-2) and reported Table 107. The main goal of this analysis performed with the forecast is to study how and if the model performances decrease in quality. Results we obtained are extremely positive and much better than expectations. For all the atmospherical parameters that we analyzed (temperature, wind speed and direction) we found that the PODs of forecasts are basically the same of the PODs of analyses, just a few percents lower. The reader can find in the next section of this Chapter the results obtained with scattering plots, individual nights (cumulative distribution) and temporal evolution). The most relevant result we obtained is therefore that the configuration that we chose

3.1 Cerro Paranal - 129 nights in 2007, 2010 and 2010

3.1.1 Scattered plots

	Absolute temperature (^{o}C)			
PARANAL	129 nights		20 nights	
ΔX = 500 m	2 m	30 m	2 m	30 m
BIAS	-0.02	-0.26	0.14	-0.17
RMSE	1.09	1.09	1.09	0.96
σ	1.09	1.06	1.08	0.94

Table 59: Near surface temperature **bias**, **RMSE** and bias-corrected RMSE σ (Meson-NH minus Observations), at Cerro Paranal. Initial conditions: ECMWF forecasts. Left: from the 129 nights sample. Right: from the 20 nights sample of Phase A.

	Wind speed (m$\cdot$s^{-1})			
PARANAL	129 nights		20 nights	
ΔX = 100 m	10 m	30 m	10 m	30 m
BIAS	-1.42	-0.60	-0.91	-0.46
RMSE	3.07	2.96	2.86	3.06
σ	2.73	2.90	2.71	3.02

Table 60: Near surface wind speed **bias**, **RMSE** and bias-corrected RMSE σ (Meson-NH with the high horizontal resolution configuration - $\mathbf{\Delta X = 100}$ **m** - minus Observations), at Cerro Paranal. Initial conditions: ECMWF forecasts. Left: from the 129 nights sample. Right: from the 20 nights sample of Phase A.

	Wind direction (^{o})			
PARANAL	129 nights		20 nights	
ΔX = 500 m	10 m	30 m	10 m	30 m
BIAS	3.7	-0.5	-1.0	-3.7
RMSE	38.6	37.6	43.3	41.3
RMSE$_{rel}$	21.4%	20.9%	24.0%	22.9%
σ	38.4	37.5	43.3	41.1

Table 61: Near surface wind direction **bias**, **RMSE** and bias-corrected RMSE σ (Meson-NH with the standard configuration - maximum ΔX = 500 m - minus Observations), at Cerro Paranal. Data with observed wind speed inferior to 3 m·s^{-1} are discarded. Initial conditions: ECMWF forecasts. Left: from the 129 nights sample. Right: from the 20 nights sample of Phase A.

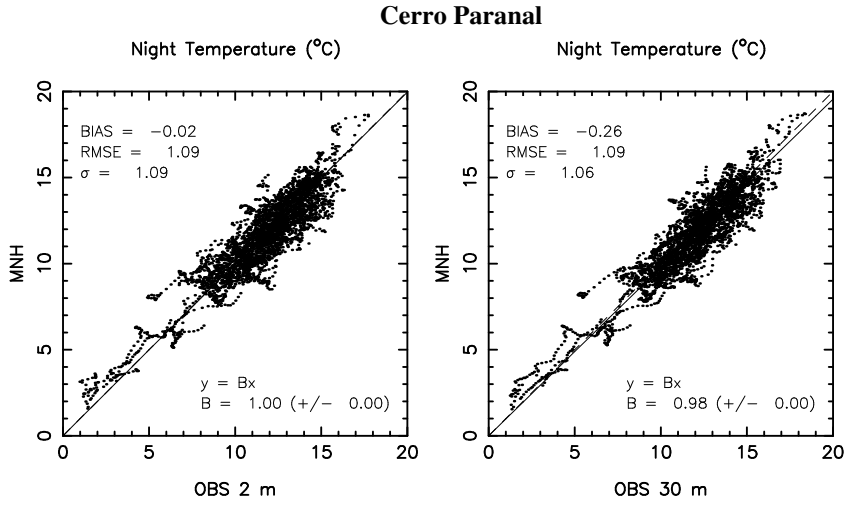

Figure 42: Scattered plot of Meso-NH **temperature** against observations, at 2 m and 30 m at **Cerro Paranal**, with the $\Delta X = 500$ m configuration. Initial conditions: ECMWF forecasts.

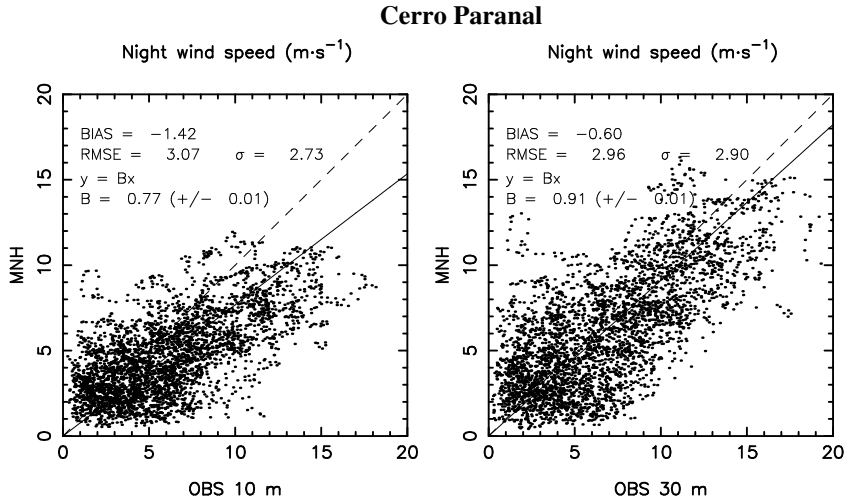

Figure 43: Scattered plot of Meso-NH **wind speed** against observations, at 10 m and 30 m at **Cerro Paranal**, with the $\Delta X = 500$ m configuration. Initial conditions: ECMWF forecasts.

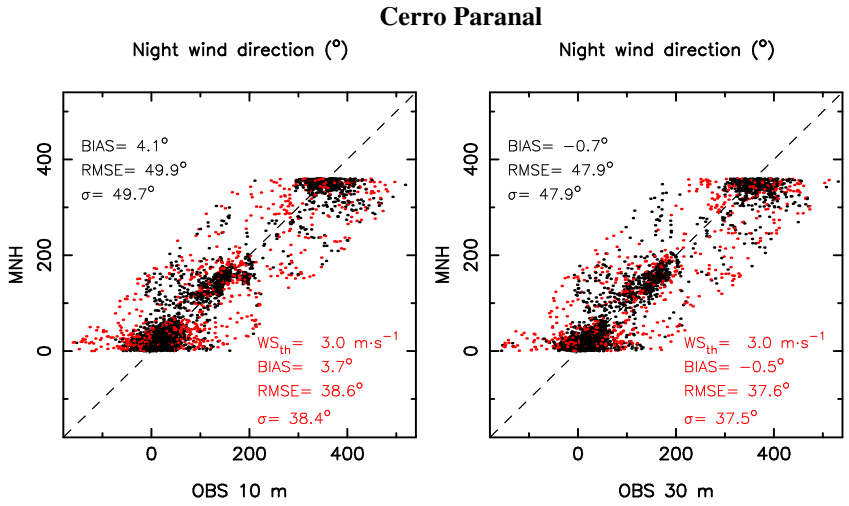

Figure 44: Scattered plot of Meso-NH **wind direction** against observations, at 10 m and 30 m at **Cerro Paranal**, with the $\Delta X = 500$ m configuration. Initial conditions: ECMWF forecasts. The dots in red are dots for which the wind speed was inferior to 3 m·s^{-1}. The values of bias, RMSE and σ reported in red corresponds to statistical computations with the red dots excluded.

3.1.2 Temporal evolutions

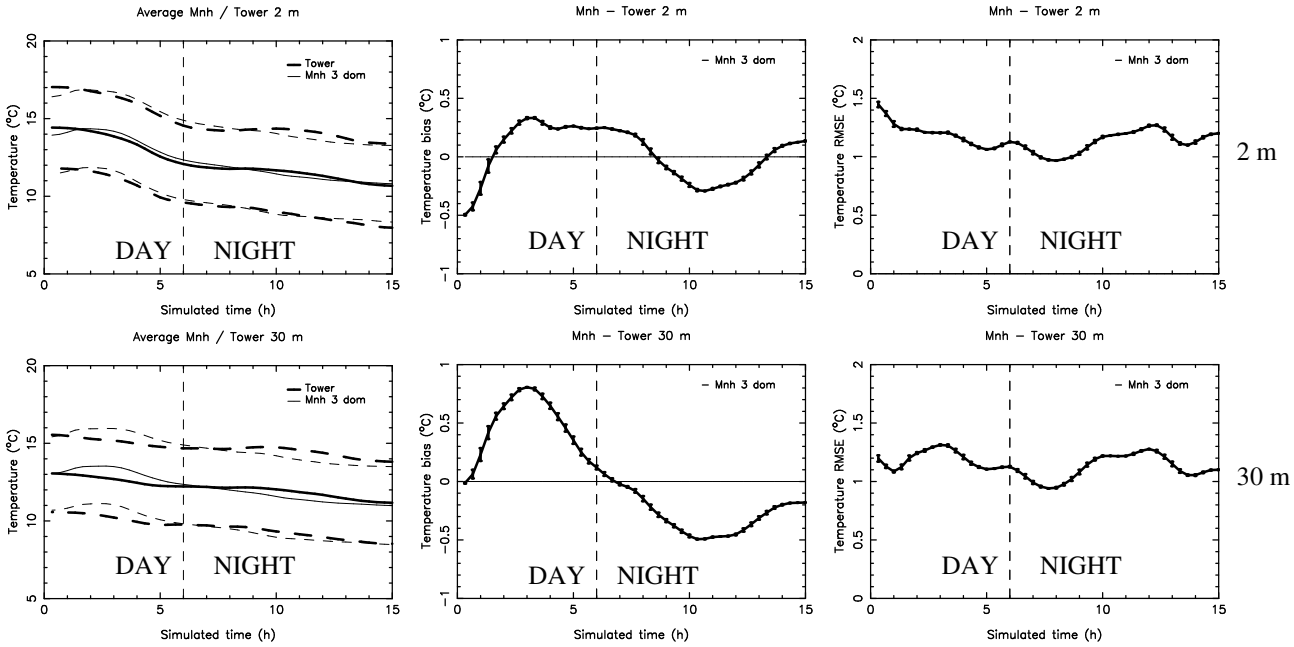

Figure 45: Temporal evolution of the **absolute temperature average** computed on the 129 nights sample (the bold line is the observation average and the thin line is Meso-NH average), **bias** (Mnh - Observations) and **RMSE** at **Cerro Paranal** (top: at 2 m); bottom: at 30 m). Initial conditions: **ECMWF forecasts**. The x-axis represents the time from the beginning of the simulation (00 h is 18 UT of the day before, 06 h is 00 UT, and 15 h is 09 UT). The nights starts at around 06 h (00 UT - 20 LT) and is delimited by the vertical dashed line. Meso-NH is with the $\Delta X = 500$ m configuration. The error bars represent $\pm$ the standard deviation.

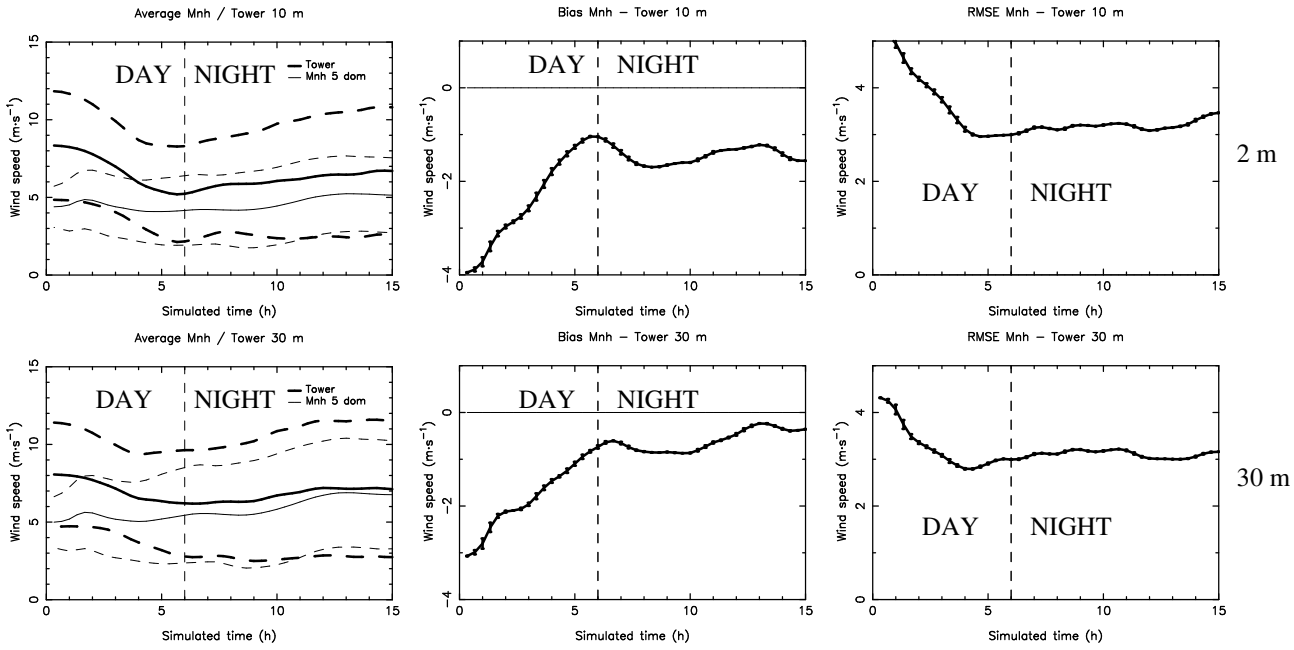

Figure 46: Same as Fig. 45 but for the **wind speed** at **Cerro Paranal** (top: at 10 m; bottom: at 30 m). Meso-NH is used with $\Delta X = 100$ m configuration.

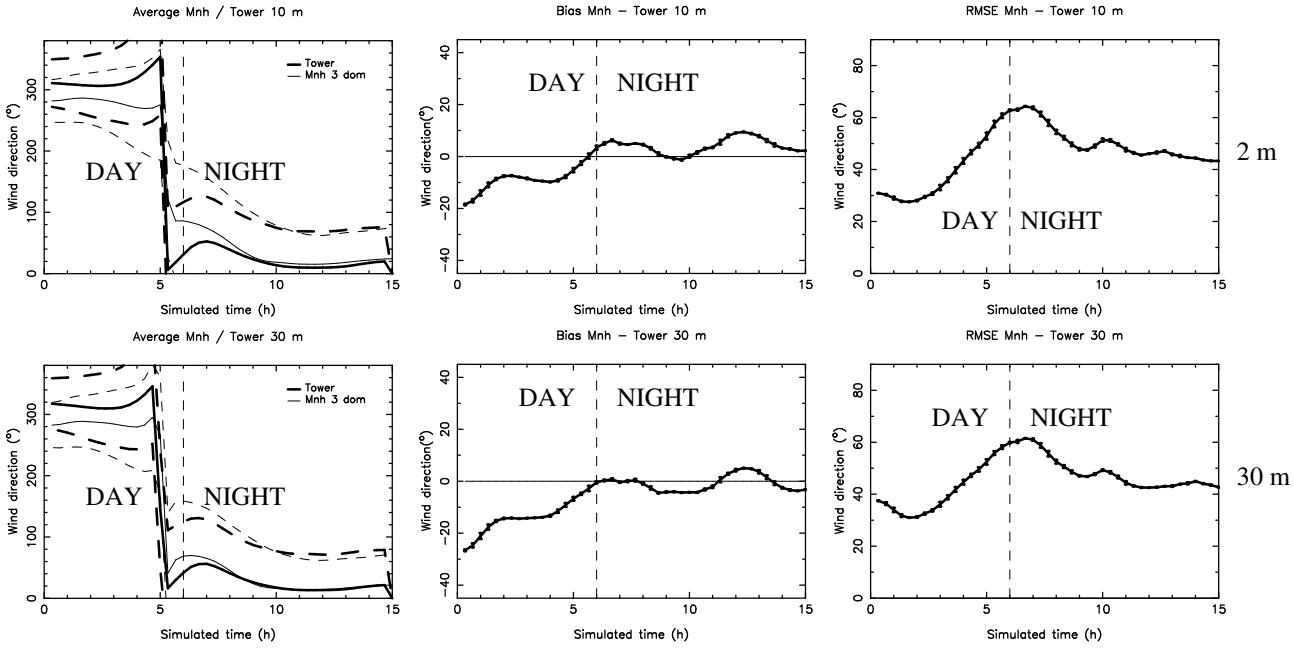

Figure 47: Same as Fig. 45 but for the **wind direction** at **Cerro Paranal** (top: at 10 m; bottom: at 30 m).

3.1.3 Contingency tables

TEMPERATURE

Division by tertiles (climatology) C. Paranal - 2 m		**OBSERVATIONS** $T < 11°C$	$11°C < T < 13.5°C$	$T > 13.5°C$
MODEL	$T < 11°C$	1103	285	4
	$11°C < T < 13.5°C$	158	979	278
	$T > 13.5°C$	0	201	475

Total points = 3483; PC=73.4%; EBD=0.1%
POD_1=87.5%; POD_2=66.8%; POD_3=62.7%

Table 62: 3×3 contingency table for the absolute temperature during the night, at 2 m a.g.l. at Cerro Paranal, on the 129 nights sample. Initial conditions: ECMWF forecasts. We use the Meso-NH ΔX = 500 m configuration.

Division by tertiles (climatology) C. Paranal - 30 m		**OBSERVATIONS** $T < 11.5°C$	$11.5°C < T < 13.5°C$	$T > 13.5°C$
MODEL	$T < 11.5°C$	1206	366	18
	$11.5°C < T < 13.5°C$	110	689	314
	$T > 13.5°C$	18	147	615

Total points = 3483; PC=72.1%; EBD=1.0%
POD_1=90.4%; POD_2=57.3%; POD_3=64.9%

Table 63: 3×3 contingency table for the absolute temperature during the night, at 30 m a.g.l. at Cerro Paranal, on the 129 nights sample. Initial conditions: ECMWF forecasts. We use the Meso-NH ΔX = 500 m configuration.

WIND SPEED

Division by tertiles (climatology) C. Paranal - 10 m		**OBSERVATIONS** $WS < 4\ m{\cdot}s^{-1}$	$4\ m{\cdot}s^{-1} < WS < 7\ m{\cdot}s^{-1}$	$WS > 7\ m{\cdot}s^{-1}$
MODEL	$WS < 4\ m{\cdot}s^{-1}$	629	399	88
	$4\ m{\cdot}s^{-1} < WS < 7\ m{\cdot}s^{-1}$	419	449	334
	$WS > 7\ m{\cdot}s^{-1}$	91	226	821

Total points = 3456; PC=54.9%; EBD=5.2%
POD_1=55.2%; POD_2=41.8%; POD_3=66.0%

Table 64: 3×3 contingency table for the wind speed during the night, at 10 m a.g.l. at Cerro Paranal, on the 129 nights sample. Initial conditions: ECMWF forecasts. We use the Meso-NH ΔX = 100 m configuration with the wind corrected by the multiplicative bias.

Division by tertiles (climatology) C. Paranal - 30 m		**OBSERVATIONS** $WS < 4\ m{\cdot}s^{-1}$	$4\ m{\cdot}s^{-1} < WS < 8\ m{\cdot}s^{-1}$	$WS > 8\ m{\cdot}s^{-1}$
MODEL	$WS < 4\ m{\cdot}s^{-1}$	541	406	34
	$4\ m{\cdot}s^{-1} < WS < 8\ m{\cdot}s^{-1}$	419	497	305
	$WS > 8\ m{\cdot}s^{-1}$	95	256	903

Total points = 3456; PC=56.2%; EBD=3.7%
POD_1=51.3%; POD_2=42.9%; POD_3=72.7%

Table 65: 3×3 contingency table for the wind speed during the night, at 30 m a.g.l. at Cerro Paranal, on the 129 nights sample. Initial conditions: ECMWF forecasts. We use the Meso-NH ΔX = 100 m configuration with the wind corrected by the multiplicative bias.

WIND DIRECTION

		OBSERVATIONS			
C. Paranal - all levels		N-E	S-E	S-W	N-W
MODEL	N-E	2649	150	36	739
	S-E	166	832	100	40
	S-W	47	68	70	48
	N-W	577	70	20	641

Total points = 6253 ; PC=67.0%; EBD=3.1%
$POD(NE)$=77.0%; $POD(SE)$=74.3%
$POD(SW)$=44.2%; $POD(NW)$=43.7%

Table 66: 4×4 contingency table for the wind direction α during the night, at 10 m, and 30 m a.g.l. at Cerro Paranal, on the 129 nights sample. Initial conditions: ECMWF forecasts. We use the Meso-NH ΔX = 500 m configuration. We filter out the data with an observed wind inferior to 3 $m{\cdot}s^{-1}$. NW corresponds to $0° < \alpha < 90°$; SW corresponds to $90° < \alpha < 180°$; SE corresponds to $180° < \alpha < 270°$; NE corresponds to $270° < \alpha < 360°$.

		OBSERVATIONS			
C. Paranal - all levels		N	E	S	W
MODEL	N	3751	447	41	110
	E	237	479	116	6
	S	49	191	544	36
	W	68	63	36	79

Total points = 6253; PC=77.6% ; EBD=2.5%
$POD(N)$=91.4%; $POD(E)$=40.6%
$POD(S)$=73.8%; $POD(W)$=34.2%

Table 67: 4×4 contingency table for the wind direction α during the night, at 10 m, and 30 m a.g.l. at Cerro Paranal, on the 129 nights sample. Initial conditions: ECMWF forecasts. We use the Meso-NH ΔX = 500 m configuration. We filter out the observed wind inferior to 3 $m{\cdot}s^{-1}$. N corresponds to $-45° < \alpha < 45°$; E corresponds to $45° < \alpha < 135°$; S corresponds to $135° < \alpha < 225°$; W corresponds to $225° < \alpha < 315°$.

3.1.4 Wind direction contingency tables, under strong wind speed conditions ($WS > 12\ m{\cdot}s^{-1}$)

Here we present the contingency tables for the wind direction between model and observation, with a filter on the wind speed. We consider in these tables only the points for which the observed wind speed is superior to 12 $m{\cdot}s^{-1}$. The reason of this test is to investigate how good or bad is the model behavior in reconstructing the wind direction in the most critical conditions from an astronomical point of view i.e. when the wind speed is particularly strong. Table 68 is the contingency table for the wind direction at 10m and 30m. Results tell us that the model performances in reconstructing the wind flowing from the North-East (NE) is excellent (> 90%) even better for the wind direction at 10 m. This is also the sector in which the wind speed is more frequent. The model has also an excellent behavior (100%) in reconstructing the wind direction from the South-East (SE) also if it is not so frequent that wind flows from this direction when the wind speed is > 12 ms^{-1}. The POD(NW) is equal to 71.1% (at 10 m) and 56.4% (at 30 m) that is still very good even if slightly inferior with respect to the previous cases. To conclude, the model correctly do not reconstruct wind direction flowing from the SW. The wind direction basically never flows from this direction.

		OBSERVATIONS			
C. Paranal - (10 m / 30 m)		N-E	S-E	S-W	N-W
MODEL	N-E	367/462	0/0	0/0	37/71
	S-E	1/0	9/49	0/0	0/0
	S-W	0/0	0/0	0/0	0/0
	N-W	18/49	0/0	0/0	91/92

Total points = 523/723 ; PC=89.3%/83.4%; EBD=0%/0%
$POD(NE)$=95.1%/90.4%; $POD(SE)$=100%/100%
$POD(SW)$=NaN / NaN; $POD(NW)$=71.1%/56.4%

Table 68: 4×4 contingency table for the wind direction α during the night, at 10 m (left values), and 30 m (right values) a.g.l. at Cerro Paranal, on the 129 nights sample. Initial conditions: ECMWF forecasts. We use the Meso-NH ΔX = 500 m configuration. We filter out the data with an observed wind inferior to 12 $m{\cdot}s^{-1}$. NW corresponds to $0° < \alpha < 90°$; SW corresponds to $90° < \alpha < 180°$; SE corresponds to $180° < \alpha < 270°$; NE corresponds to $270° < \alpha < 360°$.

3.1.5 Individual nights model performances

In this section we present the analysis done on the model performances in reconstructing the atmospheric parameters, night by night, on the 129 nights sample, at Cerro Paranal, using the ECMWF forecasts as initial conditions and forcing.

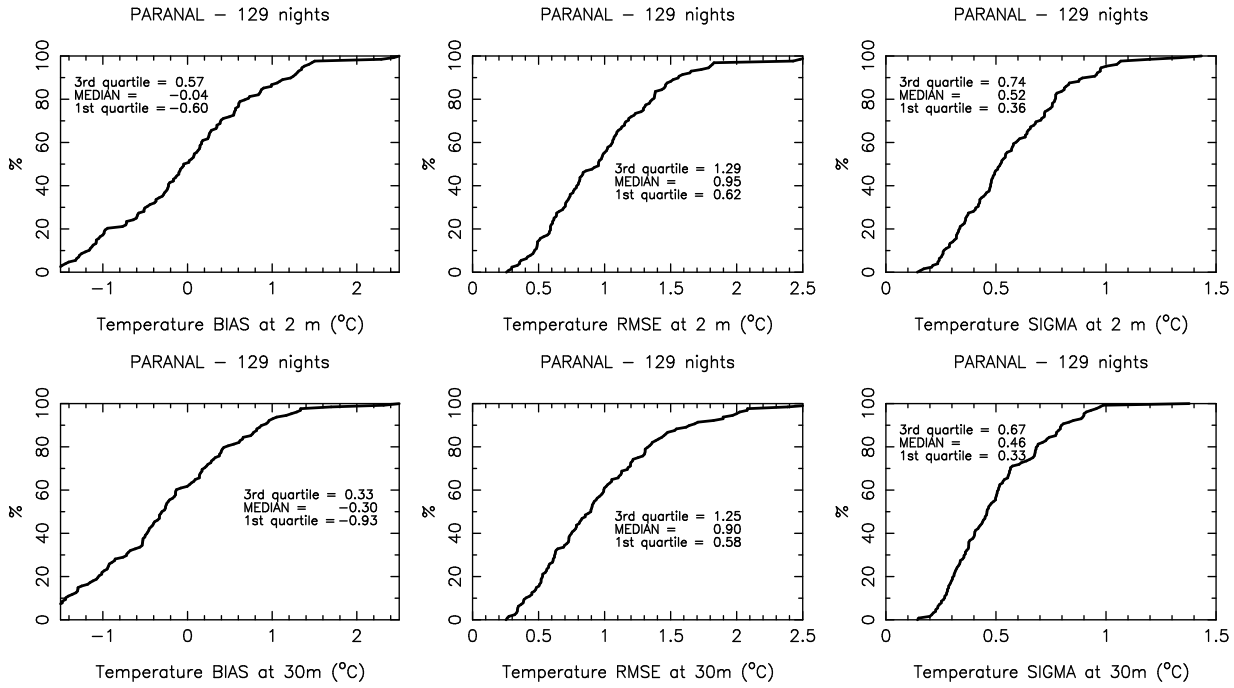

Figure 48: Cumulative distributions of the single nights bias (left), RMSE (middle) and bias-corrected RMSE (right) for the absolute temperature at Cerro Paranal, for the sample of 129 nights of 2007, 2010 and 2011. Initial conditions: ECMWF forecasts.

Absolute temperature (^{o}C)

	PARANAL - 20 nights		PARANAL - 129 nights	
	2 m	30 m	2 m	30 m
BIAS	$0.25^{+0.80}_{-0.42}$	$-0.19^{+0.58}_{-0.70}$	$-0.04^{+0.57}_{-0.60}$	$-0.30^{+0.33}_{-0.93}$
RMSE	$1.05^{+1.30}_{+0.69}$	$0.80^{+1.05}_{+0.62}$	$0.95^{+1.29}_{+0.62}$	$0.90^{+1.25}_{+0.58}$
σ	$0.56^{+0.97}_{+0.33}$	$0.46^{+0.70}_{+0.33}$	$0.52^{+0.74}_{+0.36}$	$0.46^{+0.67}_{+0.33}$

Table 69: Near surface median, **bias**, **RMSE** and **bias-corrected RMSE** σ (Meson-NH minus Observations), of the **temperature** from the single nights values, from the original 20 nights sample on the left, and from the extended 129 nights sample on the right (see Fig. 48). In small fonts, the 1st and 3rd quartiles.

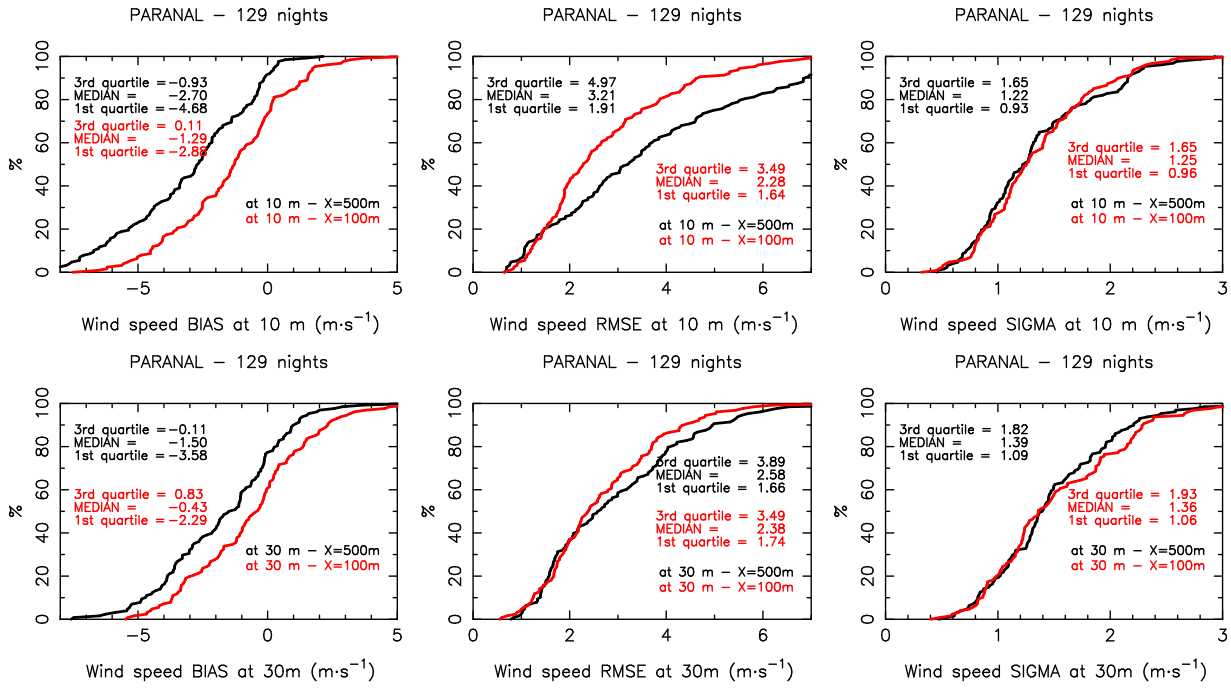

Figure 49: Cumulative distributions of the single nights bias (left), RMSE (middle) and bias-corrected RMSE (right) for the wind speed at Cerro Paranal, for the sample of 129 nights of 2007, 2010 and 2011. The results for both $\Delta X = 500$ m (in black) and $\Delta X = 100$ m (in red) configurations are reported. Initial conditions: ECMWF forecasts.

Wind speed (m·s^{-1})

	PARANAL - 20 nights		PARANAL - 129 nights	
	10 m	30 m	10 m	30 m
BIAS	$-0.98^{+0.12}_{-1.72}$	$-0.60^{+0.51}_{-2.02}$	$-1.29^{+0.11}_{-2.88}$	$-0.43^{+0.83}_{-2.29}$
RMSE	$1.77^{+2.76}_{+1.41}$	$1.90^{+3.28}_{+1.25}$	$2.28^{+3.49}_{+1.64}$	$2.38^{+3.49}_{+1.74}$
σ	$1.13^{+1.34}_{+1.01}$	$1.17^{+1.27}_{+0.95}$	$1.25^{+1.65}_{+0.96}$	$1.36^{+1.93}_{+1.06}$

Table 70: Near surface median, **bias**, **RMSE**, and **bias-corrected RMSE** σ (Meson-NH minus Observations), of the **wind speed** with the $\Delta X = 100$ m configuration. from the single nights values, from the original 20 nights sample on the left, and from the extended 129 nights sample on the right (see Fig. 49). In small fonts, the 1st and 3rd quartiles.

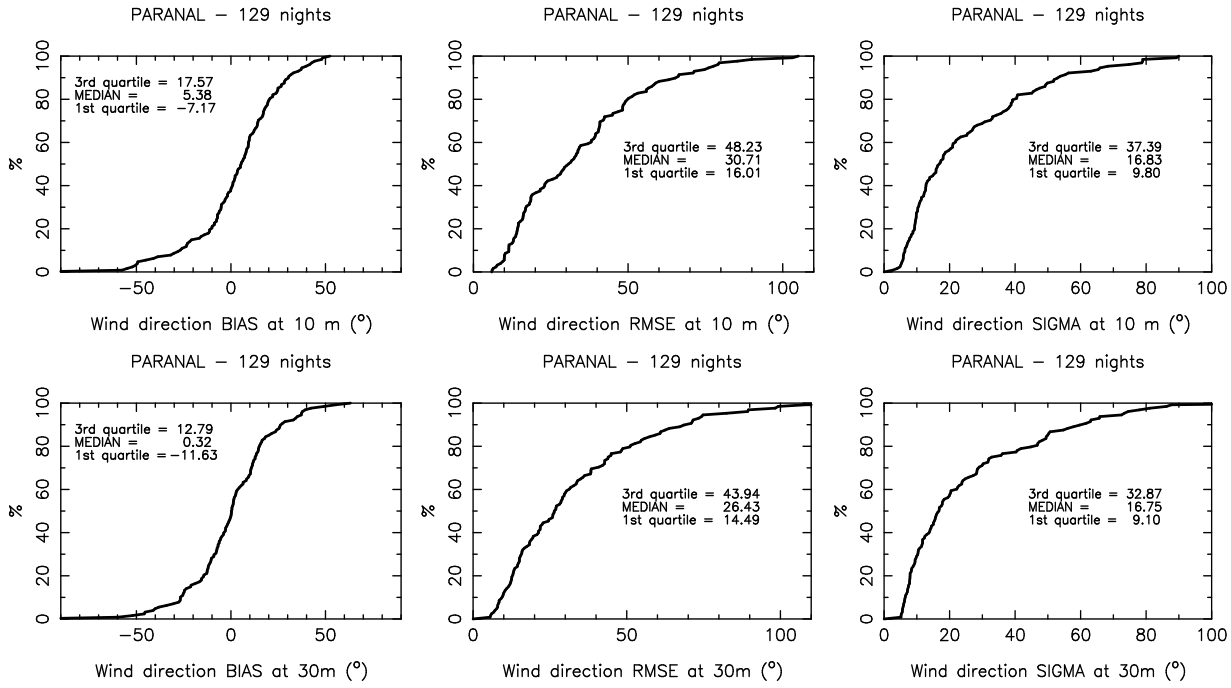

Figure 50: Cumulative distributions of the single nights bias (left), RMSE (middle) and bias-corrected RMSE (right) for the wind direction at Cerro Paranal, for the sample of 129 nights of 2007, 2010 and 2011. The data with a wind velocity inferior to 3 m·s^{-1} are filtered out from the sample. Initial conditions: ECMWF forecasts.

Wind direction (^{o})

	PARANAL - 20 nights		PARANAL - 129 nights	
	10 m	30 m	10 m	30 m
BIAS	$2.20^{+15.07}_{-11.54}$	$-4.1^{+4.06}_{-14.10}$	$5.38^{+17.57}_{-7.17}$	$0.32^{+12.79}_{-11.63}$
RMSE	$39.87^{+50.44}_{+24.39}$	$28.08^{+48.75}_{+19.38}$	$30.71^{+48.23}_{+16.01}$	$26.43^{+43.94}_{+14.49}$
σ	$19.55^{+39.97}_{+11.58}$	$17.12^{+41.25}_{+10.80}$	$16.83^{+37.39}_{+9.80}$	$16.75^{+32.87}_{+9.10}$

Table 71: Near surface median, **bias**, **RMSE**, and **bias-corrected RMSE** σ (Meson-NH minus Observations), of the **wind direction** from the single nights values, from the original 20 nights sample on the left, and from the extended 129 nights sample on the right (see Fig. 50). The data with a wind velocity inferior to 3 m·s^{-1}) are filtered out from the samples. In small fonts, the 1st and 3rd quartiles.

3.1.6 Trends

In this section we present the results of the contingency tables for the wind speed trend. We analyze the performance of the model in reproducing the good trend for the wind speed during the night. The night is divided in N parts where the wind speed is averaged, and we define the trend Δ as the difference between two successive averaged wind speed between two contiguous regions. We have then N-1 values for Δ for each night, both for observations (Δ_{obs}) and Meso-NH model (Δ_{mnh}). We compare (Δ_{obs}) and (Δ_{mnh}) using 3×3 contingency tables, divided in three sectors: negative trend, stable trend and positive trend. A trend is negative when $\Delta < \Delta_{lim1}$ (where $\Delta_{lim1} < 0$), positive when $\Delta > \Delta_{lim2}$ (where $\Delta_{lim2} > 0$), and stable when $\Delta_{lim1} < \Delta < \Delta_{lim2}$. To have an idea of the order of magnitude of Δ_{lim1} and Δ_{lim2}, we have computed the median values of the observations. They are summarized in Table 72. We see that the median value of the absolute values is of the order of 1.5 ms^{-1} or even less. Also we observe that, as it is normal to expect, the median values decreases with the N.

First, we look at the case $\Delta_{lim1} = \Delta_{lim2} = 0$ i.e. we consider only the positive and negative trends. This means

Medians at 10 m - in $m{\cdot}s^{-1}$

Number of intervals per night	All $\lvert\Delta_{obs}\rvert$	Only $\Delta_{obs} < 0$	Only $\Delta_{obs} > 0$
N=2	1.59	-1.28	2.30
N=3	1.33	-1.30	1.51
N=5	0.93	-0.79	1.00

Medians at 30 m - in $m{\cdot}s^{-1}$

Number of intervals per night	All $\lvert\Delta_{obs}\rvert$	Only $\Delta_{obs} < 0$	Only $\Delta_{obs} > 0$
N=2	2.01	-1.38	2.31
N=3	1.63	-1.58	1.64
N=5	1.02	-0.99	1.05

Table 72: Median values of the observed trends for rhe wind speed, in $m{\cdot}s^{-1}$.

that the contingency tables is not 3×3 but a simpler 2×2 (Tables 73 and 74). When N=3 the night is divided in 3 parts, when N=5 the night is divided in 5 parts. The results are very satisfactory, with POD_i between 55.6% and 83.2% (for N=3). For N=5 (not reported here), the POD_i are good, only slightly lower than for N=3, between 52.5% and 72.9%. The results are very close to the POD_i obtained for simulations initialized with the analyses of the ECMWF instead of the forecasts (between 59.4% and 82.2% for N=3, not reported here).

If we choose Δ_{lim1} and Δ_{lim2} different from 0, thus analysing 3×3 contingency tables, the division between

3 intervals of 3 hours per night		**OBSERVATIONS**	
	C. Paranal - 10 m	Negative trend	Positive trend
MODEL	Negative trend	55	30
	Positive trend	44	127

Total points = 256; PC=71.1%
POD_1=55.6%; POD_2=80.9%

Table 73: 2×2 contingency table for the wind speed trend during the night, at 10 m a.g.l. at Cerro Paranal, on the 129 nights sample. The nights are divided in three intervals of 180 min each. Initial conditions: ECMWF forecasts. We use the Meso-NH ΔX = 100 m configuration with the wind corrected by the multiplicative bias.

negative/stable/positive seems less reliable than the division negative/positive. First we selected as a thresholds

3 intervals of 3 hours per night		OBSERVATIONS	
	C. Paranal - 30 m	Negative trend	Positive trend
MODEL	Negative trend	59	26
	Positive trend	42	129

Total points = 256; PC=73.4%
POD_1=58.4%; POD_2=83.2%

Table 74: 2×2 contingency table for the wind speed trend during the night, at 10 m a.g.l. at Cerro Paranal, on the 129 nights sample. The nights are divided in three intervals of 180 min each. Initial conditions: ECMWF forecasts. We use the Meso-NH ΔX = 100 m configuration with the wind corrected by the multiplicative bias.

the median values of the Δs. For N=3 (Table 75 and Table 76), with $\Delta_{lim1} = -1.3\ m{\cdot}s^{-1}$ and $\Delta_{lim2} = 1.5\ m{\cdot}s^{-1}$ (median values), the POD_i are between 39.6% (POD_1 at 10 m) and 76% (POD_2 at 30 m), with a PC around 60%. Doing successive tests simply changing a little the thresholds ($\Delta_{lim1} = -1\ m{\cdot}s^{-1}$ and $\Delta_{lim2} = 1\ m{\cdot}s^{-1}$ close to those values, Tables 77 and 78), we obtained similar results but with a better POD_3 (from 43.3% to 57.7% at 10 m and from 56.1% to 66% at 30 m).

In general, when the number of intervals that divide the night is higher (N=5, cf. the corresponding powerpoint slides available in the BSCW), PC_i and POD_i are a bit lower.

We also tested with the thresholds defined as a ratio of the wind speed between two consecutive intervals, instead of the difference. However, the results are not much different than the ones using the differences presented before. For example, using 20% as a threshold, the PC_i are now around 59%, and the POD_i between 43.6% and 66%.

In occasion of the Final Review of MOSE - Phase it has been observed that a negative/stable/positive might be useful but only for large values of Δ that could force ESO staff to close the dome or interrupt observations. We therefore included here a further calculation. First we highlight that the data have been treated, as all the other data in the report, with a moving average of 1 hour and resampled with a time scale of 20 minutes. This means that the high frequencies are filtered out. In other words we are considering the trends at low spatial frequency. It is therefore a no sense to consider large delta values because there are no observed events in which the variation of the wind intensity is larger than 3 ms^{-1}, even in the case in which we take N=2 (the case in which typically we can observe the largest value of Δ). We tested this extreme case with N=2 (as requested by the ESO Board) and Δ_{lim1} = -3 and Δ_{lim1} = 3 (the largest observed Δ) and we verified that the POD_3 is equal to 65% at 10 m, and it is equal to 75% at 30m. This tells us that the system should be able to detect with good performances the sudden increasing of the wind speed with a good score of success.

$\Delta_{lim1} = -1.3$ $m{\cdot}s^{-1}$ - $\Delta_{lim2} = 1.5$ $m{\cdot}s^{-1}$ - $N = 3$		**OBSERVATIONS**		
C. Paranal - 10 m		Negative trend	Stable trend	Positive trend
MODEL	Negative trend	21	12	1
	Stable trend	26	90	36
	Positive trend	1	27	42

Total points = 256; PC=59.8%; EBD=0.8%
POD_1=43.7%; POD_2=69.8%; POD_3=53.2%

Table 75: 3×3 contingency table for the wind speed trend during the night, at 10 m a.g.l. at Cerro Paranal, on the 129 nights sample. The nights are divided in three intervals of 180 min each. Initial conditions: ECMWF forecasts. We use the Meso-NH ΔX = 100 m configuration with the wind corrected by the multiplicative bias.

$\Delta_{lim1} = -1.6$ $m{\cdot}s^{-1}$ - $\Delta_{lim2} = 1.6$ $m{\cdot}s^{-1}$ - $N = 3$		**OBSERVATIONS**		
C. Paranal - 30 m		Negative trend	Stable trend	Positive trend
MODEL	Negative trend	22	11	1
	Stable trend	23	87	30
	Positive trend	3	28	51

Total points = 256; PC=62.5%; EBD=1.6%
POD_1=45.8%; POD_2=69.0%; POD_3=62.2%

Table 76: 3×3 contingency table for the wind speed trend during the night, at 30 m a.g.l. at Cerro Paranal, on the 129 nights sample. The nights are divided in three intervals of 180 min each. Initial conditions: ECMWF forecasts. We use the Meso-NH ΔX = 100 m configuration with the wind corrected by the multiplicative bias.

$\Delta_{lim1} = -1$ $m{\cdot}s^{-1}$ - $\Delta_{lim2} = 1$ $m{\cdot}s^{-1}$ - N=3		**OBSERVATIONS**		
C. Paranal - 10 m		Negative trend	Stable trend	Positive trend
MODEL	Negative trend	27	11	4
	Stable trend	21	54	36
	Positive trend	8	31	64

Total points = 256; PC=56.6%; EBD=4.7%
POD_1=48.2%; POD_2=56.2%; POD_3=61.5%

Table 77: 3×3 contingency table for the wind speed trend during the night, at 10 m a.g.l. at Cerro Paranal, on the 129 nights sample. The nights are divided in three intervals of 180 min each. Initial conditions: ECMWF forecasts. We use the Meso-NH ΔX = 100 m configuration with the wind corrected by the multiplicative bias.

$\Delta_{lim1} = -1\ m{\cdot}s^{-1}$ - $\Delta_{lim2} = 1\ m{\cdot}s^{-1}$ - N=3 C. Paranal - 30 m		**OBSERVATIONS** Negative trend	Stable trend	Positive trend
MODEL	Negative trend	31	13	3
	Stable trend	21	47	31
	Positive trend	12	30	69

Total points = 256; PC=57.4%; EBD=5.9%
POD_1=48.4%; POD_2=52.8%; POD_3=67.0%

Table 78: 3×3 contingency table for the wind speed trend during the night, at 30 m a.g.l. at Cerro Paranal, on the 129 nights sample. The nights are divided in three intervals of 180 min each. Initial conditions: ECMWF forecasts. We use the Meso-NH ΔX = 100 m configuration with the wind corrected by the multiplicative bias.

4 Work Package 1.4 - Figures of merit

As widely discussed in our previous reports/articles (see among other the MOSE Report - Phase A and [53]), the identification of the figures of merit to quantify the model performances is a very delicate topic. Because of arguments presented in [53]-Introduction we decided, in agreement with the ESO Board, to consider a set of figure of merit that, all together, should contribute to provide indicators of the goodness of the model prediction.

The first three fundamental parameters are the bias, the RMSE and the sigma (as defined in [51]) on a as rich as possible sample of nights. The bias provides informations on the systematic errors, the RMSE on the statistical errors, the sigma on the statistical errors at which we have subtracted the systematic errors. The values of sigma tells us the ultimate uncertainty expressed in statistical terms. It is very important to consider the respective values of bias, RMSE and sigma obtained considering different instruments to have a reference with respect to which compare the model performances. We remind that the values of sigma calculated between different instruments provides an order of magnitude of the accuracy of the individual parameters that have to be taken into account when the model performances is analyzed.

Beside to this statistical operators, we think it can be interesting to consider the trend as described in Section 3.1.6. For what concerns the atmospherical parameters at present we have considered the trends only for the wind speed. Because of the arguments presented in Section 1 we think that such a figure of merit is not useful for the relative humidity close to the ground. For what concerns the temperature close to the ground it is possible to calculate that even if we think that the most useful information is the temporal evolution during the time, particularly at the beginning of the night to thermalize the telescopes's domes.

At the end of MOSE - Phase A we proposed to use, beside to the cited operators, also a few further parameters retrieved from the contingency tables (see [53] for more details) (3×3 for all the atmospheric parameters and astroclimatic parameters with exception of the wind direction that requires a 4×4 contingency table). These parameters are: (1) the percent of correct forecast (PC) (see definition in [53]), (2) the probability to forecast the parameter X with values included in a particular rnage of values (POD) (see definition in [53]) and (3) extremely bad detection (EBD) (see definition in [53]).

In the case of 3×3 contingency tables, the three subranges are: $x_i < 1^{st}$ tertile, 1^{st} tertile $< x_i < 3^{rd}$ tertile and $x_i > 3^{rd}$ tertile. The tertiles are calculated on a rich statistical sample of observations. In the case of 4×4 contingency table i.e. for the wind direction the sub-ranges we considered so far are: (a) North-East, South-West, South-East, North-West and (b) North, East, South, West.

5 Work Package 2.1 - Improvement of the optical turbulence algorithm in the free atmosphere

The state of art is that we have 20 nights (calibration sample) plus the validation sample made by 53 nights in 2010/2011 and 36 nights in 2007 for a total of 89 nights. The latter represents the validation sample.
In order to improve the peak-to-valley temporal evolution of some astroclimatic parameters (free-atmosphere seeing, isoplanatic angle), the OT algorithm has been modified. Scientific justifications for such a modification will be presented in a forthcoming paper.

The C_N^2 is corrected by a term depending on the wind shear:

$$\begin{aligned} &For\ h < 700\ m,\ C_N^2(h)^* = C_N^2(h) \\ &For\ h > 700\ m,\ C_N^2(h)^* = \mathbf{A} \cdot C_N^2(h) \end{aligned} \tag{1}$$

with

$$\mathbf{A} = \begin{cases} \mathbf{A_1} = [(\frac{dV_x}{dz})^2 + (\frac{dV_y}{dz})^2]^\beta / < [(\frac{dV_x}{dz})^2 + (\frac{dV_y}{dz})^2]^\beta > \ with\ \beta\ \epsilon\ [\frac{1}{2}, 1, \frac{3}{2}] \\ or \\ \mathbf{A_2} = [(\frac{dV}{dz})^2]^\beta / < [(\frac{dV}{dz})^2]^\beta > \ with\ \beta\ \epsilon\ [\frac{1}{2}, 1, \frac{3}{2}] \end{cases} \tag{2}$$

V_x and V_y are the horizontal components of the wind speed. V is the module of the horizontal wind. We highlight that originally our model outputs provided only the module of the wind speed. In the context of this analysis we added to the set of the model outputs also the two components of the wind speed (V_x and V_y) and we repeated the simulations on the sub-sample of the 20 nights (of the calibration) plus the 36 nights of the 2007 so to evaluate the behavior of the algorithm using the two components V_x and V_y (instead of the modulus) on a representative statistical sub-sample. A_1 can not be tested on the all 89 nights. On the sub-sample of nights where both A_1 and A_2 have been used, we were able to conclude that the differences on the correction factor were minor (not shown in this report). Also we tested the sensibility of the threshold of 700 m applying the correction using 600 m as a threshold. In the same way we verified that the results differed by negligible quantities. That's why in the rest of this section, the C_N^2 profiles have been corrected with the coefficient A_2, allowing us to analyze the whole validation sample. We do not show all the intermediate steps, however the best fit is obtained with $\beta = \frac{3}{2}$. All the following analysis is based on these corrected C_N^2 profiles. Fig.51 shows, as an example, the temporal evolution of the C_N^2 in its standard form and after the correction. In the same picture is also shown the temporal evolution of the factor A_1. In Annex C the reader can find the correction coefficient A_1 for all the nights of the PAR2007 site testing campaign. Besides it is also reported the C_N^2 temporal evolution before and after correction of the algorithm.

We analyze 3×3 contingency tables. To appreciate the difference we would obtain using as a forecast method the climatological median (of whatever astroclimatic parameter) the reader can have a look to the contingency table shown in Table 79. **The method of the climatological median provides a probability to detect the parameter we intend to study of 100 % for values between the first and third tertiles but a probability of 0 % for values smaller or larger than the first and third tertiles. These interval are, however, the most interesting from an astronomical point of view. We also remind that, the random case has the values of PC, POD$_i$ (with i=1, 2 and 3) is equal to 33%.**

It is also important to mention that an important result of our analysis (see Report of Phase A) puts in evidence that the model calibration for seeing seeing and isoplanatic angle are *'season dependent'*. With this we mean that the model should be calibrated with different data related to the two seasons: winter and summer. However, in our study the unique available Generalized SCIDAR measurements for the calibration refer to the site testing campaign (PAR2007) performed in November and December i.e. in summer. For this two astroclimatic parameters (seeing and isoplanatic angle) we report therefore the results obtained for the validation

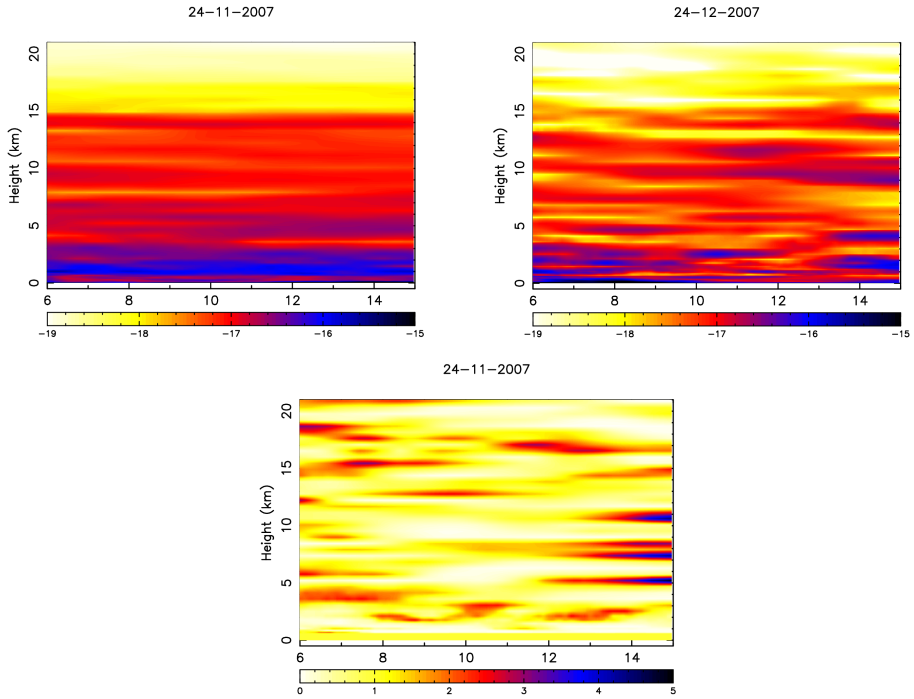

Figure 51: Temporal evolution of the C_N^2 during the night of 24/11/2007 in its standard form (top left) and after the correction with the factor A_1 (top right). On the bottom is shown the temporal evolution of the factor A_1. The x-axis report the time in hours from the beginning of the simulation. The temporal interval shown in the three figures corresponds to the whole local night. For all figures we applied a moving average of 1 hour.

sample in the summer time assuming that, using a sub-sample of SCIDAR measurements in winter time, the model will be able to be calibrated for this season. It is known that a forthcoming site testing campaign extended on a solar year will be done with a Stereo-SCIDAR (private communication M. Sarazin) in the near future at Paranal. We think therefore that a dedicated calibration will be able to be done with these measurements soon. The issue of the dependency of the model calibration from the season is almost not observed on the wavefront coherence time. We think that the reason is due to the fact that τ_0 depends on two parameters: the C_N^2 and the wind speed and probably the good model reconstruction of the wind speed can mask and overcome somehow this effect.

We remind that all measurements and simulations are treated with a moving average of 1 hour and are resampled with a temporal frequency of 20 minutes.

5.1 Total seeing

We analyse in this section 3×3 contingency tables, with 2 different sets of thresholds. For the first case (CASE 1), we use as thresholds of the total seeing the first and third tertiles of the cumulative distribution of the sample of nights considered in the validation sample. For the second case (CASE 2), we use as thresholds of the total seeing 1 arcsec and 1.4 arcsec, as decided in agreement with the ESO Board. A seing weaker than 1

	Climatology whatever N. of nights	OBS par. < X1	OBS X1 < par. < X2	OBS par.> X2
Median Value	par. < X1	0	0	0
	X1 < par. <X2	33	33	33
	par. > X2	0	0	0

PC=33%; EBD=0%
POD_1=0%; POD_2=100%; POD_3=0%

Table 79: Typical contingency table using the climatological median value (as N is undefined, we display the percent only).

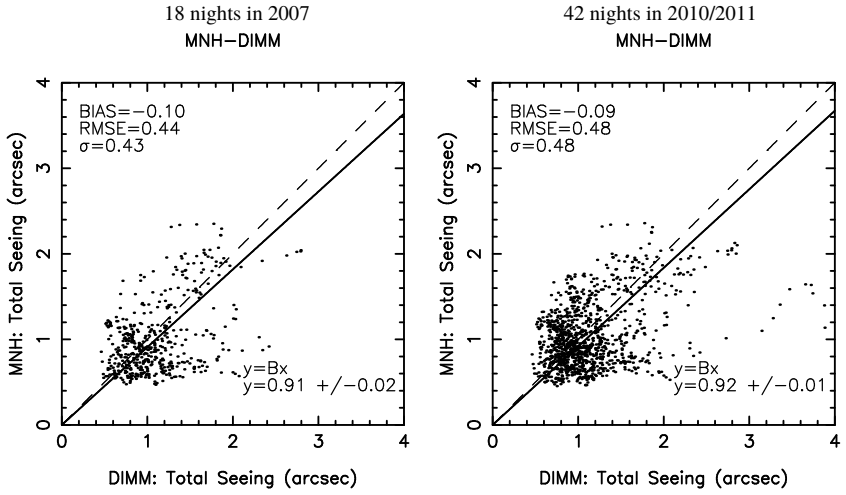

Figure 52: Scattered plot of the total seeing between Meso-NH outputs and DIMM measurements, for the summer periods of 2007, and 2010/2011. Both represent the validation sample.

arcsec and larger than 1.4 arcsec should still provide a very useful information to help for the decision to be taken *in loco*. Only the DIMM is used as a reference when we treated the large validation sample. Generalized SCIDAR measurements are available only for the small calibration sample (see MOSE Report Phase A).

5.1.1 Validation sample

We focus on the summer (42 over 89 simulated nights in 2007, 2010 and 2011 (total validation sample), and 18 over the sub-sample of 36 simulated nights in 2007), the season for which the calibration of the model was done. Tables 81 and 80 are the contingency tables for both cases (1 and 2), related to the 18 summer nights of 2007. Tables 83 and 82 are the contingency tables for both cases (1 and 2), related to the 42 summer nights of 2010/2011. Figure 52 displays the scattered plot of the total seeing between Meso-NH outputs and DIMM measurements, for the summer periods of 2007, and 2007/2010/2011.

If we look at the most interesting and critical range i.e. the POD_1 that is the probability that the model predicts seeing weaker than the first threshold we observe very good percentages. **For the total sample we have that the probability to predict a seeing weaker than 1" is 62.04 % (Table 83), while the**

	ε - SUMMER 18 nights over 36	DIMM $\varepsilon < 0.86$"	DIMM 0.86" $< \varepsilon <$ 1.20"	DIMM $\varepsilon >$ 1.20"
MNH	$\varepsilon < 0.86$"	86	87	52
MNH	0.86" $< \varepsilon <$ 1.20"	64	61	34
MNH	$\varepsilon >$ 1.20"	12	14	76

Total points = 486; PC=45.88%; EBD=13.17%
POD_1=53.09%; POD_2=37.65%; POD_3=46.91%

Table 80: Contingency tables for the total seeing, in summer (18 nights in 2007) - validation sample. Rounded values of the first and third tertiles of the climatology have been used as thresholds.

	ε - SUMMER 18 nights over 36	DIMM $\varepsilon <$ 1"	DIMM 1" $< \varepsilon <$ 1.4"	DIMM $\varepsilon >$ 1.4"
MNH	$\varepsilon <$ 1"	177	87	38
MNH	1" $< \varepsilon <$ 1.4"	58	34	14
MNH	$\varepsilon >$ 1.4"	9	18	51

Total points = 486; PC=53.91%; EBD=9.67%
POD_1=72.54%; POD_2=24.46%; POD_3=49.51%

Table 81: Contingency tables for the total seeing, in summer (18 nights in 2007) - validation sample.

probability to predict a seeing weaker than the first tertile is 48.14 % (Table 82). If we consider just the date of 2007 results are even better: we observe that the probability to predict a seeing weaker than 1" is 72.54 % (Tables 81) while the probability to predict a seeing weaker than the first tertile is 53.09 % (Tables 80). We analyzed separately the year 2007 because it gave some better results with respect to the total sample (2007/2010/2011). It might be due to the fact that the calibration sample belongs to the 2007 (also if the calibration sample is totally independent from the validation sample). This seems to indicate that there is space in the future to further improve the results with more sophisticated calibrations.

5.1.2 Calibration sample

For information, we report here the results for the calibration sample (20 nights sample). The interest of this analysis is that, for this sample, we can compare the performance of the model with respect to an instrument taken as a reference with the dispersion between two different instruments.

Tables 84 and 85 report the contingency tables of the 2 instruments (GS and DIMM). Table 86 reports the contingency table between Meso-NH and the GS, for the total seeing. Table 87 reports the contingency table between Meso-NH and the DIMM, for the total seeing. **If we look at the probability of the model to forecast a seeing weaker than the first tertile is 82.14 % (Table 86) or 88.13 % (Table 87) depending if we consider the GS or the DIMM as a reference. These results are even better than those obtained comparing the two different instruments. Indeed the probability to measure a seeing weaker than the first tertile is 64.29 % (Table 84) or 71.43 % (Table 85) depending on the reference (GS or the DIMM)**.

	ε - SUMMER 42 nights over 89	DIMM $\varepsilon < 0.88$"	DIMM 0.88" $< \varepsilon <$ 1.17"	DIMM $\varepsilon >$ 1.17"
MNH	$\varepsilon < 0.88$"	181	175	125
MNH	0.88" $< \varepsilon <$ 1.17"	129	106	83
MNH	$\varepsilon >$ 1.17"	66	95	168

Total points = 1128; PC=40.34%; EBD=16.93%
POD_1=48.14%; POD_2=28.19%; POD_3=44.68%

Table 82: Contingency tables for the total seeing, in summer (42 nights in 2010 and 2011) -validation sample. Rounded values of the first and third tertiles of the climatology have been used as thresholds.

	ε - SUMMER 42 nights over 89	DIMM $\varepsilon <$ 1"	DIMM 1" $< \varepsilon <$ 1.4"	DIMM $\varepsilon >$ 1.4"
MNH	$\varepsilon <$ 1"	353	209	77
MNH	1" $< \varepsilon <$ 1.4"	177	77	43
MNH	$\varepsilon >$ 1.4"	39	48	105

Total points = 1128; PC=47.43%; EBD=10.28%
POD_1=62.04%; POD_2=23.05%; POD_3=46.67%

Table 83: Contingency tables for the total seeing, in summer (42 nights in 2010 and 2011) - validation sample.

In Fig.53 are shown the scattering plots of the total seeing between GS and DIMM (left) and between the Meso-Nh and GS (center) and Meso-Nh and DIMM (right). We observe that the σ value between the two instruments is 0.30" while those of the model with respect to the instruments is 0.34" and 0.36" therefore substantially comparable.

	ε 20 nights	**GS** $\varepsilon < 0.97$"	$0.97" < \varepsilon < 1.24"$	$\varepsilon > 1.24$"
DIMM	$\varepsilon < 0.97$"	108	45	5
	$0.97" < \varepsilon < 1.24"$	39	60	14
	$\varepsilon > 1.24$"	21	63	149

Total points = 504; PC=62.90%; EBD=5.16%
POD_1=64.29%; POD_2=35.71%; POD_3=88.69%

Table 84: Contingency tables for the total seeing, between DIMM and GS, using GS as a reference - calibration sample (20 nights).

	ε 20 nights	**DIMM** $\varepsilon < 1$"	$1" < \varepsilon < 1.42"$	$\varepsilon > 1.42$"
GS	$\varepsilon < 1$"	120	52	13
	$1" < \varepsilon < 1.42"$	48	103	77
	$\varepsilon > 1.42$"	0	13	78

Total points = 504; PC=59.72%; EBD=2.58%
POD_1=71.43%; POD_2=61.31%; POD_3=46.43%

Table 85: Contingency tables for the total seeing, between DIMM and GS, using DIMM as a reference - calibration sample (20 nights).

	ε 20 nights	**GS** $\varepsilon < 0.97$"	$0.97" < \varepsilon < 1.24"$	$\varepsilon > 1.24$"
MODEL	$\varepsilon < 0.97$"	138	115	15
	$0.97" < \varepsilon < 1.24"$	18	35	48
	$\varepsilon > 1.24$"	12	18	105

Total points = 504; PC=55.16%; EBD=5.36%
POD_1=82.14%; POD_2=20.84%; POD_3=62.50%

Table 86: Contingency tables for the total seeing, between Meso-NH and GS - calibration sample (20 nights).

	ε 20 nights	DIMM $\varepsilon < 1$"	DIMM 1" $< \varepsilon <$ 1.42"	DIMM $\varepsilon >$ 1.42"
MODEL	$\varepsilon < 1$"	156	102	27
	1" $< \varepsilon <$ 1.42"	17	60	70
	$\varepsilon >$ 1.42"	4	14	79

Total points = 529; PC=55.76%; EBD=5.86%
POD_1=88.13%; POD_2=34.10%; POD_3=44.89%

Table 87: Contingency tables for the total seeing, between Meso-NH and DIMM - calibration sample (20 nights).

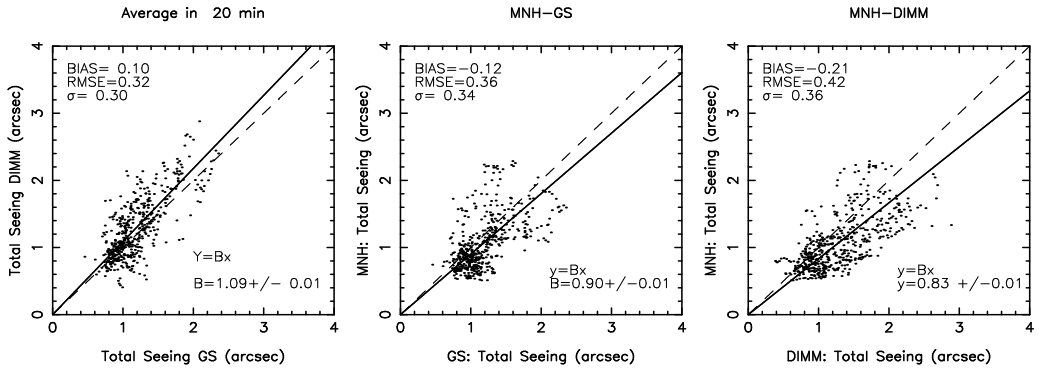

Figure 53: Scattered plot of the total seeing between Meso-NH outputs and DIMM and GS measurements (center and right) and between the GS and the DIMM (left) for the calibration sample of 20 nights.